DISSERTATIONES
CHIMICAE
UNIVERSITATIS
TARTUENSIS
161

ANU TEEARU

Development of MALDI-FT-ICR-MS methodology for the analysis of resinous materials

DISSERTATIONES CHIMICAE UNIVERSITATIS TARTUENSIS
161

DISSERTATIONES CHIMICAE UNIVERSITATIS TARTUENSIS
161

ANU TEEARU

Development of MALDI-FT-ICR-MS methodology for the analysis of resinous materials

UNIVERSITY OF TARTU
Press

Institute of Chemistry, Faculty of Science and Technology, University of Tartu, Estonia.

Dissertation is accepted for the commencement of the Degree of *doctor philosophiae* (PhD) in Physical and Analytical Chemistry on June 14, 2017, by the Doctoral Committee of Institute of Chemistry, University of Tartu.

Supervisors: Research fellow Signe Vahur
Institute of Chemistry, University of Tartu, Estonia

Professor Ivo Leito
Institute of Chemistry, University of Tartu, Estonia

Opponent: Prof. emer. Jean-Francois Gal
Institut de Chemie de Nice, France

Commencement: August 16th, 2017, 12.00
Ravila Street 14a, Tartu (Chemicum), auditorium 1021

Publication of this dissertation is granted by University of Tartu.

This work has been partially supported by Graduate School of Functional materials and technologies receiving funding from the European Regional Development Fund in University of Tartu, Estonia

ISSN 1406-0299
ISBN 978-9949-77-497-5 (print)
ISBN 978-9949-77-498-2 (pdf)

University of Tartu Press
www.tyk.ee

When nature gives you resin, you make art.

TABLE OF CONTENTS

LIST OF ORIGINAL PUBLICATIONS

This thesis is based on three articles listed below and referred in the text by Roman numbers.

I. Vahur, S.; **Teearu, A.**; Haljasorg, T.; Burk, P.; Leito, I.; Kaljurand, I. Analysis of dammar resin with MALDI-FT-ICR-MS and APCI-FT-ICR-MS. *J Mass Spectrom*, **2012**, 47 (3), 392−409.

II. **Teearu, A.**; Vahur, S.; Haljasorg, U.; Leito, I.; Haljasorg, T.; Toom, L. 2,5-Dihydroxybenzoic acid solution in MALDI-MS: ageing and use for mass calibration. *J Mass Spectrom*, **2014**, 49 (10), 970−979.

III. **Teearu, A.**; Vahur, S.; Rodima, T.; Herodes, K.; Bonrath, W.; Netscher, T.; Tshepelevitsh, S.; Trummal, A.; Lõkov, M.; Leito, I. Method development for the analysis of resinous materials with MALDI-FT-ICR-MS: novel internal standards and a new matrix material for negative ion mode. *J Mass Spectrom*, published online 04.05.2017, DOI: 10.1002/jms.3943.

Author's contribution

I. Performed experiments and helped in data analysis.
II. Main person for planning and writing the manuscript. Performed all the experimental work and data processing.
III. Main person for planning and writing the manuscript. Performed all of the experimental work and data processing.

ABBREVIATIONS

^{1}H NMR	proton nuclear magnetic resonance
AA	aminoacridine
ACTH	adrenocorticotropic hormone
ADC	analog-to-digital converter
APCI	atmospheric pressure chemical ionisation
ATR	attenuated total reflectance
CHCA	α-cyano-4-hydroxycinnamic acid
Da	Dalton
DE	direct exposure
DFT	density functional theory
DHB[1]	dihydroxybenzoic acid
dma	dimethylamino
DT	direct temperature
ESI	electrospray ionisation
FT	Fourier transform
GB	gas phase
GC	gas chromatography
ICR	ion cyclotron resonance
IR	infrared
LC	liquid chromatography
MALDI	matrix-assisted laser desorption/ionisation
MS	mass spectrometry
Nd:YAG	neodymium-doped yttrium aluminium garnet
PCR	polymerase chain reaction
pyrr	pyrrolidino
SA	sinapic acid
T	Tesla
TD	time dependent
ToF	time of flight

[1] In this work, DHB is used as an abbreviation for 2,5-dihydroxybenzoic acid.

1. INTRODUCTION

Natural resins and resinous materials, such as tars and pitches are known to humanity since prehistoric times. These materials have found extensive use as adhesives, coating materials, water-repellents, etc. One of the most important application of natural resins has been their use in the production of varnishes for the coating of paintings, polychrome objects, woodwork, furniture, etc. Therefore, the resins play an important role in the preserving of historical artefacts and the knowledge of their chemical composition and ageing processes is very valuable.

The composition of natural resins and their products is intrinsically complex and difficult to elucidate because they contain numerous compounds that have very similar structures. Determining the composition of such materials is significantly complicated by the extensive oxidation/degradation and by the small sample size usually available from the works of art and cultural heritage objects.

The composition and ageing of natural resins has been studied with various analytical methods, such as infrared spectroscopy (IR), gas chromatography (GC) and liquid chromatography (LC) coupled with mass spectrometry (MS), etc. Nowadays, direct mass-spectrometric methods are increasingly taking the central role in the investigation of different types of materials. The development of different mass analysers, such as tandem (MS/MS), time of flight (ToF), Fourier transform ion cyclotron resonance (FT-ICR), and a range of novel ionisation techniques, like matrix-assisted laser desorption/ionisation (MALDI), electrospray ionisation (ESI) and atmospheric pressure chemical ionisation (APCI), have expanded the capabilities to analyse almost any type of complex materials (including resinous substances).

MALDI has a number of advantages regarding the analysis of complex resinous materials: (1) it does not require complete solubility of the sample, (2) for the analysis very small sample size is needed and (3) components present at very low levels can be determined. At the same time, a mass spectrum obtained from a resinous material without prior component separation is usually very complex. To obtain as much information about the composition of the material as possible the resolution and *m/z* accuracy in such mass spectrum should be as high as possible. Currently, the instrument offering the highest possible resolution and *m/z* measurement accuracy is the FT-ICR mass spectrometer. Combined with MALDI ionisation technique it is a promising analysis method for resinous materials.

A key aspect in MALDI-MS analysis is the choice of matrix material. The number of different matrices proposed for MALDI-MS is extensive. A large number of the matrix materials in regular use are acidic (derivatives of benzoic and cinnamic acids, etc.) but also a number of basic matrix materials have been successfully incorporated to this method (pyridines, anilines, etc.). Finding the suitable matrix compound is usually associated with the specific application and

type of material. The chemical properties of the material – the solubility, the nature of its components, etc. influence the behaviour of the matrix material. Therefore, a matrix that can be suitable for one type of material may not be suitable for another similar substance.

The second important factor in the mass-spectrometric analysis of resinous materials is achieving the highest possible *m/z* accuracy. In order to obtain high *m/z* accuracy with FT-ICR-MS instruments, the *m/z* axis must be calibrated. Currently, the selection of commercially available calibration standards that offer a flexible selection of *m/z* values under *m/z* 1000 is limited to a few peptides, polyethylene glycols, and some other substances. Therefore, the number of calibration standards suitable for the analysis of resinous materials that mostly have characteristic peaks under *m/z* 1000, is low and restricted to only a few options.

Last but not least, the sample preparation stage has also critical influence on the success of the MALDI-MS analysis. Resinous materials are complex in their nature, and over time, this complexity increases via oxidation, polymerisation, degradation processes. Thereby, also the properties of the material change (e.g. solubility), making it necessary to modify the sample preparation stage.

The general aim of the study is the development of a MALDI-FT-ICR-MS methodology for the comprehensive analysis of resinous materials in the positive and negative ion mode focusing mainly on the natural resins used for the production of varnishes, such as dammar, mastic, sandarac, colophony and shellac resins.

The hypothesis of the study is the following: MALDI-FT-ICR-MS is a capable technique for the analysis of resinous materials that allows to obtain a wealth of high accuracy data from these complex and problematic materials if the sample preparation and choice of matrix are suitable and the *m/z* accuracy is increased by the use of internal standards.

The PhD study is divided into the following stages:

- Assessment of the capabilities of MALDI-FT-ICR-MS method for the analysis of natural resins with dammar resin as a representative; [publication I]
- Investigation of 2,5-dihydroxybenzoic acid (DHB) as a matrix compound for the analysis of natural resins and its suitability for internal calibration; [publication II]
- Introduction of a new matrix compound (2-aminoacridine) in the negative ion mode for the analysis of resinous materials with MALDI-FT-ICR-MS; [publication III]
- Application of novel calibration standards with *m/z* values below *m/z* 1000 for both, positive and negative ion mode; [publication III]

- Demonstration of the applicability of the developed MALDI-FT-ICR-MS methodology during the analysis of three case studies from different cultural heritage objects representing Estonian history and artworks. [publication III]

All the stages listed above include also the modifications to sample preparation and the development of individual sets of parameters for different resins and resinous materials. [publications I, II, III]

2. LITERATURE OVERVIEW

2.1 Natural resins

Natural resins are sticky and water insoluble by-products secreted by a great number of trees and plants but also by some insects. [1, 2] In their raw and non-purified form they consist of numerous organic compounds, such as terpenoids, alcohols, esters, essential oils, phenolic compounds, water, etc. [1, 3]

Due to the useful properties and wide availability natural resins have been used for centuries (and still are) in many different applications:

- as coating and adhesive materials (e.g. to waterproof or decorate objects, etc.);
- for medicinal use: for the healing and disinfecting of wounds, as pain relief, also for the production of medicaments;
- as a remedy for toothache and as filler for tooth cavities;
- for mummification;
- for incense;
- as food or drink additive;
- in the production of cosmetics and perfumes;
- for making jewellery and sculptures, etc. [2, 3]

From the point of view of cultural heritage objects and works of art one of the most important products of natural resins are varnishes. Varnishes are prepared by dissolving a resin in a liquid, such as linseed oil, turpentine, spirit, etc. [1] Upon drying the varnish forms a hard and usually transparent film that offers protection to the object from humidity, dust and sunlight, also from smaller physical damages. It also accentuates the colours on the paintings and highlights the structure of the wood. The chemistry and properties of the varnish are mainly determined by the resin(s) used for the production of it, therefore, an extended knowledge about the composition, ageing processes and overall properties of natural resins is desirable.

Natural resins can be divided according to their origin to tree (plant) and insect resins. Natural tree resins, in turn, are divided into fossilised and recent resins. Fossilised resins, such as amber and copals are very old resins (≥40000 years). [3] They are very hard due to extensive polymerisation, and are mainly used for making small sculptures, jewellery, and beads, but also varnishes (oil-based). The recent tree resins are easily soluble in spirit- and oil-based solvents and are therefore often used for the preparation of varnishes and in the composition of paints. [1, 2, 4]

Hereafter a more detailed description for some of the more important varnish resins (di- and triterpenoid and insect resins) is presented. The discussed resins are also the analysis objects of this study.

2.1.1 Tree resins

The number of trees secreting resin is very high: most of the trees are producing viscous substance that offers protection against dehydration and helps to heal the (smaller) wounds on the bark and trunk of the trees.

By their chemical nature, the tree resins are divided into terpenoid and phenolic resins.

Phenolic resins (known also as balsamic resins) are composed of aromatic compounds, mainly cinnamic and benzoic acids and their esters. Phenolic resins, such as benzoe resin and storax resin have found extensive use in medicinal applications and in the production of cosmetics. [1, 3]

The majority of tree resins are composed of terpenoids. Terpenoids are chemically altered (oxidised, dehydrogenated, etc.) terpenes. The building block for the latter one is isoprene (C_5H_8). The smallest terpene – monoterpene is made up of two isoprene units, sesquiterpenes contain three isoprene units, diterpenes four, the very rare sesterterpenes consists of five isoprene units, triterpenes are made up of six isoprene units, and so on. Tree resins usually contain di- or triterpenoids along with mono- and sesquiterpenoids. As di- and triterpenoids are never found together in one resin the tree resins can be divided respectively. [1, 3]

Below, an overview of the most important tri- and diterpenoid resins used in the production of varnishes is given.

Triterpenoid resins

There are several triterpenoid resins that have found use in different applications. Among these resins, dammar and mastic resin are the most important triterpenoid resins used for the production of high-quality picture varnishes.

Dammar resin is a pale-yellow resin that is obtained from various species of trees belonging to the *Dipterocarpaceae* family (mainly species of *Shorea* and *Hopea*). These are very tall tropical trees (up to 70–85 m) with broad leaves, that grow in the East Indies (particularly in Malaysia, Indonesia, Sumatra and Borneo). [1–3, 5, 6] The resin is collected by making incisions into the trunk of the tree (tapping). Before the collection, the secreted resin is allowed to harden. The gathered resin is purified and sorted according to the size and quality of the resin clumps. [2, 7]

The chemical composition of dammar resin is complex. The resin mainly consists of tetracyclic triterpenoids (hydroxydammarenone, dammarenolic acid, dammaradienone, etc.), but also contains pentacyclic triterpenoids of the series of olanane, ursane and hopane, e.g. oleanonic/ursonic acid or aldehyde, oleanolic/ursolic acid or aldehyde, nor-amyrone, etc. (see Figure 1). The resin also contains a small amount of sesquiterpenoids (volatile fraction) and a polymeric fraction based on the sesquiterpene cadinene ($C_{15}H_{24}$). [1–3, 8]

With time, the complexity of dammar resin increases. Dietemann *et al.* demonstrated that oxidation in dammar resin (also in dammar varnish) takes place

over a short period of time (roughly 6 months). [9] The oxidation process is extensive even if the resin is kept in the dark. The rapid oxidation is accompanied by partial polymerisation and decomposition of the original compounds of dammar resin. [10, 11] From every individual original component of the resin numerous new compounds are formed. Since the original composition of dammar resin already has a large number of different components then the diversity of the different compounds present in the aged resin (also varnish) is very high. [I]

Dammar resin is fully soluble in organic solvents, such as turpentine, white spirit, toluene, dichloromethane, etc. but dissolves only partially in alcohols (the polymeric fraction is not soluble in alcohols). Dammar resin has good optical and adhesive properties; also, the acidity of dammar resin is lower compared to other terpenoid resins (less damaging to basic pigments and linen canvas). [3, 7] Due to these properties dammar resin has been extensively used for the production of painting varnish since the first half of 19th century and is still used nowadays. [2, 3] The varnish layer left by dammar varnish is thin, colourless, bright and elastic. In addition to the protective properties, it also enhances the colour nuances. With time, dammar resin gradually yellows, although to a lesser extent than varnishes made from e.g. diterpenoid resins. The aged varnish layer on the painting becomes brittle (cracks appear) and the solubility of it decreases. Therefore, during the restoration and conservation of artworks, stronger and more damaging solvents are needed for the removal of the varnish. [7, 8]

Mastic resin is collected from small trees or shrubs of the *Pistacia* genus (*Anacardiaceae* family) growing in the Mediterranean area. The main source of this pale-yellow resin is the pistachio tree *Pistacia lentiscus*. Since the Middle Ages, mastic resin is exclusively produced on the island of Chios (Greece). The best-quality resin is collected from male trees growing in the South-eastern areas of the island. Also, the time of collection affects the quality of the resin, therefore it is gathered only from the middle of July to mid-October.

Mastic resin has been used since ancient times. The remnants of the resin found at different sites in the Mediterranean area date back to the establishment of the first permanent settlements in this area (5500–5000 BC). [2] The selection of different applications that mastic resin has been (and still is) used is broad: from an adhesive for wounds and a filler for tooth cavities and relief for toothache to a flavouring component in alcoholic beverages. In fact, the name of the resin comes from the Greek word for chew, and the resin is used for masticatory purposes even nowadays. [2]

Even if the origin of mastic resin is traceable to a very specific and small geographical area, the chemical composition of mastic resins is still very complex and even more diverse compared to dammar resin. The resin consists mainly of triterpenoids, such as masticadienonic acid, isomasticadienonic acid and moronic acid, lupeol. It also shares a number of compounds that are present in the composition of dammar resin: hydroxydammarenone, oleanonic acid, oleanonic aldehyde, nor-amyrone, etc. (see Figure 1). [1, 2, 8, 10, 12] Compared to dammar resin, mastic resin is lacking in ursane-type compounds. [3, 8, 13] In

addition to triterpenoids, mastic resin contains a fraction of monoterpenes, e.g. *α*-pinene, *β*-pinene, limonene, *β*-myrcene, etc. [2] Similarly to dammar resin mastic resin also contains a polymeric fraction that has been identified as cis-1,4-poly-*β*-myrcene [$(C_{10}H_{16})_n$]. [1, 3, 8, 14]

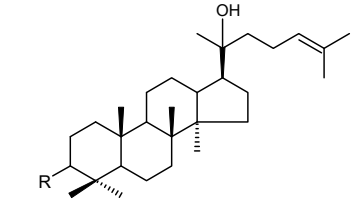

R	Compound
O	Hydroxydammarenone ($C_{30}H_{50}O_2$)
OH	Dammarenediol ($C_{30}H_{52}O_2$)

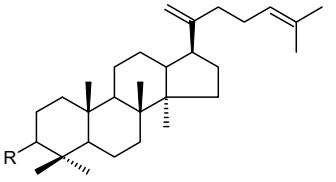

R	Compound
O	Dammaradienone ($C_{30}H_{46}O$)
OH	Dammaradienol ($C_{30}H_{50}O$)

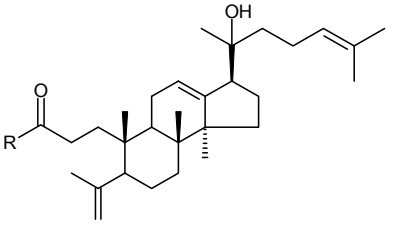

R	Compound
OH	Dammarenolic acid ($C_{30}H_{50}O_3$)
OMe	Dammarenolic acid methyl ester ($C_{31}H_{52}O_3$)

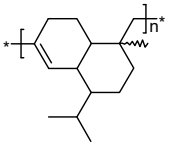

Polycadinene ($[C_{15}H_{24}]_n$)

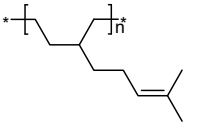

cis-1,4-poly-*β*-myrcene ($[C_{10}H_{16}]_n$)

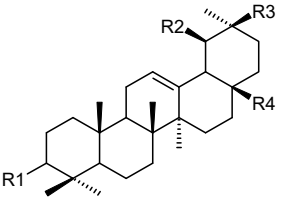

R1	R2	R3	R4	Compound
O	CH_3	H	H	Nor-*α*-amyrone ($C_{29}H_{46}O$)
O	H	CH_3	H	Nor-*β*-amyrone ($C_{29}H_{46}O$)
O	H	CH_3	CHO	Oleanonic aldehyde ($C_{30}H_{46}O_2$)
O	CH_3	H	CHO	Ursonic aldehyde ($C_{30}H_{46}O_2$)
O	H	CH_3	COOH	Oleanonic acid ($C_{30}H_{46}O_3$)
O	CH_3	H	COOH	Ursonic acid ($C_{30}H_{46}O_3$)
OH	H	CH_3	CHO	Oleanolic aldehyde ($C_{30}H_{48}O_2$)
OH	CH_3	H	CHO	Ursolic aldehyde ($C_{30}H_{48}O_2$)
OH	H	CH_3	COOH	Oleanolic acid ($C_{30}H_{48}O_3$)
OH	CH_3	H	COOH	Ursolic acid ($C_{30}H_{48}O_3$)

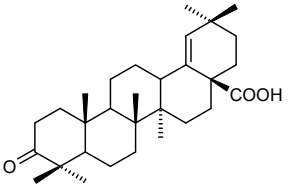

Moronic acid ($C_{30}H_{46}O_3$)

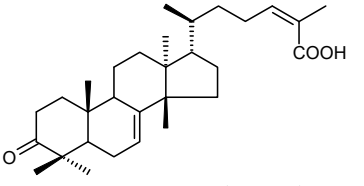

Masticadienonic acid ($C_{30}H_{46}O_3$)

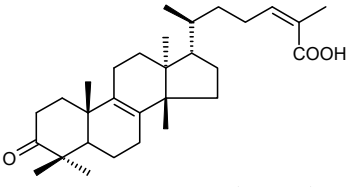

Isomasticadienonic acid ($C_{30}H_{46}O_3$)

Figure 1. Selection of components present in dammar and mastic resins. [1, 8] The compounds present in both resins are highlighted with blue text.

The composition of mastic resin and varnish becomes more diverse with time. The original compounds undergo oxidation, polymerisation and also some degradation may occur. [10] This leads to changes in the properties of the resin and the varnish: the solubility of the material decreases, it becomes yellow and more brittle.

Mastic resin is soluble in turpentine and aromatic solvents (toluene, benzene, etc.), and partially soluble in alcohols (similarly to dammar resin, the polymeric fraction of mastic resin is not soluble in alcohols). The resin is the basis of oil-, spirit- and watercolour varnishes that have been used since the Middle Ages. The properties of mastic varnish are similar to dammar picture varnish: it leaves a clear and elastic film that offers protection to the object and helps to highlight and brighten the colours. [2] At the same time, the layer of mastic varnish yellows more and thereby becomes more brittle than dammar varnish.

Diterpenoid resins

Diterpenoid resins are collected from trees belonging mainly to the Coniferae family. [1, 7] The diterpenoids used during this study are sandarac resin and colophony resin.

Sandarac resin is obtained from trees belonging to the *Cupressaceae* subfamily of the Coniferae family (African sandarac is obtained from the species of *Tetraclinis articulate*, Australian sandarac comes from species of *Callitris*). [2, 3] The resin is collected by tapping the tree or by natural secreting. The colour of the resin may vary from pale yellow to orange. [1, 2]

Sandarac resin consists mainly of polymerised communic acid (about 70%) making it harder compared to colophony or the triterpenoid resins. The resin also contains sandaracopimaric acid along with its derivatives, and some phenolic compounds, such as totarol and ferruginol (see Figure 2). With time, the level of oxidation and polymerisation increases and simultaneously the solubility of the resin decreases. [1, 3, 7, 15]

The resin has found use in various applications and is known since ancient times. Its main use is for the production of varnish (both, oil- and spirit-based) for paintings, but it has been used as a coating material for leather, stone and metal objects, as well for calligraphy. [2, 3, 16] For the preparation of oil varnish, sandarac resin is usually pulverised and mixed with hot linseed oil. [1, 16] The layer of sandarac oil varnish is glossy and hard and it is fairly difficult to remove it due to the mainly polymeric composition of the resin. The heat treatment also alters the composition of the resin (fragmentation and decarboxylation of polycommunic acid) and this, in turn, affects the stability, solubility, and the colouring of the varnish. The similar disadvantages exist also in the case of the spirit-based sandarac varnish, but in a lesser extent because of the missing heat-treatment stage. At the same time, the spirit varnish prepared from sandarac resin is not so elastic as the oil varnish and becomes brittle with time. [2]

Colophony resin (also called rosin) is a by-product of the resinous material obtained from pine trees (*Pinus* subfamily), turpentine being the other. It is a yellow to brown coloured soft resin that is soluble in alcohols, turpentine, etc.

The main component of fresh colophony resin (after the extraction of turpentine) is abietic acid, also neoabietic acid, pimaric acid, etc. are present in small amounts in the composition of the resin. Abietic acid readily oxidises to give dehydroabietic acid, this, in turn, oxidises to 7-oxodehydroabietic acid (see Figure 2). [1, 7, 17]

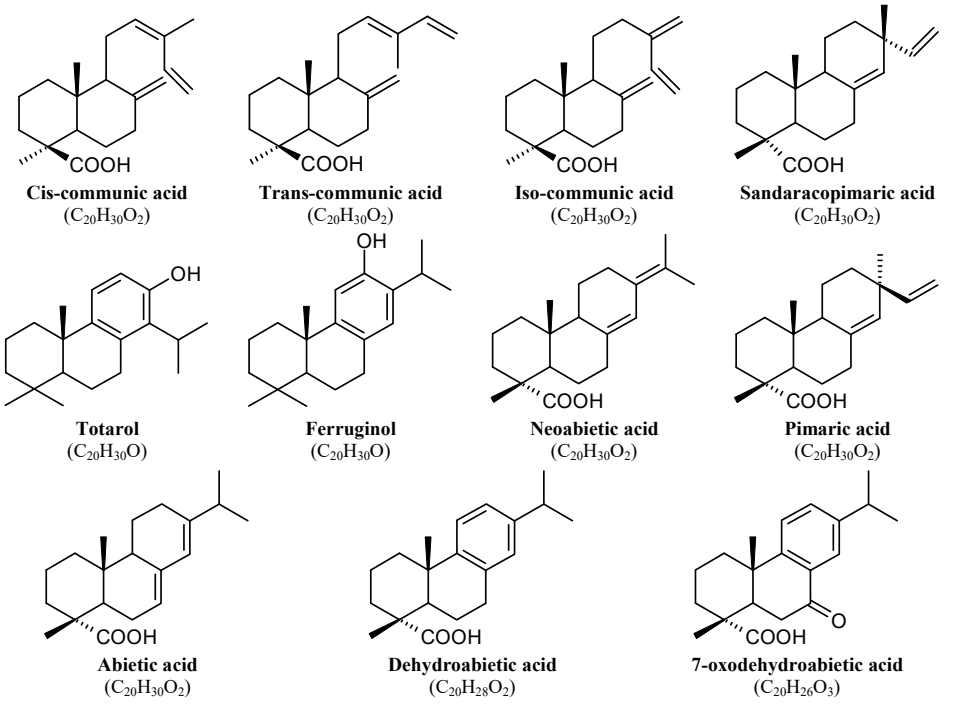

Figure 2. Selection of components present in sandarac and colophony resins. [1]

Colophony resin has many drawbacks due to its mainly acidic composition: it has a damaging effect on basic materials (e.g. some pigments, linen canvas, etc.), also the rapid oxidation leads to the darkening of the resin. Therefore, also the varnish (mainly oil-based) containing colophony resin has low quality. Nevertheless, colophony resin has been extensively used as a varnish component, especially in Europe as a cheap alternative for more expensive resins, such as mastic and sandarac. [7]

Besides being in the composition of varnish, colophony resin has been applied for various other applications. It has extensively been used in the naval industry (as a waterproofing agent), in fact, the term “naval stores” is regarded as a synonym for the industry dealing with the producing, processing and handling of colophony resin (in Northern America). [18] The resin has been an additive in

paper, oil and tempera mediums. Nowadays it is used more in the composition of synthetic rubber, printing ink, chewing gum (E915), etc. Athletes, dancers and players of string instruments use it as a friction-increasing material. [2]

2.1.2 Insect resins

Also, some insects produce resinous material during their lifetime. The most important animal origin resin is shellac resin.

Shellac (also known as lac) resin is produced by the *Kerria lacca* Kerr insect (Coccidae family) that is living on tropical trees in the South-East Asian region, mainly in India. The scale insects cover the branches of trees with the deep red to brown gum-like fluid for self-defence purposes. [7] The substance hardens with time and the "crust" is collected once a year by scraping it off the branches. The raw resin, known as stick-lac, mainly consists of resinous components, but also contains wax (6–7%), dyestuffs (4–8%), and bits of wood and bark, also dead insects, etc.

The colour of the resin depends on the purification procedure and varies from a pale-yellow (bleached shellac) to deep reddish-brown. In the first purification stage, the stick-lac is washed with water to remove the wooden material and other impurities, including water-soluble components. The product obtained during this stage is known as seedlac. Depending on the further treatment of seedlac a resin with different quality and properties is produced. Shellac that also contains wax is obtained by melting and filtrating the seedlac. The purified resin is sold as flakes or as small drops (known as button lac). [1] For the removal of wax, solvent extraction with ethanol is used. Shellac wax along with the remaining impurities is filtrated and the remaining resin is treated with activated carbon. The latter is removed during second filtration and the resin film is cooled and broken into sheets. [19] In order to obtain colourless shellac resin (bleached shellac), the solution of seedlac in water-based alkaline is treated with sodium hypochlorite and the resin is precipitated with sulphuric acid. This treatment affects the composition of the resin by making the components more reactive and thereby decreasing the stability of the resin. [1, 19]

Shellac resin consists mainly of aliphatic acids, such as aleuritic and butolic acids. It also contains a small amount of sesquiterpenoids like shellolic, jalaric and laccijalaric acids (see Figure 3). [1, 19] With time the level of cross-linkage increases (esterification), resulting in deterioration of the solubility of the resin. [1, 19, 20]

One of the most important products of shellac resin is the spirit varnish that is mainly used for wooden objects (furniture, also musical instruments). The dried varnish coat left by the spirit-based shellac varnish is hard and thick. At the same time, it is lustrous and although usually coloured it is still very transparent and it helps to accentuate the structure of the wood. The main drawback of this varnish is the sensitivity to moisture, heat and sunlight. [20] In addition

to being an important varnish resin, shellac has also found use as an additive in colours, in dental application (dental boards and trays), etc. [19, 20]

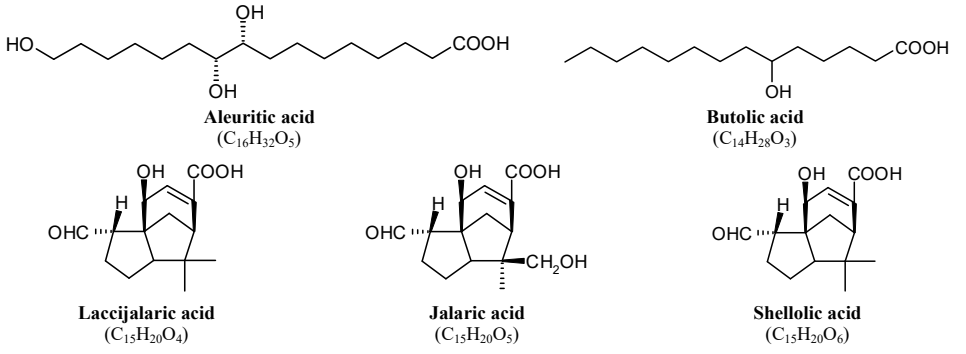

Figure 3. Selection of components present in shellac resin. [1, 19]

2.1.3 Tars and pitches obtained from resinous wood

Historically, also tars and pitches have been very important resinous materials, especially in the Northern parts of Eurasia. These materials have been used for very practical purposes – for waterproofing and caulking different objects, such as ships, pots, barrels, arrow and spear heads, etc. also for medicinal use for wounds and toothache, etc. The earlier finds of these materials date back to Mesolithic and Neolithic times (approximately 10000–2000 BC). [7, 15]

The sticky and viscous material is obtained during the pyrolytic heat-treatment of resinous wood. The undistilled product of this process is known as pitch and tar is obtained by the distillation of pitch. Usually, pine, spruce, fir (diterpenoids) and birch (triterpenoids) have been used for the production of tars and pitches. [1, 3]

Tars and pitches are chemically very complex. Their composition is mainly related to the resin obtained from the trees used for the production of tar or pitch. But the heat-treatment and also components present in the wood are responsible for the alterations of the original resin compounds, usually leading to components with lower molecular weight. [1, 3] For the diterpenoid tars and pitches, the components of the resin undergo demethylation and decarboxylation, also the aromatisation of these compounds has been found to be common. E.g. the polycyclic hydrocarbon retene ($C_{18}H_{18}$) has been identified as a characteristic compound in aged pine tar and pitch. The marker components in birch bark tar and pitch are lupeol and betulin, a smaller fraction of lupenone, betulone and betulinic acid have been identified (triterpenoids with the lupane skeleton). [3]

2.2 Analytical methods for the analysis of resinous materials

2.2.1. General overview of the analysis of resinous materials

As described above, the composition of natural resinous materials is very complex, and the level of complexity increases during ageing and/or different treatments that the resins undergo in order to be used in various applications. Furthermore, usually the samples available from cultural heritage objects (and archaeological finds) are very small, analyte concentrations in them are low, and the samples consist of many components, including impurities and their decomposition products. Therefore, the requirements for the analysis technique are high.

The chemical composition (and ageing) of natural resinous materials has been an investigation object for over 100 years and different analysis methods have been applied. One very useful tool in the characterisation and differentiation, also in the monitoring of ageing and determining the origin (botanical and geographical) of resinous materials has been infrared (IR) spectroscopy. [4, 5, 21–30]

Mass spectrometry, especially if coupled with gas chromatography has found extensive use in the analysis of resinous materials. [3, 12, 31–34] However, the sample treatment prior to GC-MS analysis is extensive and demanding, requiring derivatisation and/or hydrolysis of the sample, and the full dissolution of the sample. This, in turn, sets some limitations on sample size. In addition, the possible oligomeric part of the resins usually remains undetected. [I, 15] In addition to GC-MS, also liquid chromatography coupled with MS is used. [35] This method has fewer limitations regarding the sample but it still needs a fairly comprehensive sample preparation: only the soluble part of the sample can be analysed and the selection of solvents is restricted to only these solvents that are compatible with the instrument. Furthermore, there is currently no ion source available that would be compatible with LC-MS and would at the same time give ions of all sample components, irrespective of their chemical nature.

As an alternative, direct MS ionisation methods, such as direct temperature (DT) and direct exposure (DE) electron ionisation have been used for the analysis and identification of the resinous materials. [16, 36, 37] Also, the modern ionisation techniques, such as matrix-assisted laser desorption/ionisation (MALDI), electrospray ionisation (ESI), and atmospheric pressure chemical ionisation (APCI), that are able to produce ions from compounds with low volatility, are increasingly used for the analysis of a wide variety of complex materials, including resinous samples. [38, 39]

In order to maximise the information from the mass spectrum of a resinous material, the resolution and *m/z* accuracy have to be as high as possible. The best option currently available is Fourier transform ion cyclotron resonance (FT-ICR) mass spectrometer. Under routine conditions a resolution up to a hundred thousand and *m/z* errors almost always below 2 ppm for mass spectra with internally calibrated *m/z* axes are obtained. [I, II, III, 40, 41]

Out of the above-mentioned ionisation methods, MALDI is an especially promising technique for the analysis of resinous samples because it enables the analysis of very small samples and does not require the sample to be fully dissolved.

2.2.2. Matrix-assisted laser desorption/ionisation (MALDI)

Matrix-assisted laser desorption/ionisation is suitable for the mass-spectrometric analysis of non-volatile, non-soluble, highly oxidised, polymerised and thermally labile samples. [39, 40] Initially developed for the analysis of large molecules, such as proteins and polymers, it is also applicable to smaller molecules, like lipids, carboxylic acids, etc. The technique was introduced around 30 years ago simultaneously by the groups of Hillenkamp [42], and Tanaka [43].

MALDI is based on the (almost) simultaneous desorption and ionisation of solid mixture of matrix and sample deposits by laser radiation (see Figure 4). In the positive ion mode, MALDI produces ions mainly in the form of adducts with H^+, Na^+ or other cations, i.e. $[M+H]^+$, $[M+Na]^+$, etc. with almost no fragmentation. [I, II, 44] In the negative ion mode, MALDI produces mainly deprotonated ions ($[M-H]^-$).

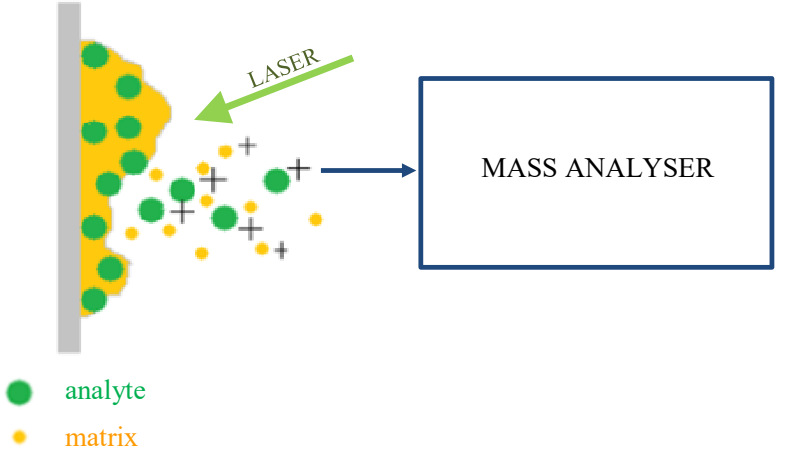

Figure 4. The principle of MALDI technique: the solid mixture of sample (analytes) and matrix particles is irradiated with the laser that initiates the desorption and also the ionisation of the analyte molecules. Here, the generation of positive ions is depicted but the process is similar for the negative ion mode.

MALDI matrices

One of the most important aspects of MALDI-MS analysis is the correct choice of matrix. [38, 45] So far an universal MALDI matrix substance that is suitable in both, positive and negative ion mode and enables the analysis of different

type of materials (proteins, lipids, carbohydrates, resins, etc.) has not been discovered. Mostly, the choice of matrix compound is dependent on the type of materials analysed and therefore, the selection of different matrices is quite extensive. [38, 39]

A useful matrix compound should have the following properties: (1) it co-crystallises with the sample molecules when the solvent is evaporated, (2) it absorbs the laser radiation, (3) it ionises sample molecules either by proton transfer or by transfer of some other ion, (4) it does not itself produce intense interfering peaks in the mass spectrum. [39, 40, 44] In addition, the matrix compound should be sufficiently pure so that no significant extraneous peaks would be observed. [44] However, in some cases, the peaks belonging to the matrix can be very useful for internal calibration. [I, II, III] Additionally, from a practical point of view, it is important to know how matrix compounds behave (especially in solution) on long-term usage. [II]

Many MALDI matrix compounds are acidic in character – 2,5-dihydroxy-benzoic acid and its derivatives, α-cyano-4-hydroxycinnamic acid (CHCA), sinapic acid (SA), etc. They enable the analysis of different types of samples – mostly peptides and proteins, but also polymers, saccharides, resins, dyes, etc. and are applicable in both, positive and negative ion mode. [I, II, III, 39]

Among the most widely used MALDI matrices is 2,5-dihydroxybenzoic acid. [46–54] It is a yellowish crystalline compound that absorbs UV radiation in the range of 290–370 nm [47, 55], which embraces the wavelengths of the lasers commonly used for MALDI: N_2 laser at 337 nm, Nd:YAG laser at 355 nm or 266 nm. [I, II, III, 46–49, 56–59] DHB was introduced as a MALDI matrix in the early 1990s. [56] The properties of DHB have been studied by several groups making it possibly the most investigated MALDI matrix compound. [46–54]

In addition, several basic matrices have been proposed, for example derivatives of pyridines, pyrimidines, anilines, etc. for the negative ion mode. [60] In 2002 a novel basic matrix – 9-aminoacridine (9-AA) – was introduced for the analysis of molecules with acidic protons, such as carboxylic acids, phenols, alcohols, etc. specifically for the negative ion mode. [61] The study showed that in some cases the already known and established matrices, such as DHB and CHCA had problems in generating analyte ions, which the newly proposed matrix compound could overcome.

2.2.3 Fourier transform ion cyclotron resonance mass spectrometry

The principle of Fourier transform ion cyclotron resonance (FT-ICR) mass spectrometer is based on the movement of ions in the magnetic field at their frequency of circular motion, ω_c,

$$\omega_c = \frac{zB}{m}, \quad (1)$$

where z is the charge, B the magnetic field strength, and m is the mass of the ion. [62] If B is constant then the frequency is determined by the m/z ratio and ions with different m/z ratios have different frequencies. If cyclotroning is monitored during sufficiently long time then the frequency can be measured with extremely high accuracy and discrimination between very similar frequencies is possible. The former enables extremely high mass accuracy and the latter – extremely high resolving power.

An FT-ICR-MS instrument consists of five components: an ion source, an analyser cell, a magnet, a vacuum system and a data system. [38] The main function of the ion source is the generation of ions. In the early days, the ion source was inside the magnet, but nowadays external ion sources (outside the magnetic field), such as MALDI, ESI, APCI, etc. are used. In the analyser cell (nowadays mainly a cylinder consisting of curved plates) the ions are isolated (or ejected) according to their frequencies (m/z values). [38] The magnet, namely strength of the magnetic field determines the m/z accuracy, resolution, but also the m/z range of the instrument. The higher the magnetic field strength, B, the better results can be obtained. Currently, superconducting magnets with field strengths in the range of 4.7 Tesla (T) up to 12 T (or even 15 T) are used for FT-ICR-MS instruments. [38] The FT-ICR-MS system must be equipped with ultra-high vacuum (obtained with turbomolecular or cryopumps). The data system is also important because it helps to control the timing of numerous events necessary for the FT-ICR-MS analysis.

Equation 1 relating ω_c to m/z is valid only under idealised conditions. In practice, the following empirical equation is used:

$$m/z = \frac{A}{f + C} \tag{2}$$

where A and C are calibration parameters and A relates the m/z value to the magnetic field strength, B. Thus, for achieving high accuracy with an FT-ICR-MS instrument the m/z axis needs to be calibrated. Calibration can be either external or internal. When externally calibrating the m/z axis the calibration standards are analysed separately from the samples and the obtained calibration constants are used for adjusting the m/z axes of all the mass spectra recorded thereafter. Internal calibration is carried out using the m/z values of the reference compounds (either natively present in the sample or matrix, or added on purpose) from the obtained mass spectrum itself. [40, 41]

The need for Equation 2 comes from the space-charge effects between trapped ions (also the potential applied to the trapping plates affects this). These effects shift the cyclotron frequency f by Δf. [63, 64] The number of trapped ions per volume unit in the ICR cell cannot be well predicted and depends on a number of parameters. If MALDI source is used then the main parameters influencing the number of trapped ions are the choice of matrix material, its crystallisation, the laser intensity, etc. For internal calibration, the parameter C is directly related to the frequency shift of the particular spectrum in question, and

therefore is very accurate. In the case of external calibration, the determined value of *C* is applied to other spectra with different ion abundances. Thus, the space-charge effects will not be accurately compensated and inferior *m/z* accuracy is obtained.

2.2.4 Importance of internal calibration of *m/z* axis of mass spectra

During the analysis of complex samples, such as natural resins high *m/z* accuracy aids in the ion identification process by reducing the number of potential matches. Therefore, it is reasonable to use mass spectra with internally calibrated *m/z* axis.

In case of internal calibration, the *m/z* values of the peaks may originate from (1) the sample, (2) from the matrix compound or (3) from internal standards – compounds that are intentionally added to the sample. [I, 41, 62, 65] The first two methods are convenient: they do not require adding substances to the sample. However, using peaks originating from the resinous materials (chemically complex samples) for internal calibration increases the risk of misinterpretation because it is not reliably known what compounds are present in the sample. Employing the matrix material for the internal calibration of the *m/z* axis of mass spectra is a common practice. [I, II, 62, 66, 67] Unfortunately, the occurrence of the matrix peaks in the mass spectra is not always reproducible, especially when analysing materials that require modified sample preparations. For these reasons, adding internal standards to the sample (or matrix) solution is the most reliable approach for the *m/z* axis calibration of complex materials. [I, 41]

The most popular compounds used as calibration standards in MALDI-MS analysis are peptides and proteins (for example Angiotensin II, Bradykinin fragment 1-7, etc.). [I, II, 41] The *m/z* range of commercially available protein-based calibration standards starts from ca. *m/z* 500 and in the range of *m/z* 500–1000 only few options are available. This is insufficient for the analysis of resinous materials because the most valuable information about the composition is in the range of (roughly) *m/z* 200 to *m/z* 600. [I, 1, 3, 10]

Also, other materials have been used, such as polymers (dendrimers, dendrons, functionalised polyethylene glycol, polymethyl methacrylate, etc.) [68–70], silicone and silicone oil [71] and elemental compounds (sulphur) [72] as calibration standards. The calibration range of polymer and silicone-based standards is about *m/z* 200–1000. The elemental compounds provide a range of polyatomic ions with *m/z* values under *m/z* 500. But the location of these peaks is fixed and the mass range covered by them is too limited at times. All in all, the selection of *m/z* calibration standards in the *m/z* range under *m/z* 1000 is limited.

3. EXPERIMENTAL

3.1 Preparation of calibration standard solutions

3.1.1 Preparation of standard solutions for external calibration [I, II, III]

During the analysis of dammar resin in the positive ion mode the ProteoMass™ Peptide MALDI-MS calibration kit was used (see Table 1). Bradykinin fragment 1–7 and insulin chain B standards were dissolved in 1 ml of a 1:1 mixture of acetonitrile (Sigma-Aldrich) and 0.1% trifluoroacetic acid (Sigma-Aldrich) solution in Milli-Q water (Milli-Q® Advantage A 10, Millipore). Angiotensin II, $P_{14}R$ and ACTH fragment 18–39 were dissolved in 1 ml of 0.1% trifluoroacetic acid solution in Milli-Q water. 10 µl of each of the calibration standard solution was pipetted to a 1.5 ml PCR clean Eppendorf® Safe-Lock tube and 50 µl of DHB solution was added.

Table 1. The calibration standards used for the external calibration of the *m/z* axes of the obtained MALDI-FT-ICR-MS spectra. The calibration standards highlighted with blue text were also used as internal standards during the positive ion mode analysis of dammar and shellac resins (see also Table 5).

No	Compound	Molecular formula	$[M^2+H]^+$ [a]	Amount per vial
ProteoMass™ Peptide MALDI-MS calibration kit (Sigma Aldrich)				
1	Bradykinin fragment 1–7	$C_{35}H_{52}N_{10}O_9$	757.39915	10 nmol
2	Angiotensin II (human)	$C_{50}H_{71}N_{13}O_{12}$	1046.54179	
3	$P_{14}R$ (synthetic peptide)	$C_{76}H_{112}N_{18}O_{16}$	1533.85765	
4	ACTH fragment 18–39 (human)	$C_{112}H_{165}N_{27}O_{36}$	2465.19833	
5	Insulin oxidised B chain (bovine)	$C_{157}H_{232}N_{40}O_{47}S_2$	3494.65077	
ProteoMass™ MALDI calibration kit for LTQ XL and LTQ Hybrids – Normal mass calibration (Sigma Aldrich)				
6	MRFA	$C_{23}H_{37}N_7O_5S$	524.26496	1217 pmol
7	Bradykinin fragment 1–7	$C_{35}H_{52}N_{10}O_9$	757.39915	453 pmol
8	Bradykinin	$C_{50}H_{73}N_{15}O_{11}$	1060.56867	680 pmol
9	Angiotensin I	$C_{62}H_{89}N_{17}O_{14}$	1296.68477	924 pmol
10	Neurotensin	$C_{78}H_{121}N_{21}O_{20}$	1672.91695	667 pmol
11	Renin Substrate	$C_{85}H_{123}N_{21}O_{20}$	1758.93260	868 pmol

[a] The *m/z* value is calculated for the monoisotopic ion.

[2] M denotes the corresponding neutral molecule and this notation is used throughout the study.

Thereafter, the ProteoMass™ MALDI calibration kit for LTQ XL and LTQ Hybrids – normal mass calibration mixture was used (see Table 1). The components of this kit are provided by the manufacturer as a mixture. First, the calibration mixture was reconstituted by adding 58 µl of 20% acetonitrile solution in Milli-Q water to the vial. Thereafter, the solution was incubated at room temperature for 30 minutes. 5 µl of this solution was mixed with 45 µl of the DHB solution.

3.1.2 Preparation of the internal calibration standard solutions [I, II, III]

Preparation of the phosphazene and sulpho-compound solutions [III]

During this study, 15 different phosphazenes yielding cations in the *m/z* range of *m/z* 257–916, and anions of 2 sulphonimides and 2 sulphonyl methanes covering the *m/z* range from *m/z* 410 to *m/z* 978 were tested as internal standards (see Table 2 and Figure 5).

The phosphazenes (in the form of HBF_4 and $HBPh_4$ salts) have been synthesised in our workgroup. [73–78] The sulpho-compounds have been synthesised at DSM Nutritional Products laboratories, Switzerland. [79, 80]

The stock solutions of the phosphazenes and sulpho-compounds were prepared in 1.5 ml Eppendorf® Safe-Lock tubes and sealed with Parafilm M (Pechiney Plastic Packaging). The solutions were stored at 4 ºC.

A few milligrams of the phosphazene salt was dissolved in acetonitrile. For H-P_1(pyrr)$_3$·HBF_4 and 4-Br-C_6H_4-P_1(pyrr)$_3$·$HBPh_4$ a 1:1 mixture of acetonitrile and Milli-Q water was used. The concentrations of the solutions ranged from 0.005 to 0.013 mmol/ml, in the case of H-P_1(pyrr)$_3$·HBF_4 the concentration was 0.040 mmol/ml.

For the preparation of the stock solutions of the sulpho-compounds, a few milligrams of $(CF_3SO_2)_3CH$, $[CF_3(CF_2)_3SO_2]_2NH$ and $[CF_3(CF_2)_3SO_2]NH[CF_3(CF_2)_7SO_2]$ were dissolved in acetonitrile, in the case of $[CF_3(CF_2)_7SO_2]_2CH_2$ isopropanol (Merck) was used as a solvent. The concentrations of the stock solutions were in the range of 0.028 to 0.049 mmol/ml.

The calibration standards were used as mixtures to enable a more convenient sample preparation procedure. The prepared mixtures were diluted 1000 times before adding them to the sample or matrix solutions. During the analysis in the positive ion mode acetonitrile and in the negative ion mode methanol (Sigma-Aldrich) was used for the dilution.

Table 2. Formulas (see Figure 5 for structures) and exact *m/z* values of the cations and anions of the phosphazene salts and sulpho-compounds used for internal calibration. Compounds used in this study are highlighted in blue text.

No	Phosphazene salt[a]	$[M+H]^+$ formula	Exact *m/z*[3]
1	H-P_1(pyrr)$_3$·HBF_4	$C_{12}H_{26}N_4P^+$	257.18896
2	H_2N-P_1(pyrr)$_3$·$HBPh_4$	$C_{12}H_{27}N_5P^+$	272.19986
3	2-Cl-C_6H_4-P_1(dma)$_3$·$HBPh_4$	$C_{12}H_{23}N_4ClP^+$	289.13434
4	Et-P_2(dma)$_5$·$HBPh_4$	$C_{12}H_{36}N_7P_2^+$	340.25019
5	4-MeO-C_6H_4-P_1(pyrr)$_3$·HBF_4	$C_{19}H_{32}N_4OP^+$	363.23082
6	t-Bu-P_2(dma)$_5$·HBF_4	$C_{14}H_{40}N_7P_2^+$	368.28149
7	4-Br-C_6H_4-P_1(pyrr)$_3$·$HBPh_4$	$C_{18}H_{29}N_4BrP^+$	411.13077
8	Ph-P_2(pyrr)$_5$·$HBPh_4$	$C_{26}H_{46}N_7P_2^+$	518.32844
9	2-Cl-C_6H_4-P_2(pyrr)$_5$·$HBPh_4$	$C_{26}H_{45}N_7ClP_2^+$	552.28947
10	4-CF_3-C_6H_4-P_2(pyrr)$_5$·$HBPh_4$	$C_{27}H_{45}N_7F_3P_2^+$	586.31583
11	4-Br-C_6H_4-P_2(pyrr)$_5$·$HBPh_4$	$C_{26}H_{45}N_7BrP_2^+$	596.23896
12	t-Bu-P_4(dma)$_9$·HBF_4	$C_{22}H_{64}N_{13}P_4^+$	634.43526
13	Ph(CH_3)CH-P_4(dma)$_9$·HBF_4	$C_{26}H_{64}N_{13}P_4^+$	682.43526
14	Ph-P_4(pyrr)$_9$·HBF_4	$C_{42}H_{78}N_{13}P_4^+$	888.54481
15	Ph(CH_3)CH-P_4(pyrr)$_9$·HBF_4	$C_{44}H_{82}N_{13}P_4^+$	916.57611
No	**Sulpho-compound**	**$[M-H]^-$ formula**	**Exact *m/z***
16	$(CF_3SO_2)_3CH$	$C_4F_9O_6S_3^-$	410.87188
17	$[CF_3(CF_2)_3SO_2]_2NH$	$C_8F_{18}NO_4S_2^-$	579.89868
18	$[CF_3(CF_2)_3SO_2]NH[CF_3(CF_2)_7SO_2]$	$C_{12}F_{26}NO_4S_2^-$	779.88591
19	$[CF_3(CF_2)_7SO_2]_2CH_2$	$C_{17}HF_{34}O_4S_2^-$	978.87788

[a] For phosphazenes the Schwesinger's [81] nomenclature is used.

[3] Exact *m/z* represents the *m/z* value of the monoisotopic ion.

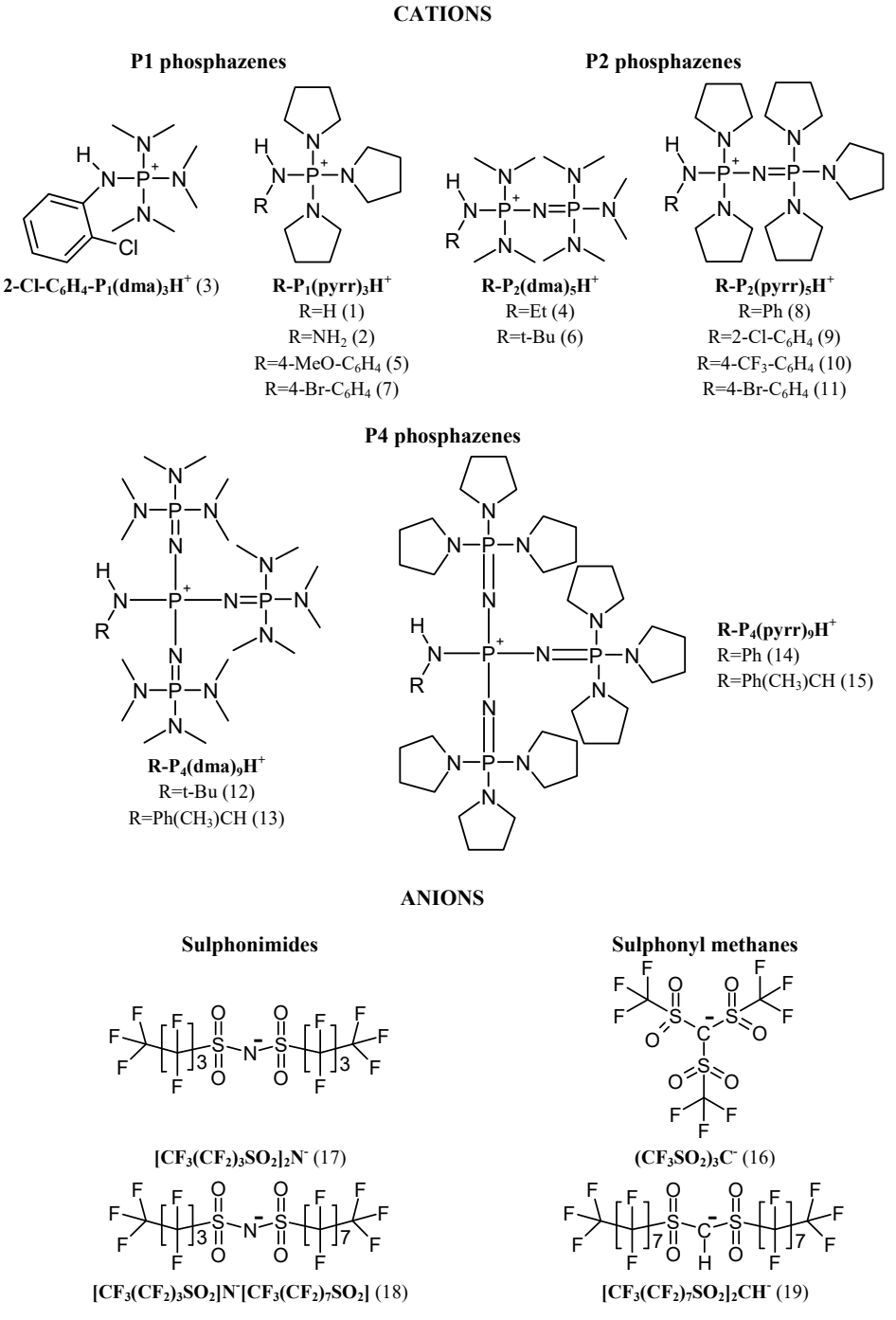

Figure 5. Cation and anion structures of the compounds used for internal calibration (the numbers in parentheses correspond to the numbers in Table 2).

3.2 Preparation of the matrix solutions for MALDI-FT-ICR-MS analysis

For the positive ion mode analysis, DHB was used as a matrix. 150 mg of DHB was mixed with 0.5 ml of acetonitrile and 0.5 ml 0.1% trifluoroacetic acid solution in Milli-Q water. During the analysis of dammar resin, also CHCA was tested as a matrix material. The results obtained were worse compared to DHB: the matrix itself displayed a great number of peaks in the mass spectra (that interfered with the peaks originating from the resin), also the peaks belonging to the resin had lower intensities. Therefore, the analysis of resinous materials in the positive ion mode was continued only with DHB.

For the analysis of dammar resin, a few tens of µl of ACTH fragment 18–39 solution was mixed with a few hundreds of µl of DHB solution. During the ageing of DHB solution, Angiotensin II was added to the matrix solution (concentration in DHB was 1 nmol/ml). In case of colophony resin and the real-life samples analysed in positive ion mode, 0.2 µl of the specific calibration solution of phosphazenes was mixed with 25 µl of the matrix solution (see Table 5 and Table 7).

For the negative ion mode analysis, a novel matrix substance, 2-aminoacridine (Reakhim) was used as a matrix material. 15 mg of 2-AA (recrystallised) was dissolved in 1 ml of methanol. In the case of real-life sample analysis, 15 µl of the matrix solution was mixed with 0.1 µl of the internal calibration solution prior to the next step (see Table 6 and Table 8 for specific compounds).

3.3 Preparation of resin solutions for MALDI-FT-ICR-MS analysis

Table 3 lists general information about all the natural resins analysed during this study.

Table 3. Natural resins analysed during this study.

Resin	Manufacturer/ source	Product code	Type	Description
Dammar	Kremer Pigmente GmbH & Co. KG	60000	Triterpenoid resin	Pale yellow soft resin
Mastic		60050		Yellow soft resin
Sandarac		61000	Diterpenoid resin	Dark yellow semi-soft resin
Colophony (light)		60300		Yellow soft resin
Shellac		60400	Insect resin	Reddish brown resin flakes

3.3.1 Preparation of resins for positive ion mode MALD-FT-ICR-MS analysis

In the framework of this PhD study, dammar resin was the first resin analysed with MALDI-FT-ICR-MS. Therefore, a more comprehensive sample preparation was carried out to study the different solvents and solvent systems for dissolving the resin, and assess the compatibility of different solvents with DHB.

Table 4 lists 10 different solvents or solvent systems that were used for dissolving dammar resin. It also evaluates the capability of the solvents and solvent mixtures to dissolve the resin and their compatibility with DHB. During the study, different volume ratios were tested for the solvent systems and the volume ratio 1:1 was proved to be the most suitable.

6 mg of powdered dammar resin was mixed with 200 µl of the solvent or solvent mixture. In case of solvent mixtures, dichloromethane (Sigma-Aldrich) was added first, followed by the second solvent.

Table 4. The solvents and solvent systems used for dissolving dammar resin.

Solvent system	Solubility of dammar resin	Compatibility with DHB
Dichloromethane	Completely soluble	Very poor
Ethanol	Partly soluble	Good
Acetone (Sigma-Aldrich)	Partly soluble	Good
Toluene (Sigma-Aldrich)	Completely soluble	Very poor
Acetonitrile	Partly soluble	Mediocre
Chloroform (Lach:ner)	Completely soluble	Very poor
Acetone:dichloromethane (1:1)	Almost soluble	Very good
Ethanol:dichloromethane (1:1)	Almost soluble	Very good
Toluene:dichloromethane (1:1)	Completely soluble	Very poor
Acetonitrile:dichloromethane (1:1)	Partly soluble	Poor

For the preparation of shellac resin solution, 5 mg of the resin was dissolved in 200 µl of ethanol (Premium, Estonian Spirit OÜ) and the mixture was sonicated for 10 minutes at 35 ºC. 20 µl of the prepared shellac resin solution was mixed with 10 µl of solution containing equivalent volumes of bradykinin fragment 1–7 and angiotensin II.

In the case of mastic, sandarac, and colophony resins, approximately 10 mg of each of the resins were dissolved in 200 µl of solvent. For mastic and sandarac resins, a 1:1 mixture of dichloromethane:ethanol was used, colophony resin was dissolved in a 1:1 mixture of dichloromethane:acetonitrile.

During the analysis of mastic and sandarac resins, the internal calibration mixture was added to the resin solution: 50 µl of mastic resin's solution was mixed with 1 µl of the calibration solution, the ratio for the analysis of sandarac resin was 50 µl and 0.2 µl, respectively. For the analysis of colophony resin, the

calibration mixture was added to the matrix solution. The latter was done in order to mimic the analysis of real-life samples. The concentration of the internal standards in the resin and matrix solutions was in the range of few pmol/ml. The specific compounds used as internal standards in the positive ion mode analysis of resin samples are presented in Table 5.

Table 5. Internal standards used for the calibration of the *m/z* axes of the positive ion mode mass spectra of natural resins.

Resin	Internal standard	Exact *m/z*
Dammar	DHB	137.02332
	ACTH fragment 18–39	2465.19833
Shellac	DHB	137.02332
	Bradykinin fragment 1–7	757.39915
	Angiotensin II	1046.54179
Mastic	H-$P_1(pyrr)_3 \cdot HBF_4$	257.18896
	Et-$P_2(dma)_5 \cdot HBPh_4$	340.25019
	2-Cl-C_6H_4-$P_2(pyrr)_5 \cdot HBPh_4$	552.28947
	t-Bu-$P_4(dma)_9 \cdot HBF_4$	634.43526
	Ph(CH_3)CH-$P_4(pyrr)_9 \cdot HBF_4$	916.57611
Colophony	H-$P_1(pyrr)_3 \cdot HBF_4$	257.18896
	t-Bu-$P_2(dma)_5 \cdot HBF_4$	368.28149
	Ph-$P_2(pyrr)_5 \cdot HBPh_4$	518.32844
	Ph(CH_3)CH-$P_4(pyrr)_9 \cdot HBF_4$	916.57611
Sandarac	H-$P_1(pyrr)_3 \cdot HBF_4$	257.18896
	t-Bu-$P_2(dma)_5 \cdot HBF_4$	368.28149
	4-Br-C_6H_4-$P_2(pyrr)_5 \cdot HBPh_4$	596.23896
	Ph-$P_4(pyrr)_9 \cdot HBF_4$	888.54481

3.3.2 Preparation of resins for negative ion mode MALDI-FT-ICR-MS analysis

For the analysis of dammar, mastic, sandarac, colophony, and shellac resins in the negative ion mode, 5 mg of each of the resins was dissolved in 200 µl of solvent. For mastic, colophony and sandarac resins, methanol was used; shellac resin was dissolved in ethanol and for dammar resin, a 1:1 mixture of dichloromethane:methanol was used. The solution of shellac resin was also sonicated prior analysis for 10 minutes at 35 °C.

60 µl of the prepared resin solution was mixed with the internal calibration mixture. In Table 6, the compounds used as internal standards for the calibration of the *m/z* axes of the negative ion mode mass spectra are listed. In case of dammar and mastic resins, 1.0–1.2 µl, for colophony and sandarac

resins, 0.4 µl and for shellac resin, 0.3 µl of the internal calibration mixture was added to the sample solution before the analysis. The concentration of the internal standards added to the sample solution was in the range of a few dozen pmol/ml.

Table 6. Internal standards used for the calibration of the *m/z* axes of the negative ion mode mass spectra of different resinous samples.

Resin	Internal standard	Exact *m/z*
Mastic	2-AA	193.07712
	$[CF_3(CF_2)_3SO_2]_2NH$	579.89868
	$[CF_3(CF_2)_7SO_2]_2CH_2$	978.87788
Dammar, colophony, sandarac	2-AA	193.07712
	$(CF_3SO_2)_3CH$	410.87188
	$[CF_3(CF_2)_3SO_2]_2NH$	579.89868
	$[CF_3(CF_2)_3SO_2]NH[CF_3(CF_2)_7SO_2]$	779.88591
Shellac	2-AA	193.07712
	$(CF_3SO_2)_3CH$	410.87188
	$[CF_3(CF_2)_3SO_2]_2NH$	579.89868
	$[CF_3(CF_2)_3SO_2]NH[CF_3(CF_2)_7SO_2]$	779.88591
	$[CF_3(CF_2)_7SO_2]_2CH_2$	978.87788

3.4 Preparation of real-life samples for MALDI-FT-ICR-MS analysis

During this study, three real-life resinous samples were analysed with the modified MALDI-FT-ICR-MS methodology:

- the varnish sample from a 19th century drop-leaf sewing table (from Estonian National Museum);
- the sample of a resinous material obtained from the wreck of an unknown 16th century ship (from Estonian Maritime Museum);
- the varnish sample from the late 19th century painting “Dream” by Wilhelm Kotarbiński (1848–1921) (from Narva Museum, Estonia).

All real-life samples were dissolved in dichloromethane:ethanol (1:1) mixture. In case of the sewing table’s varnish sample, 0.15 mg of sample was dissolved in 40 µl of solvent mixture; 3 mg of the resinous material found on the 16th century shipwreck was dissolved in 100 µl of solvent mixture; and for the varnish sample from the painting “Dream”, approximately 0.15 mg of the sample was dissolved in 20 µl of solvent mixture.

In the case of real-life samples, the calibration standards were added to the matrix solution to minimise the sample consumption and to make the sample

preparation stage more convenient. Table 7 and Table 8 give an overview of the internal standards used for the adjusting of the *m/z* axes of the corresponding mass spectra.

Table 7. Internal standards used for the calibration of the *m/z* axes of the positive ion mode mass spectra of different real-life samples.

Sample	Internal standard	Exact *m/z*
Varnish sample from the 19th century drop-leaf sewing table	H-P_1(pyrr)$_3$·HBF_4	257.18896
	Et-P_2(dma)$_5$·$HBPh_4$	340.25019
	Ph(CH_3)CH-P_4(dma)$_9$·HBF_4	682.43526
	Ph(CH_3)CH-P_4(pyrr)$_9$·HBF_4	916.57611
Resinous material from the unknown ship wreck from the 16th century	DHB	187.03897
	H-P_1(pyrr)$_3$·HBF_4	257.18896
	Et-P_2(dma)$_5$·$HBPh_4$	340.25019
	Ph(CH_3)CH-P_4(dma)$_9$·HBF_4	682.43526
	Ph(CH_3)CH-P_4(pyrr)$_9$·HBF_4	916.57611
Varnish sample from the painting "Dream" by W. Kotarbiński	t-Bu-P_2(dma)$_5$·HBF_4	368.28149
	Ph-P_2(pyrr)$_5$·$HBPh_4$	518.32844
	Ph(CH_3)CH-P_4(dma)$_9$·HBF_4	682.43526

Table 8. Internal standards used for the calibration of the *m/z* axes of the negative ion mode mass spectra of different real-life samples.

Sample	Internal standard	Exact *m/z*
Varnish sample from the 19th century drop-leaf sewing table	2-AA	193.07712
	$[CF_3(CF_2)_3SO_2]_2NH$	579.89868
	$[CF_3(CF_2)_3SO_2]NH[CF_3(CF_2)_7SO_2]$	779.88591
	$[CF_3(CF_2)_7SO_2]_2CH_2$	978.87788
Resinous material from the unknown 16th century ship wreck	2-AA	193.07712
	$[CF_3(CF_2)_3SO_2]_2NH$	579.89868
	$[CF_3(CF_2)_7SO_2]_2CH_2$	978.87788

3.5 MALDI-FT-ICR-MS analysis

3.5.1 The instrument

MALDI mass spectra were obtained with Varian 930 FT-ICR-MS that uses an intermittent pressure (10^{-3} mbar) MALDI ion source, New Wave Orion 50083 Nd:YAG laser (355 nm) and a 7 T superconducting magnet for the generation and detection of ions. The magnet is also used by an ESI cart; thus, it is a dual instrument.

Typical pressure in the analyser region is $n \cdot 10^{-10}$ mbar (usually $n \leq 4$) and during the introduction of cooling gas (nitrogen) it increases to the $n \cdot 10^{-8} – n \cdot 10^{-7}$ mbar range for a short time period. The pressure of the instrument is dependent on the cleanness of the vacuum system. As this instrument is also used for the gas-phase basicity and acidity measurements of superbases and superacids, the system needs thorough bake-out before a MALDI-FT-ICR-MS measurement: the instrument is "baked" before measurement sessions at alternating temperatures of 150 ºC and 100 ºC in repeated cycles (lasting few hours at a time). Also, continuous heating at 100–110 ºC (overnight) is routinely applied. Bake-out temperatures above 150 °C cannot be used with this instrument, because the signal preamplifier is located in the vicinity of the ICR cell.

The mass spectra were acquired in the direct broadband mode, the ADC rate was 4 MHz and the transient length 524 ms. For the analysis of dammar resin in positive ion mode, the mass spectra were accumulated on 7 laser shots. Afterwards, the number of laser shots was lowered to 5 because this was found to be sufficient. The laser intensity varied from 33–55%, depending greatly on the specific sample, used solvents and thus, on the crystals formed during spotting. Ion guide amplitude was varied in the range of 120–200 V(b-p) and the corresponding range for arbitrary waveform amplitude was 125–200 V(b-p). These parameters were adjusted according to the specific sample, but they were also influenced by the varying cleanliness of the system (see above). These changing conditions of the FT-ICR-MS system increased the need for internal calibration even more.

Varian OMEGA 9.1.21 software was used to operate the instrument and process the mass spectra.

3.5.2 Spotting of the sample solutions on the MALDI target plate

Applied Biosystems stainless steel 198 sample spot MALDI plate was used for the spotting of the samples. At the start of each experiment day (and during the day if necessary) the MALDI plate was cleaned with methanol, warm tap water and detergent, Milli-Q water, acetone, and acetonitrile. Occasionally the MALDI plate was polished with polishing paste (Brasso).

For the **analysis of dammar resin in the positive ion mode**, a 0.7 µl drop of DHB solution was spotted on the MALDI plate and the solvent was allowed to evaporate at ambient pressure and temperature. Thereafter, 1 µl of the sample solution was added on the solid matrix crystals. The DHB crystals partially dissolved in the sample solution and crystallised again, now, together with the sample, resulting in widely spread spots with crystals of different sizes.

During the **analysis of shellac resin in the positive ion mode**, the same spotting technique was applied as in the dammar resin analysis. However, the amount of resin solution (with calibration standards) spotted on the DHB crystals was 1.4 µl. The spots spread extensively (to about 2 mm in diameter) due to the

content of ethanol. The formed crystals were small and they were distributed more evenly compared to the spots obtained for dammar resin.

For the **analysis of mastic, sandarac and colophony resins in the positive ion mode**, a new spotting technique was introduced: 0.7 µl of sample solution was mixed on the MALDI plate with the same volume of DHB solution and then dried under vacuum conditions. This technique enables to obtain sample spots with evenly distributed small crystals, but the spots did not spread so extensively.

During the **negative ion mode analysis**, the resin solutions were mixed with the solution of new matrix compound, 2-AA, before the spotting. In case of dammar, mastic and shellac resins and real-life samples, the ratio of sample solution to matrix solution was 1:1; for colophony and sandarac resins, the ratio of sample and matrix solutions was 2:1. 0.7 µl of this mixture was then spotted on the MALDI plate. The solvents rapidly evaporated under ambient conditions; the dried spots consisted of very small crystals that were evenly distributed.

4. RESULTS AND DISCUSSION

This PhD study focuses on the development of MALDI-FT-ICR-MS methodology for the analysis of natural resins. The development of the methodology includes:

- finding and testing of matrix compounds suitable for the analysis of resinous materials in the positive and negative ion modes,
- expanding the selection of positive and negative ion mode internal calibration standards for the region under *m/z* 1000,
- modifying the sample preparation procedure and set of parameters suitable for the analysis of different type and age of resinous materials.

The novel methodology was applied for the analysis of three real-life resinous samples.

The determination of chemical composition of the analysed resins and real-life resinous samples is only briefly discussed during this study.

The results of this PhD thesis are discussed in chronological order to visualise the development of the MALDI-FT-ICR-MS methodology for the analysis of resinous materials.

4.1 Analysis of dammar resin with MALDI-FT-ICR-MS [I]

The objective of this stage of the study was to evaluate the capabilities of MALDI-FT-ICR mass spectrometry in the analysis of natural resins. Dammar resin was chosen as the test object for this analysis because it is the basis for one of the most popular picture varnishes – dammar varnish. At the same time, dammar resin is a good representative of terpenoid resins – the resin consists of a number of different triterpenoids that have similar structures (see Figure 1).

At this stage of the study, the sample preparation procedure was developed for the analysis of natural resins. During this, numerous solvents and solvent systems were tested in order to find one that is compatible with dammar resin and DHB. Also, a preliminary set of parameters was found that enabled analysing resinous materials in a broad *m/z* range of *m/z* 100–2500.

The study also incorporated APCI-FT-ICR-MS for the analysis of dammar resin, the results obtained with this method are presented in publication I.

4.1.1 Solvents and solvent mixtures suitable for the analysis of dammar resin

One of the aims of the study was to find a solvent or solvent system that is compatible with the chosen matrix material (DHB) but at the same time, is suitable for dissolving dammar resin as well.

As described above, dammar resin is fully soluble in organic solvents like toluene and dichloromethane, but only the monomeric fraction of the resin can be dissolved in alcohols. The solubility of the resin (and the varnish) decreases with ageing. In order to obtain the maximum amount of information from the resin during the MALDI-FT-ICR-MS analysis, a good knowledge about the suitable solvent or solvent system is necessary.

In total, 6 solvents and 4 two-component solvent mixtures were tested during this study. A solvent or solvent system is suitable if it (1) readily dissolves the sample and the matrix, (2) is volatile, (3) leaves small matrix crystals upon evaporation, and (4) supports the co-crystallisation of the sample with the matrix.

Table 4 (in section 3.3.1) lists all the solvents and solvent systems that were used for the dissolving of dammar resin. As can be seen from Table 4, dichloromethane, toluene, chloroform and the mixture of toluene:dichloromethane (1:1) completely dissolve dammar resin. However, these solvents are not compatible with DHB. The crystals formed upon the evaporation of these solvents were large and the sample was not incorporated into the crystals, therefore, the matrix and the analyte did not co-crystallise very well. No good quality mass spectra from the resin were obtained with these solvents.

Acetonitrile is a suitable solvent for DHB but it only partly dissolves dammar resin. Adding dichloromethane to acetonitrile does not improve the situation because the formed DHB crystals are still quite big and the sample distribution is poor.

Acetone and ethanol only partially dissolve dammar resin but combined with dichloromethane the solubility of the resin increases. The slightly hazy solution obtained by dissolving the resin in a 1:1 mixture of dichloromethane: acetone or dichloromethane:ethanol was also compatible with DHB. The crystals formed upon evaporation of these solvents were very small and the sample was evenly distributed on the spot (no separate areas of sample solution residue and matrix crystals were noticed). Thus, dammar resin dissolved in dichloromethane: acetone or dichloromethane:ethanol gave mass spectra with equally good quality.

The mass spectrum chosen for further discussion was acquired using the dichloromethane:ethanol solvent system (see Figure 6).

4.1.2 Analysis of MALDI-FT-ICR-MS spectrum of dammar resin

The high-resolution positive ion mode mass spectrum of dammar resin obtained with MALDI-FT-ICR-MS is presented in Figure 6. Table 9 presents the summarised ion assignments for some of the more prominent peaks present in the first cluster along with the corresponding *m/z* errors in the case of internal and external calibration. A more comprehensive assignment of peaks present in all the clusters of the mass spectrum of dammar resin and the corresponding *m/z* errors for internal and external calibration can be found in Table A1[4] in Appendix 1.

[4] The tables and one figure in the Appendices are labelled with A and a number.

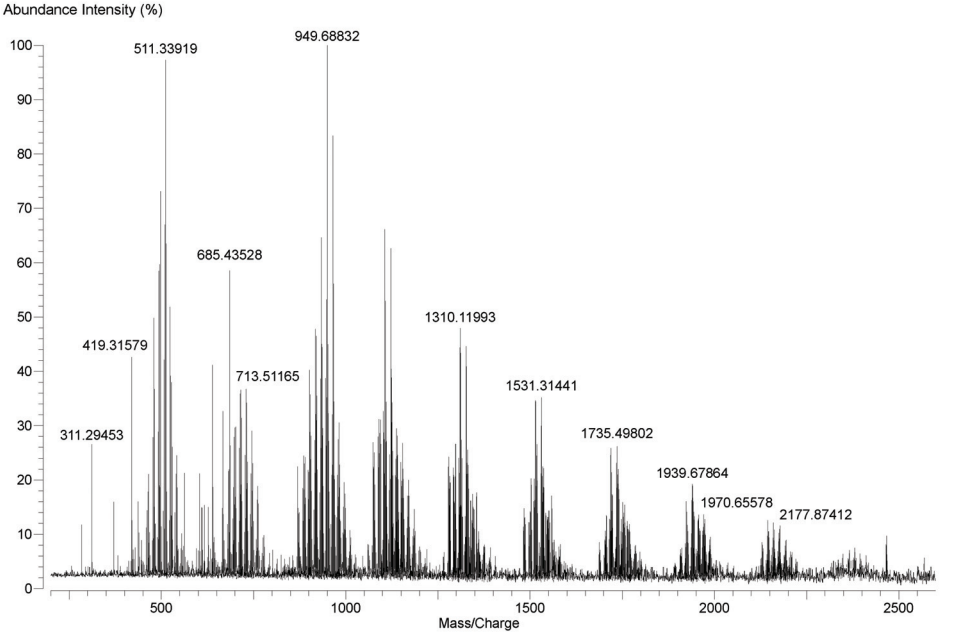

Figure 6. The MALDI-FT-ICR-MS spectrum of dammar resin (with internally calibrated *m/z* axis).

Table 9. Summary of the assignment of the more characteristic peaks in the first cluster of the MALDI-FT-ICR-MS spectrum of dammar resin.

Cation formula	Internal calibration		External calibration	
	Measured *m/z*	*m/z* error[5](ppm)	Measured *m/z*	*m/z* error (ppm)
$C_{29}H_{43}O_2^+$	423.32545	–0.73	423.32766	4.49
$C_{29}H_{46}O_3Na^+$	465.33398	0.13	465.33664	5.84
$C_{29}H_{44}O_4Na^+$	479.31346	0.57	479.31628	6.46
$C_{29}H_{46}O_5Na^+$	497.32385	0.20	497.32688	6.29
$C_{30}H_{50}O_4Na^+$	497.36011	–0.04	497.36314	6.05
$C_{29}H_{44}O_6Na^+$	511.30292	–0.18	511.30613	6.09
$C_{30}H_{48}O_5Na^+$	511.33919	–0.41	511.34240	5.86
$C_{30}H_{44}O_6Na^+$	523.30321	0.38	523.30656	6.79
$C_{31}H_{48}O_5Na^+$	523.34013	1.39	523.34348	7.80
$C_{30}H_{46}O_7Na^+$	541.31406	0.89	541.31765	7.51
$C_{30}H_{44}O_8Na^+$	555.29330	0.83	555.29707	7.61

[5] The *m/z* error is calculated as follows: $\frac{((m/z)_{measured}-(m/z)_{exact})\cdot 1000000}{(m/z)_{exact}}$.

The peaks assigned in the mass spectrum of dammar resin correspond mainly to sodium adducts of compounds originating from terpenoids, also, some protonated compounds of dammar resin were detected (see Table 9 and for more information Table A1 in Appendix 1). The high number of sodium adducts is related to the fact that most of the components of dammar resin are oxygen bases that preferably interact with alkali metal cations via the charge-charge attraction mechanism. [82] Thus, ion formation with the addition of alkaline metal cations is favoured over the formation of covalent bond that is characteristic to protonation. This in turn means that in the MALDI-FT-ICR-MS spectrum of dammar resin compounds with less than two oxygen atoms (compounds with low polarity) are rarely detectable. That is because the formation of sodium adducts in case of oxygen compounds requires at least two oxygen atoms in the molecule. [83]

The MALDI-FT-ICR-MS spectrum of dammar resin consists of 9 clusters of peaks (in the *m/z* range of 400–2200). The steps between the clusters are approximately 204 Daltons (Da). This mass corresponds to the sesquiterpene cadinene ($C_{15}H_{24}$) – the compound identified as the backbone of the polymeric fraction in dammar resin. [10, 35, 84] It is possible to identify a series of peaks across the clusters that have a *m/z* difference corresponding to this compound (see Table 10).

All the clusters present in the mass spectrum of dammar resin are composed of sub-clusters that correspond to oxidation products of the terpenes. Figure 7 presents the first cluster of the MALDI-FT-ICR-MS spectrum of dammar resin; it also illustrates the basis of the formation of sub-clusters. The attachment of an oxygen atom results in a mass increment of approximately 16 Da. Oxidation is often accompanied by simultaneous loss of two or a multiple of two hydrogen atoms (e.g. allylic oxidation or oxidation of an alcohol to acid [11]).

The majority of the peaks assigned in the positive ion mode MALDI-FT-ICR mass spectrum of dammar resin correspond to terpenoid compounds with the C_{30} skeleton. With only single-stage mass spectrometry (i.e. without tandem mass spectrometry) it is impossible to distinguish compounds that share the same elemental composition, e.g. triterpenoids, such as ursonic and oleanonic acid ($C_{30}H_{46}O_3$), ursonic and oleanonic aldehyde ($C_{30}H_{46}O_2$), ursolic and oleanolic acid ($C_{30}H_{48}O_3$), etc. (see Figure 1).

In addition to the compounds with the C_{30} skeleton, also compounds containing 27, 28, 29 and 31 carbon atoms were detected. The compounds with different number of carbon atoms shared the same nominal *m/z* value and could be assigned (and identified) only because of the good resolution of the FT-ICR-MS instrument (see Figure 8a). The C_{29} compounds were identified as derivatives of nor-amyrone and C_{31} compounds were assigned as derivatives of dammarenolic acid methyl ester (see Figure 1). [35, 85, 86] Seldom, compounds with C_{28} and C_{27} skeletons were detected in the mass spectrum of dammar resin. These compounds most probably correspond to additional demethylated (“nor”) derivatives of the triterpenoids.

Table 10. Series of peaks identified in the MALDI-FT-ICR-MS spectrum of dammar resin displaying the *m/z* differences that correspond to $C_{15}H_{24}$. In the first row, the measured *m/z* value is presented (highlighted in bold), the second row displays the *m/z* error (in ppm) and the third row presents the ion formula assigned to the peak.

Cluster 1	Cluster 2	Cluster 3	Cluster 4	Cluster 5	Cluster 6	Cluster 7	Cluster 8	Cluster 9
No peak	**697.55345** 0.62 $C_{46}H_{74}O_3Na^+$	**901.74020** –0.69 $C_{61}H_{98}O_3Na^+$	**1105.92420** –4.0 $C_{76}H_{122}O_3Na^+$	**1310.11993** 2.68 $C_{91}H_{146}O_3Na^+$	**1514.30840** 2.76 $C_{106}H_{170}O_3Na^+$	**1718.49489** 1.67 $C_{121}H_{194}O_3Na^+$	**1922.68081** 0.51 $C_{136}H_{218}O_3Na^+$	No peak
497.36011 –0.04 $C_{30}H_{50}O_4Na^+$	**701.54812** 0.27 $C_{45}H_{74}O_4Na^+$	**905.73512** –0.67 $C_{60}H_{98}O_4Na^+$	**1109.92010** –3.09 $C_{75}H_{122}O_4Na^+$	**1314.11233** 0.76 $C_{90}H_{146}O_4Na^+$	**1518.30326** 2.72 $C_{105}H_{170}O_4Na^+$	**1722.49026** 1.93 $C_{120}H_{194}O_4Na^+$	**1926.67784** 1.61 $C_{135}H_{218}O_4Na^+$	No peak
513.35497 –0.16 $C_{30}H_{50}O_5Na^+$	**717.54447** 2.26 $C_{45}H_{74}O_5Na^+$	**921.72685** –4.12 $C_{60}H_{98}O_5Na^+$	**1125.91515** –2.93 $C_{75}H_{122}O_5Na^+$	**1330.10484** –1.06 $C_{90}H_{146}O_5Na^+$	**1534.29470** 0.42 $C_{105}H_{170}O_5Na^+$	**1738.47991** –1.12 $C_{120}H_{194}O_5Na^+$	**1942.67044** 0.41 $C_{135}H_{218}O_5Na^+$	**2146.85925** 0.84 $C_{150}H_{242}O_5Na^+$
529.35021 0.47 $C_{30}H_{50}O_6Na^+$	**733.53844** 0.93 $C_{45}H_{74}O_6Na^+$	**937.72675** 1.27 $C_{60}H_{98}O_6Na^+$	**1141.91495** 1.39 $C_{75}H_{122}O_6Na^+$	**1346.10110** –0.04 $C_{90}H_{146}O_6Na^+$	**1550.28772** –0.80 $C_{105}H_{170}O_6Na^+$	**1754.47780** 0.59 $C_{120}H_{194}O_6Na^+$	**1958.66098** –1.83 $C_{135}H_{218}O_6Na^+$	No peak

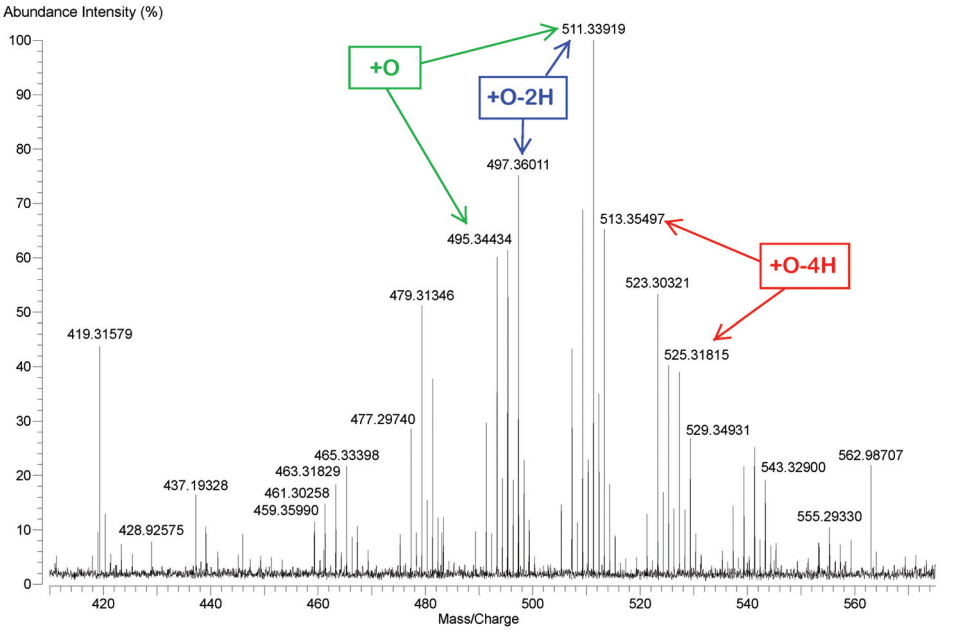

Figure 7. The first cluster of peaks in the MALDI-FT-ICR-MS spectrum of dammar resin.

During the analysis of dammar resin in the positive ion mode, also the peaks detected in the higher clusters were assigned (the *m/z* range of 665–2200; clusters 2 to 9). The peaks present in these clusters are related to the polymeric/ oligomeric fraction of dammar resin. According to literature, these could be the polymerisation and condensation products of cadinene and its oxidation products. [10, 35] Based on the analysis of the mass spectra obtained during this study this is indeed fully possible, however, other compounds are also not ruled out. E.g. in the 3rd cluster, the peaks can also belong to dimers of the triterpenoid compounds. Following this pattern, the 5th cluster in the MALDI-FT-ICR-MS spectrum of dammar resin can contain trimers, the 7th cluster tetramers (dimer + dimer) and the 9th cluster pentamers. So, the "cadinene hypothesis" can conditionally be also so called the "x-mer hypothesis".

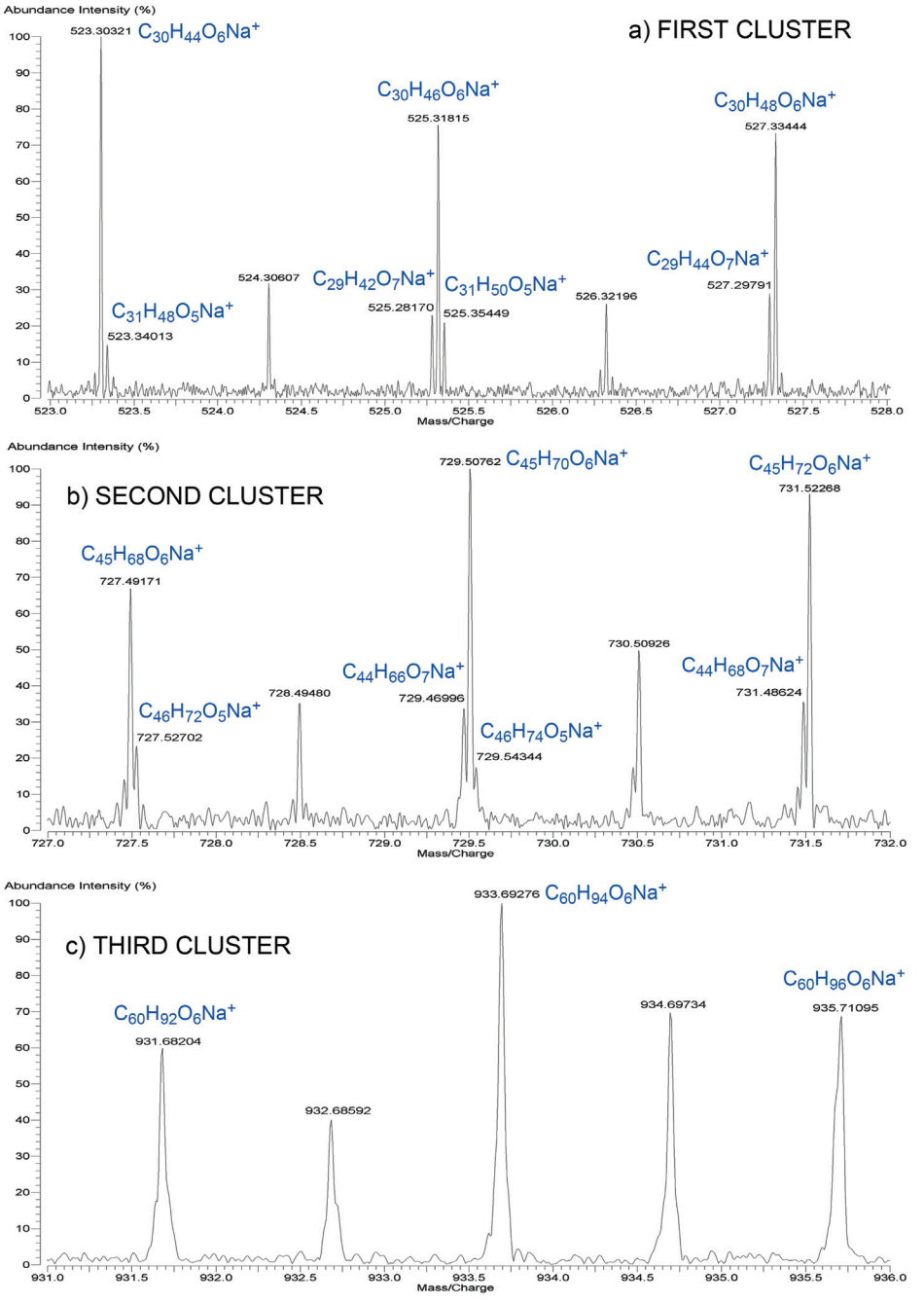

Figure 8. The decrease in resolving power illustrated by a selection of peaks present in the a) first, b) second and c) third cluster of the mass spectrum of dammar resin.

The good resolution obtained in the 1st cluster was also observed in the 2nd cluster of the MALDI-FT-ICR-MS spectrum of dammar resin. As Figure 8b demonstrates, the resolving power in the 2nd cluster is still sufficient to separate peaks that share the same nominal *m/z* value. E.g. three peaks that share the nominal *m/z* of 729 are assigned as $C_{44}H_{66}O_7Na^+$, $C_{45}H_{70}O_6Na^+$ and $C_{46}H_{74}O_5Na^+$ (corresponding to $C_{29}H_{42}O_7Na^+$+$C_{15}H_{24}$, $C_{30}H_{46}O_6Na^+$+$C_{15}H_{24}$, $C_{31}H_{50}O_5Na^+$+ $C_{15}H_{24}$, respectively). However, starting from the 3rd cluster, the peaks with the same nominal *m/z* value start to overlap due to loss of resolving power at higher *m/z* values and thus, only peaks that correspond to C_{60} compounds are detected (related to C_{30} triterpenoids+2($C_{15}H_{24}$)). The decrease in resolving power is also the reason for the fact that many *m/z* values in the 3rd cluster had to be adjusted manually (see Table A1 in Appendix 1).

The *m/z* accuracy for all the assigned peaks in the mass spectrum of dammar resin was also assessed during this stage of the study. In the mass spectrum with externally calibrated *m/z* axis, the *m/z* errors ranged from 3.5 ppm to 30.8 ppm (see Table A1 in Appendix 1). The corresponding range obtained for the peaks in the mass spectrum of dammar resin with internally calibrated *m/z* axis was –8.42 ppm to 9.89 ppm (see Table A1 in Appendix 1). As expected, internal calibration lowered the *m/z* errors but they were still on the higher side. However, it was noticed that the *m/z* errors were generally lower for peaks that were closer to peaks corresponding to the calibration compounds (see Table 5) – in the first and last third of the mass spectrum.

4.1.3 Main conclusions

As a result of this study, a customised preliminary methodology for the analysis of resinous materials with MALDI-FT-ICR-MS was developed. In the sample preparation stage, numerous solvents and solvent mixtures were tested and the most suitable was selected. The testing of different solvents provided reference for the upcoming investigations as well: the most suitable solvent systems for DHB – dichloromethane:ethanol is frequently used in the future stages of the study.

The results obtained during the analysis of dammar resin demonstrate well the capability of MALDI-FT-ICR-MS in positive ion mode to handle such complex and problematic materials. The MALDI-FT-ICR-MS method enabled to obtain a high number of *m/z* values corresponding to the resin that can be used as reference material during the analysis of resinous samples with unknown composition. In addition, the method provided information about the oxidation, polymerisation and oligomerisation, also about the (de)hydrogenation, and (de)methylation of dammar resin compounds.

Although, the method enabled to detect ions of the resin compounds in a wide *m/z* range (*m/z* 400–2200), it was concluded that restricting the *m/z* region up to *m/z* 1000 is reasonable. The region of *m/z* 100–1000 is suitable for the analysis of resinous materials because (1) it is possible to obtain information

about the original components and polymeric fraction of the resin, (2) the resolution of the MALDI-FT-ICR-MS instrument is sufficient for resolving peaks sharing the same nominal *m/z* value.

One of the problems encountered during this stage of the study was poor *m/z* accuracy in the mass spectrum with internally calibrated *m/z* axis. With high probability, the main reason for this was the low number of calibration peaks. Thus, in order to obtain better *m/z* accuracy, a higher number of calibration peaks are necessary.

During the analysis of dammar resin, the question about the durability of the matrix solution arose. It is generally recommended that a new DHB solution should be prepared on a weekly basis. During this work, the DHB solution was used for a considerably longer period of time (approximately 6 months).

Therefore, it was decided to examine the behaviour of DHB solution during long-term usage, and observe, if any changes occur during this period and whether these changes can affect the analysis.

4.2 DHB as matrix material in the analysis of resinous materials [II]

The aim of this stage of the work was to study the behaviour of the DHB solution during long term storage/usage and demonstrate if and how the ageing of the DHB solution affects the analysis of resinous samples. As an additional value, a thorough interpretation of peaks present in the mass spectra obtained from deposited DHB was carried out. This, in turn, expanded the number of peaks originating from DHB that can potentially be used for internal calibration of the *m/z* axis of MALDI-MS spectra.

4.2.1 Monitoring the ageing of the DHB solution with MALDI-FT-ICR-MS

The ageing of DHB solution was monitored during one year with MALDI-FT-ICR-MS in positive ion mode. The capabilities of the aged DHB solution to act as a matrix material were assessed with the analysis of shellac resin.

In addition, ATR-FT-IR spectroscopy, ESI-FT-ICR-MS and ^{1}H NMR analysis were used to gain information about the ageing of DHB solution. These results are described in more detail in publication II.

The positive ion mode MALDI-FT-ICR mass spectrum of DHB obtained from the fresh solution is presented in Figure 9a, the mass spectrum obtained from the one year old DHB solution is presented in Figure 9b. The comprehensive interpretation of the DHB mass spectra is presented in Table 11. The mass spectra corresponding to the DHB solution aged for 1 month, 2 months, 4.5 months and 6 months are presented in Figure S2 in the Supporting Information of publication II.

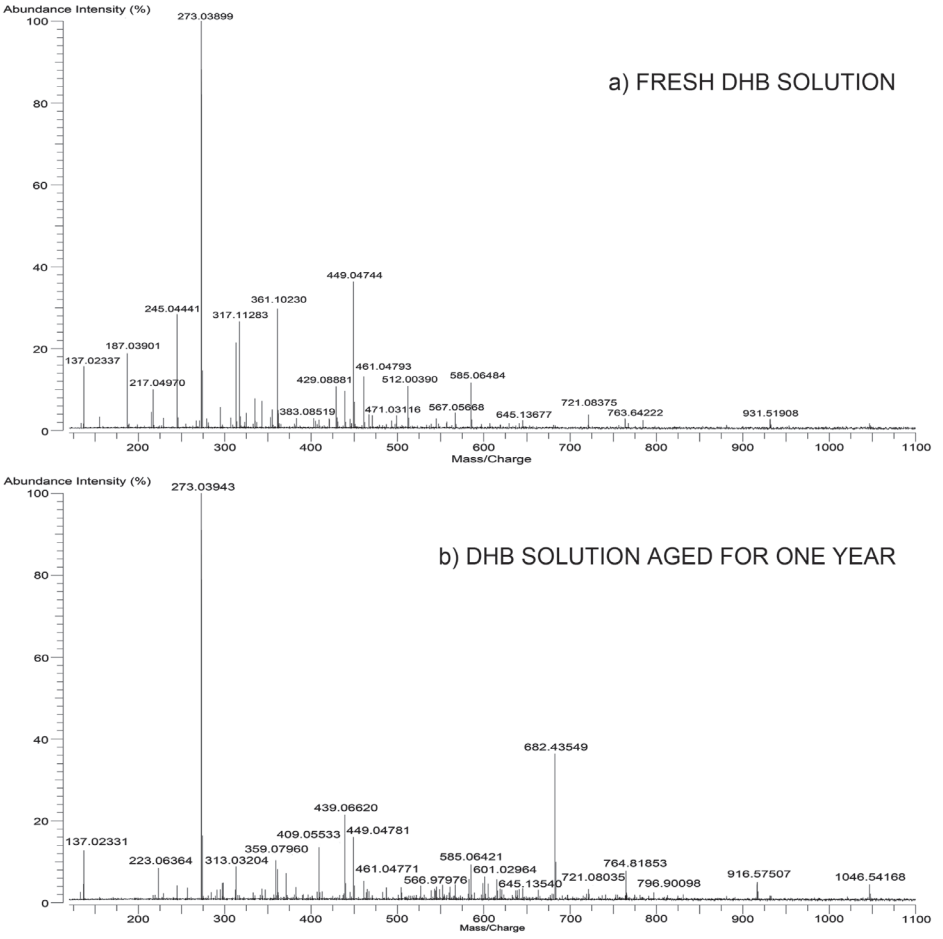

Figure 9. Comparison of MALDI-FT-ICR-MS spectra obtained from the a) fresh DHB solution and b) DHB solution aged for one year.

Peaks detected in the mass spectra obtained from the DHB solution during its ageing correspond mostly to protonated ions or sodium adducts of DHB (with possibly some lost fragments, e.g. H_2O or CO) that contain up to 5 DHB units (see Table 11). [47] Also, ions formed during the addition of two Na^+ cations with the simultaneous loss of H^+, and Al^+ adducts were occasionally detected in the measured mass spectra but these peaks had usually very low intensities. Salts containing sodium, aluminium, etc. were not intentionally added to any of the solutions. However, e.g. sodium is a common element and is present in natural samples, also in solutions that are in contact with glassware, at low levels. [83, 87]

Table 11. Interpretation of the mass spectra obtained from the DHB solution during the one-year ageing period. References are given for peaks that are reported in the literature. [a]

Cation formula	Ion formula	Exact *m/z*	Measured *m/z* and *m/z* error (ppm)	Peak present (months)					*m/z* error (ppm) during ageing
			Fresh DHB	1	2	4.5	6	12	
$C_7H_5O_3^+$	$[DHB\text{-}H_2O+H]^+$	137.02332 [46, 48, 57, 62]	137.02337 0.37	X	X	X	X	X	–0.07...0.15
$C_7H_7O_4^+$	$[DHB+H]^+$	155.03388 [46, 48, 57, 62]	155.03389 0.04						–
$C_7H_4O_3Na^+$	$[DHB\text{-}H_2O+Na]^+$	159.00526	159.00514 –0.78						–
$C_{11}H_7O_3^+$	$[2DHB\text{-}3CO\text{-}2H_2O\text{-}2H+H]^+$	187.03897	187.03901 0.22	X	X				0.06…3.48
$C_{12}H_7O_4^+$	$[2DHB\text{-}2H_2O\text{-}2CO\text{-}H]^+$	215.03388	215.03391 0.12	X					0.54
$C_{12}H_9O_4^+$	$[2DHB\text{-}2H_2O\text{-}2CO+H]^+$	217.04953	217.04970 0.76	X	X			X	–0.02...3.18
$C_{13}H_9O_5^+$	$[2DHB\text{-}2H_2O\text{-}CO+H]^+$	245.04445	245.04441 –0.16	X	X	X	X	X	–0.57...1.43
$C_{14}H_7O_6^+$	$[2DHB\text{-}2H_2O\text{-}H]^+$	271.02371	271.02424 1.94	X					0.65
$C_{14}H_9O_6^+$	$[2DHB\text{-}2H_2O+H]^+$	273.03936 [46, 48, 62]	273.03899 –1.37	X	X	X	X	X	–0.86...0.24
$C_{14}H_8O_6Na^+$	$[2DHB\text{-}2H_2O+Na]^+$	295.02131	295.02113 –0.60	X	X			X	0.28...1.23
$C_{14}H_{10}O_7Na^+$	$[2DHB\text{-}H_2O+Na]^+$	313.03187	313.03162 –0.81	X	X	X		X	–0.23...1.43
$C_{14}H_7O_6Na_2^+$	$[2DHB\text{-}2H_2O\text{-}H+2Na]^+$	317.00325	317.00380 1.72	X	X				0.65...3.68
$C_{18}H_{11}O_6^+$	$[3DHB\text{-}3H_2O\text{-}3CO\text{-}H]^+$	323.05501	323.05536 1.07						–
$C_{18}H_{13}O_6^+$	$[3DHB\text{-}3H_2O\text{-}3CO+H]^+$	325.07066	325.07097 0.94						–
$C_{14}H_{10}O_8Al^+$	$[2DHB\text{-}2H\text{-}Al]^+$	333.01856	333.01813 –1.29		X		X	X	0.09…3.99
$C_{14}H_9O_7Na_2^+$	$[2DHB\text{-}H_2O\text{-}H+2Na]^+$	335.01382	335.01417 1.05	X	X	X			0.36...1.02
$C_{20}H_{12}O_8Na^+$	$[3DHB\text{-}3H_2O\text{-}CO+Na]^+$	403.04244	403.04360 2.88	X	X				0.43...1.72
$C_{21}H_{11}O_9^+$	$[3DHB\text{-}3H_2O\text{-}H]^+$	407.03976					X	X	–0.61...0.72
$C_{21}H_{13}O_9^+$	$[3DHB\text{-}3H_2O+H]^+$	409.05541 [48, 57]	409.05665 3.04	X	X	X	X	X	–0.19...3.40

Table 11. Continued

Cation formula	Ion formula	Exact *m/z*	Measured *m/z* and *m/z* error (ppm)	Peak present (months)					*m/z* error (ppm) during ageing
			Fresh DHB	1	2	4.5	6	12	
$C_{20}H_{14}O_9Na^+$	$[3DHB\text{-}2H_2O\text{-}CO+Na]^+$	421.05300	421.05393 2.20	X					–0.51
$C_{21}H_{14}O_{10}Na^+$	$[3DHB\text{-}2H_2O+Na]^+$	449.04792 [47]	449.04744 –1.06	X	X	X	X	X	–0.24...0.99
$C_{21}H_{13}O_{10}Na_2^+$	$[3DHB\text{-}2H_2O\text{-}H+2Na]^+$	471.02986	471.03116 2.75	X	X	X			–0.71...2.78
$C_{28}H_{18}O_{13}Na^+$	$[4DHB\text{-}3H_2O+Na]^+$	585.06396	585.06484 1.50	X	X	X	X	X	0.08...0.48
$C_{28}H_{17}O_{13}Na_2^+$	$[4DHB\text{-}3H_2O\text{-}H+2Na]^+$	607.04591		X	X	X			–0.55...1.90
$C_{35}H_{22}O_{16}Na^+$	$[5DHB\text{-}4H_2O+Na]^+$	721.08001		X	X	X	X	X	–0.59...1.05

[a] Molecular formula of DHB: $C_7H_6O_4$.
"X" marks the peaks present in the mass spectra measured from the aged DHB solution.

During the one-year monitoring of the DHB solution, few changes occurred in the mass spectra of the matrix compound. The disappearing and (re)appearing of some peaks was observed (see Table 11), also, some changes in the peak intensities were detected but these were not significant enough to draw conclusions on the chemical changes taking place during the ageing of the matrix solution. The variations in the occurrence of peaks and their intensities are with high probably related to the way the crystals are formed from the deposited DHB solution. The structure, homogeneity, and density of the crystals are very important factors during the measurement of MALDI mass spectra. [I] In addition to the formed crystals, also the overall condition of the MALDI-FT-ICR-MS instrument – the cleanliness of the system and laser fluence may cause differences in the mass spectra. [88] It is also important to note that the intensity of the peaks due to DHB in the MALDI-FT-ICR-MS spectra was low, which is a normal and desired property of a good MALDI matrix compound.

There were 6 peaks in the mass spectra of DHB that were detected throughout the entire ageing period: peaks at nominal *m/z* 137, *m/z* 245, *m/z* 273, *m/z* 409, *m/z* 449, and *m/z* 585 (see Table 11 for ion assignments). In addition, several peaks with low intensities occurred occasionally in the mass spectra of DHB: peaks at nominal *m/z* 217, *m/z* 295, *m/z* 313, *m/z* 335 and *m/z* 471. The low-intensity peak that was identified as the protonated DHB (nominal *m/z* 155), and some other peaks, e.g. with nominal *m/z* 215, *m/z* 271, *m/z* 403, and *m/z* 421 were observed in the mass spectra only during the first two months of ageing.

At the beginning of the second week of monitoring the DHB solution, two new peaks were detected in the mass spectra (see Table 11). The peak at nominal *m/z* 607 identified as $[4DHB\text{-}3H_2O\text{-}H+2Na]^+$ cation and the peak with

the nominal *m/z* 721 corresponding to $[5DHB\text{-}4H_2O+Na]^+$ cation. Additionally, only one other new peak appears in the mass spectra of DHB solution during the ageing: the peak with the nominal *m/z* 407 that corresponds to $[3DHB\text{-}3H_2O\text{-}H]^+$ cation is detected from the matrix solution aged for 6 months and one year.

Examining the disappearing and emerging of the DHB peaks shows that a general increase of relative peak intensities occurs at higher *m/z* values. At the same time, the decrease of the relative peak intensities of DHB peaks at lower *m/z* values is observed. The expected reason is condensation reactions taking place in DHB solution during the ageing process, leading to different DHB oligomers. [89]

In addition to peaks corresponding to DHB, also peaks unrelated to the matrix compound were detected in the mass spectra obtained during the ageing process. E.g. the peak at nominal *m/z* 931 in the mass spectrum obtained from the fresh DHB solution is assigned as the protonated fragment of Angiotensin II ($[AngII\text{-}C_4H_6NO_3+H]^+$). Angiotensin II (nominal *m/z* 1046) was used as an internal calibration standard and was added to the DHB solution (see section 3.2). Also, some unidentified peaks were observed in the mass spectra of DHB, e.g. peaks with the nominal *m/z* values of 317, 361, 439 and 461.

During the monitoring of the DHB solution, two peaks corresponding to phosphazenes were observed occasionally in the mass spectra of the matrix material. The peak with the nominal *m/z* 682 corresponds to $Ph(CH_3)CH\text{-}P_4(dma)_9H^+$ and the peak at nominal *m/z* 916 is assigned as $Ph(CH_3)CH\text{-}P_4(pyrr)_9H^+$ (see Table 2). These two compounds are used for the measurement of gas-phase basicities (GB) of superstrong bases at our laboratory. During the acidity-basicity measurements in the gas-phase with FT-ICR-MS, vapours of these compounds (neutrals, not ions) are leaked into the ICR cell (see reference [90] for a more detailed description). After such experiments, the system is always thoroughly baked (see the description in section 3.5.1) but phosphazenes are extremely sticky and basic compounds. Therefore, a very small quantity of such a compound is sufficient for the detection of it in the mass spectra.

4.2.2 Aged DHB solution as MALDI matrix for the analysis of resins

One of the aims of this stage of the study was to determine if the aged DHB solution is applicable as a MALDI matrix material and if its age affects the analysis results of resin samples. Shellac resin was chosen as a test object during this stage of the study.

The mass spectrum of shellac resin registered using the DHB solution aged for one year is presented in Figure 10b and the mass spectrum obtained from the resin with freshly made matrix solution can be found in Figure 10a. The ion assignments of some of the more characteristic peaks of shellac resin, along with the comparison of the corresponding *m/z* errors in case of internal and external calibration is presented in Table 12 (the full assignment can be found in Table A2 in Appendix 1).

Table 12. Summary of the ion assignments for some of the more characteristic peaks in the positive ion mode mass spectrum of shellac resin along with the corresponding *m/z* errors obtained in the case of internal and external calibration.

Cation formula	Internal calibration		External calibration	
	Measured *m/z*	*m/z* error (ppm)	Measured *m/z*	*m/z* error (ppm)
$C_{15}H_{18}O_4Na^+$	285.10987	0.50	285.10929	–1.56
$C_{16}H_{30}O_4Na^+$	309.20367	0.13	309.20305	–1.88
$C_{16}H_{32}O_5Na^+$	327.21422	0.08	327.21357	–1.92
$C_{31}H_{48}O_7Na^+$	555.32906	–0.30	555.32789	–2.41
$C_{31}H_{48}O_8Na^+$	571.32421	0.12	571.32300	–2.00
$C_{32}H_{62}O_9Na^+$	613.42857	–0.06	613.42726	–2.20
$C_{46}H_{64}O_{11}Na^+$	815.43381	–0.34	815.43199	–2.56
$C_{46}H_{66}O_{12}Na^+$	833.44467	0.02	833.44280	–2.22
$C_{47}H_{78}O_{12}Na^+$	857.53826	–0.34	857.53634	–2.58

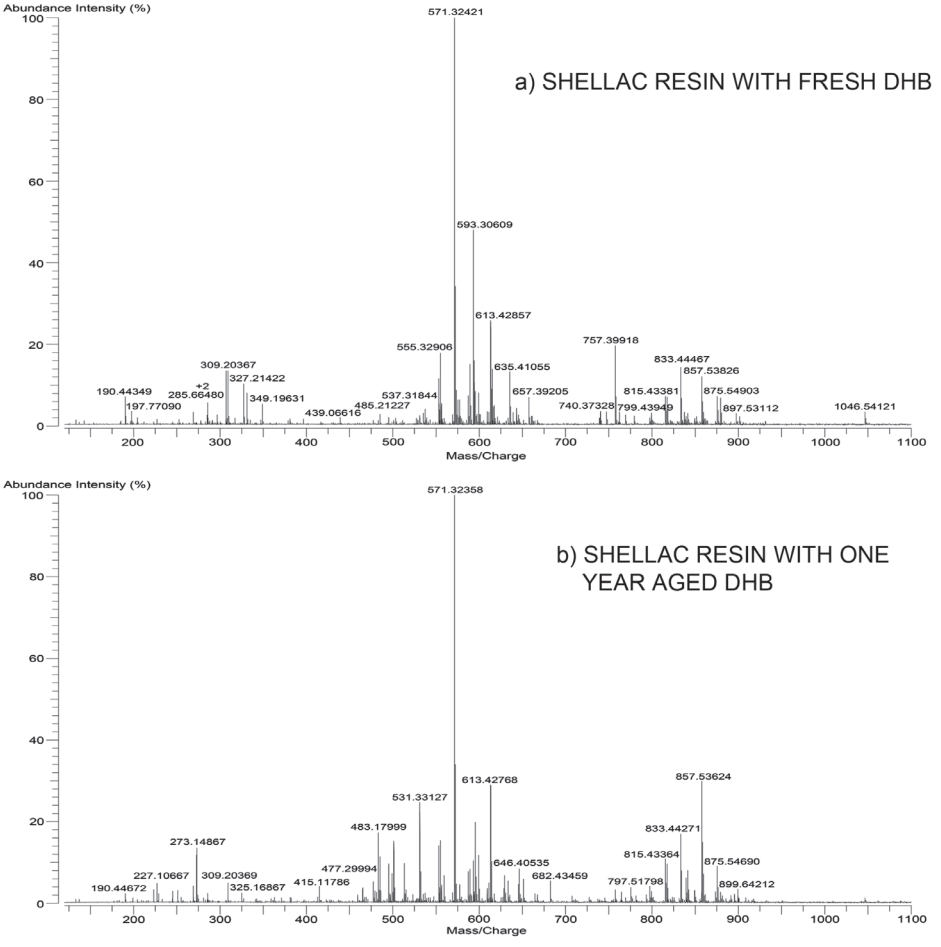

Figure 10. Comparison of mass spectra measured from shellac resin using a) freshly made DHB solution and b) DHB solution aged for one year as MALDI matrix.

There are 3 clusters of peaks visible in both mass spectra obtained from shellac resin. The first cluster consists of peaks corresponding to the original components of the resin. The peak with the nominal *m/z* value 327 corresponds to the sodium adduct of aleuritic acid ($[C_{16}H_{32}O_5+Na]^+$). The peak with the nominal *m/z* value 309 belongs to the sodium adduct of dehydrated aleuritic acid: $[C_{16}H_{32}O_5-H_2O+Na]^+$. Following this pattern, the peak at nominal *m/z* value 291 is detected as $[C_{16}H_{32}O_5-2H_2O+Na]^+$ cation. Also, the sodium adduct of dehydrated jalaric acid was detected in both mass spectra measured from shellac resin: nominal *m/z* 285 corresponds to $[C_{15}H_{20}O_5-H_2O+Na]^+$ ion (see Figure 3 for structures).

The most prominent cluster in both mass spectra presented in Figure 10 is the second cluster. The peaks in this cluster correspond to dimerisation and esterification products of shellac resin. [3] E.g. the most intensive peak in the mass spectrum is found at nominal *m/z* 571. This peak is assigned as $C_{31}H_{48}O_8Na^+$ and with high probability it corresponds to an esterification product of aleuritic acid and a sesquiterpenoid acid.

The mass spectra of shellac resin obtained with the help of fresh and aged DHB solution seem different at first but this is mainly due to the differences in peak intensities in the mass spectra. This, in turn, causes the increase in the relative intensities of the background peaks. However, after comparing the *m/z* values of the peaks originating from shellac resin in both mass spectra displayed in Figure 10, it can be concluded that the mass spectra are fairly similar to each other. The differences between these mass spectra are also caused by the variations in the peak intensities. With high probability, this is not caused by the condition of DHB solution and can be attributed to the complex nature of the analysis of resinous samples. The analysis of resinous samples with MALDI method requires a modified sample preparation and spotting method. [I] In the case of shellac resin the volume of shellac solution (in ethanol) was 2 times higher than the volume of DHB solution (see section 3.5.2) in order to obtain better results from the resin. Therefore, the formed crystals on the MALDI target plate were very small and the spots spread out extensively. The mass spectra measured from this kind of spots tend to have lower intensities because the thickness of the spots is small. In addition, the results vary more because replicating the spots is more difficult.

4.2.3 Using DHB for internal calibration

One of the practical aims of this part of the study was to use peaks originating from DHB for internal calibration of the *m/z* axis. Table 11 provides a list of peaks belonging to DHB that are potential candidates for internal calibration.

The mass spectra measured from shellac resin contain in total 4 peaks that correspond to DHB: peaks with the nominal *m/z* 137 and 273 occurred frequently, peaks at nominal *m/z* 155 and 409 were occasionally present. The small number of DHB peaks present in the mass spectra obtained from shellac resin is

with high probability connected to the fact that the ratio of resin solution vs matrix solution was 2:1. This, in turn, made it more difficult to obtain peaks corresponding to DHB in the mass spectra measured from shellac resin because the effective amount of the matrix substance in the location hit by the laser was relatively low.

Nevertheless, some of the peaks corresponding to DHB were used for internal calibration of the lower *m/z* region of the *m/z* axes of the mass spectra of shellac resin.

As can be seen from Table 12 (and Table A2 in Appendix 1), the *m/z* errors in the case of the mass spectrum with internally and externally calibrated *m/z* axis did not differ greatly. The overall *m/z* errors for internal calibration were in the range of –1.55 ppm to 1.71 ppm, in case of external calibration, the corresponding values ranged from –4.00 ppm to –0.58 ppm. The small difference between the *m/z* errors obtained during the internal and external calibration of the *m/z* axis of the mass spectrum of shellac resin is a good example of the variability of the external calibration. It is very much dependent on the specific conditions of the FT-ICR-MS instrument. Whereas internal calibration is more reliable, leading to consistently lower *m/z* errors.

4.2.4 Main conclusions

The one year ageing process of the DHB solution indicated that although some changes occur in the mass spectra of the matrix, they are mainly caused by the formed crystals and the overall conditions of the MALDI-FT-ICR-MS instrument, rather than chemical changes occurring in the matrix solution with time. The results give no strong evidence for the formation of additional products in the DHB solution during its ageing. Thus, DHB solution in a mixture of acetonitrile and 0.1 % trifluoroacetic acid can be used for at least one year.

During the analysis of DHB, 25 peaks corresponding to the matrix compound were identified, and thereby, the number of potential internal calibration peaks was increased significantly. DHB offers calibration possibilities mainly in the lower *m/z* region (below *m/z* 500) where the common calibration standards (commercial peptides, etc.) typically do not have peaks.

In this study, it was shown that with the right sample preparation and spotting technique DHB peaks are obtainable in the mass spectra of shellac resin. However, the number of DHB peaks detected in the mass spectra of shellac resin was considerably low: only 4 peaks corresponding to the matrix compound could be identified in the mass spectra of the resin. Therefore, the matrix compound is not a very abundant source for calibration peaks for resinous materials. Thus, more reliable calibration standards are needed, preferably compounds that enable to cover the *m/z* range of up to *m/z* 1000.

At this stage of the study, the question about the possibility to analyse resinous materials with the MALDI-FT-ICR-MS methodology in the negative ion mode emerged. This in turn raised additional questions: is DHB a suitable matrix compound and what compounds (and how) to use for internal calibration.

4.3 New methodological approach in MALDI-MS analysis of resins: new negative ion mode matrix and novel internal standards [III]

The aim of this part of the study was to complete the development of the MALDI-FT-ICR-MS methodology for the analysis of resinous materials, involving positive and negative ion mode. For this, 2-aminoacridine (2-AA) was introduced as a novel matrix material for the analysis of resinous materials in the negative ion mode and a selection of phosphazenes and sulpho-compounds were employed as internal standards (see Table 5 and Figure 5). For the incorporation of these novel materials, the sample preparation procedure, including the spotting of the solutions was thoroughly modified (see Experimental section for more details).

4.3.1 The properties of 2-aminoacridine

2-Aminoacridine ($C_{13}H_{10}N_2$) is a bright yellow crystalline compound that is soluble in alcohols and pyridine. The maximum UV-Vis absorption of 2-AA is approximately at 265 nm but it also has a smaller absorption maximum in the range of 350 nm (see Figure 11) making it compatible with MALDI instruments that have the Nd:YAG laser (355 nm and 266 nm). [91]

The pK_a value of 2-AA in acetonitrile is 16.39 and the gas-phase basicity (GB) value of the ground state of 2-AA calculated by G4MP2 method is 229.8 kcal mol^{-1}. The corresponding values for 9-AA are 18.35 (measured in acetonitrile) and 236.4 kcal mol^{-1}, making this compound more basic compared to 2-AA. The situation is reversed in the excited state. When protonation from the vertical S_1 state of a free base to the vertical S_1 state of respective conjugate acid is taken into account, the results of time dependent density functional theory (TD DFT) calculations using B3LYP, CAM-B3LYP, M06, M06HF, and PBE0 density functional formulations and Förster cycle approximation all suggest that the difference between excited state gas-phase basicity values (GB*) of 2-AA and 9-AA are in the range of 12 to 14 kcal mol^{-1} in favour of 2-AA. Thus, 2-AA becomes in the excited state a stronger base than 9-AA. This gives rise to the hypothesis that 2-AA is more efficient in ionising analyte molecules than 9-AA during MALDI-MS analysis if the conditions for excited state protonation are favourable.

The MALDI-FT-ICR mass spectrum of 2-AA obtained in the negative ion mode shows few peaks (see Figure 11). The most intensive peak in the mass spectrum of 2-AA is at *m/z* 193.07716 and this corresponds to the deprotonated 2-AA anion ($[C_{13}H_{10}N_2\text{-}H]^-$). Also, the peak belonging to the triply dehydrogenated anion ($[C_{13}H_{10}N_2\text{-}3H]^-$) with low intensity is present at *m/z* 191.06133. The structures of the ions corresponding to peaks with the nominal *m/z* 191 and

193 are presented in Appendix 2. The mass spectrum of 2-AA also displays the doubly charged anion of the deprotonated 2-AA molecule at *m/z* 96.53887 and the peak at *m/z* 385.14610 (assigned as $[C_{26}H_{17}N_4]^-$) belongs to the deprotonated dimer of the original compound.

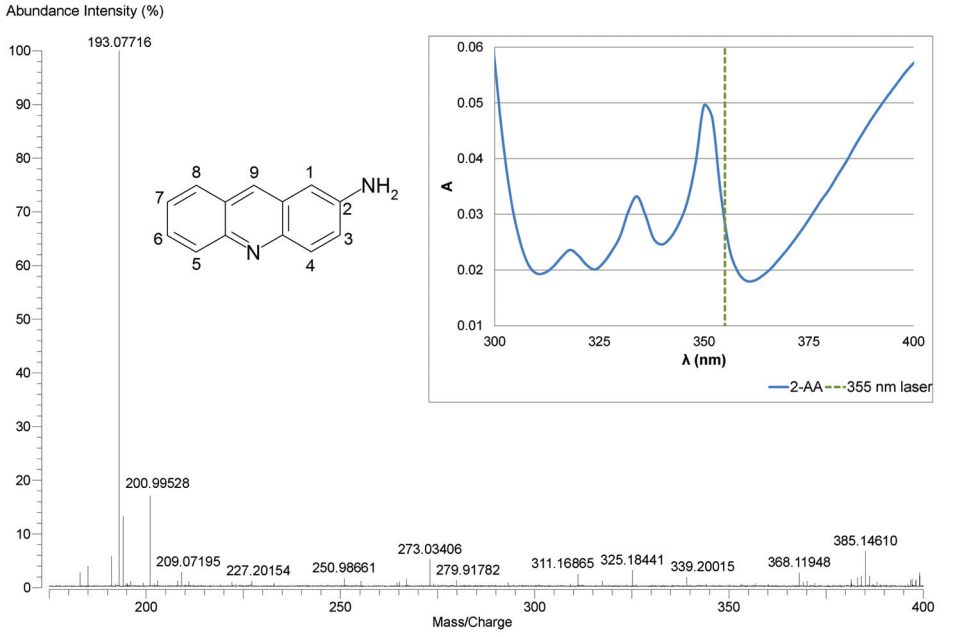

Figure 11. Negative ion mode mass spectrum, chemical structure (the Graebe and Lagodzinski numbering of nucleus is used [91]) and UV-Vis spectrum of 2-aminoacridine (obtained from a 0.008 mM solution of 2-AA in acetonitrile, the laser wavelength used during this study – 355 nm is indicated by dashed green line).

4.3.2 Ionisation characteristics of phosphazenes and sulpho-compounds

Phosphazenium cations and anions of the sulpho-compounds are very stable ions and their parent compounds are strongly basic or strongly acidic, respectively. Therefore, they readily produce gas-phase ions in the MALDI source. The phosphazenium cations and anions of sulpho-compounds, depicted in Figure 5, are formed due to the addition or loss of a proton ($[M+H]^+$ and $[M-H]^-$) to or from the parent compounds, respectively.

Although these compounds yield almost no fragments in the mass spectra, it was observed that they can produce multiply charged radical ions (the corresponding exact *m/z* values are presented in Table A11 in Appendix 3). The occurrence of doubly and triply charged ions of the phosphazenes and sulpho-compounds was confirmed by the ^{13}C satellite peak positions in the mass spectra. The detection of such peaks is with high probability related to the

strongly basic and acidic nature of the parent compounds and observing these ions is not common in MALDI-MS analysis (will be further investigated by our workgroup).

In case of phosphazenes, the relative intensities of the peaks corresponding to multiply charged ions in the mass spectra obtained from individual compounds were usually lower than 5%. Therefore, peaks belonging to multiply charged phosphazenium cations were rarely detected in the mass spectra obtained from the resins. For sulpho-compounds, the intensities of the peaks corresponding to the doubly charged ions were in the range of 30–35% and for the triply charged ions the relative intensities of the peaks were below 10%. Therefore, the $[[CF_3(CF_2)_3SO_2]_2NH\text{-}H]^{2-}$ and $[[CF_3(CF_2)_7SO_2]_2CH_2\text{-}H]^{2-}$ radical ions were occasionally present in the mass spectra obtained from the resin samples.

However, for internal calibration of the *m/z* axis only the *m/z* values of singly charged calibration peaks were used. The *m/z* values of the multiply charged ions showed higher *m/z* errors compared to the *m/z* errors obtained for the singly charged ions. This is caused by a systematic effect that originates from the *m/z* calibration equations (see Equation 2). The space-charge effects (trapped ion population size) cause the cyclotron frequency *f* to shift by Δf. [63, 64] In order to use the *m/z* values of the multiply charged ions for internal calibration this frequency shift has to be taken into account.

Multiply charged ions have been used for internal calibration in FT-ICR-MS analysis, by mathematically correcting the *m/z* values of the corresponding peaks. [64] However, in the case where the calibration constant for the *m/z* axis is calculated using theoretical (exact) *m/z* values of the selected calibration peaks, the frequency shifts caused by the space charge effect cannot be included into the equation in an easy way.

4.3.3 Phosphazenes as internal standards for the positive ion mode MALDI-FT-ICR-MS analysis of natural resins

The suitability of phosphazenes (and their salts) as internal standards for the positive ion mode MALDI-FT-ICR-MS analysis of natural resin samples was assessed via the analysis of mastic, sandarac, and colophony resins. Individual calibration mixtures containing 4–5 different phosphazenes were prepared for the analysis of these resins (see Table 5). The corresponding mass spectra are presented in Figure 12. Table 13 gives a summary of the assigned ions that corresponded to the peaks in the mass spectra of these three resins (a more comprehensive assignment is presented in Appendix 1, in Tables A3–A5). In addition, Table 13 presents the *m/z* errors corresponding to *m/z* values obtained in the mass spectra with internally and externally calibrated *m/z* axes.

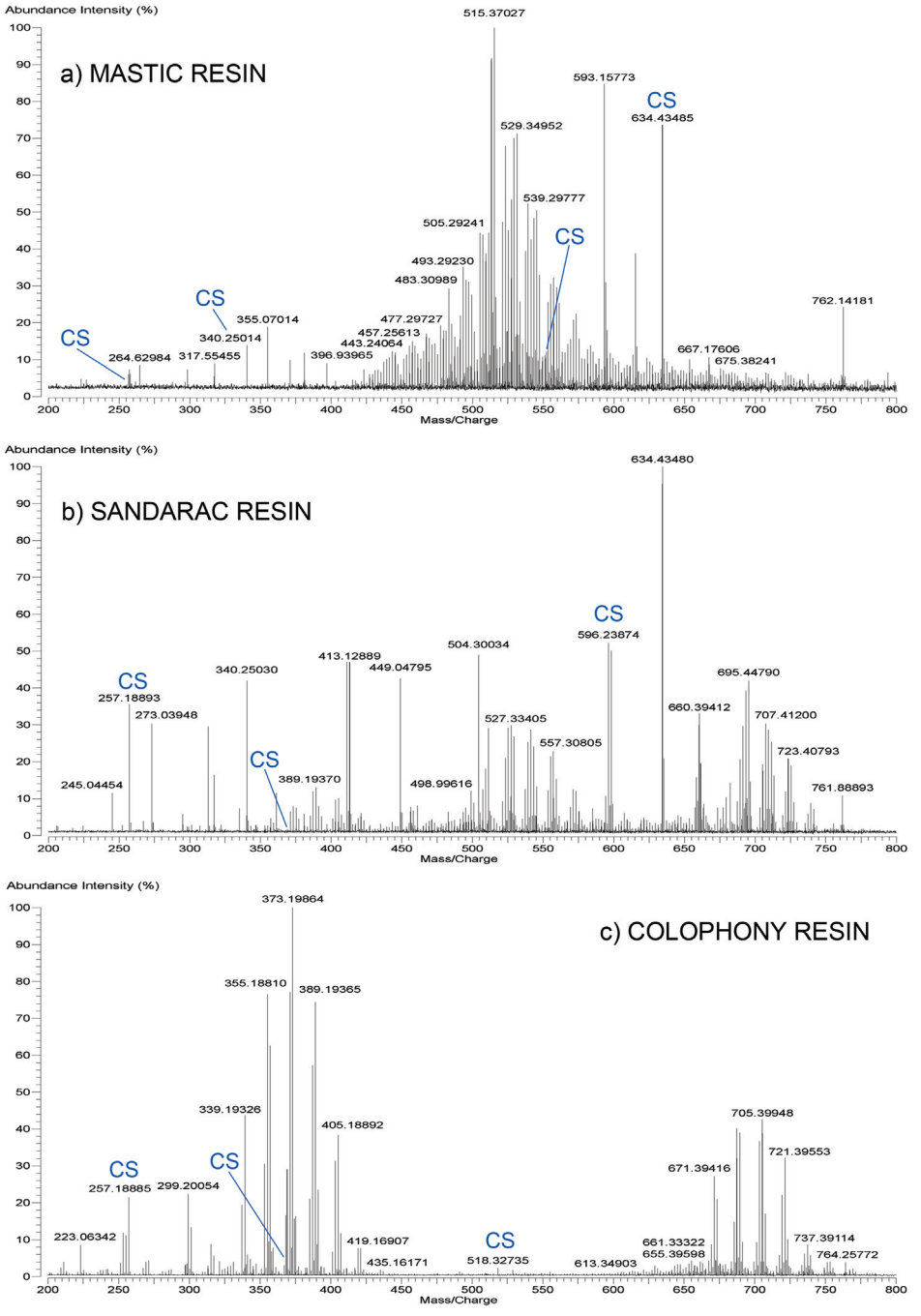

Figure 12. The positive ion mode MALDI-FT-ICR-MS mass spectra (with internally calibrated *m/z* axes) of a) mastic, b) sandarac, and c) colophony resins.[6]

[6] CS (calibration standard) is used to indicate the peaks corresponding to the calibration standards.

Table 13. Summarised assignment of cation formulas corresponding to peaks of the positive ion mode mass spectra of mastic, sandarac and colophony resins. In addition, the corresponding *m/z* errors in the case of internally and externally calibrated *m/z* axes are presented.

Resin	Cation	Internal calibration		External calibration	
		Measured *m/z*	*m/z* error (ppm)	Measured *m/z*	*m/z* error (ppm)
Mastic	$C_{27}H_{40}O_5Na^+$	467.27708	0.61	467.28316	13.63
	$C_{30}H_{43}O_5^+$	483.30989	–1.26	483.31644	12.29
	$C_{29}H_{42}O_5Na^+$	493.29230	–0.29	493.29914	13.57
	$C_{30}H_{42}O_5Na^+$	505.29241	–0.06	505.29962	14.19
	$C_{30}H_{52}O_5Na^+$	515.37027	–0.82	515.37779	13.76
	$C_{30}H_{50}O_6Na^+$	529.34952	–0.82	529.35748	14.21
	$C_{30}H_{44}O_7Na^+$	539.29777	–0.29	539.30605	15.06
	$C_{30}H_{52}O_7Na^+$	547.36015	–0.69	547.36869	14.92
	$C_{30}H_{46}O_8Na^+$	557.30880	0.56	557.31768	16.49
	$C_{30}H_{46}O_9Na^+$	573.30385	0.78	573.31328	17.23
Sandarac	$C_{20}H_{30}O_5Na^+$	373.19883	0.75	373.20951	29.39
	$C_{20}H_{30}O_6Na^+$	389.19370	0.61	389.20534	30.53
	$C_{20}H_{30}O_7Na^+$	405.18863	0.63	405.20128	31.84
	$C_{30}H_{48}O_5Na^+$	511.33887	–1.02	511.35921	38.76
	$C_{30}H_{48}O_6Na^+$	527.33405	–0.50	527.35571	40.58
	$C_{30}H_{46}O_8Na^+$	557.30805	–0.78	557.33229	42.71
	$C_{40}H_{62}O_6Na^+$	661.44281	–1.59	661.47713	50.31
	$C_{40}H_{64}O_8Na^+$	695.44790	–2.07	695.48589	52.56
	$C_{40}H_{60}O_{10}Na^+$	723.40793	0.08	723.44909	56.97
Colophony	$C_{20}H_{28}O_3Na^+$	339.19326	0.56	339.20278	28.64
	$C_{20}H_{28}O_4Na^+$	355.18810	0.35	355.19841	29.35
	$C_{20}H_{30}O_5Na^+$	373.19864	0.26	373.20985	30.30
	$C_{20}H_{30}O_6Na^+$	389.19365	0.50	389.20571	31.47
	$C_{20}H_{30}O_7Na^+$	405.18892	1.35	405.20184	33.24
	$C_{42}H_{55}O_7^+$	671.39416	–0.10	671.42589	47.16
	$C_{42}H_{57}O_9^+$	705.39948	–0.33	705.43420	48.89
	$C_{42}H_{57}O_{10}^+$	721.39553	1.25	721.43170	51.40
	$C_{40}H_{58}O_{12}Na^+$	753.38086	–1.59	753.42002	50.40

As can be seen from Table 13, the majority of the peaks present in the positive ion mode mass spectra obtained from mastic, sandarac and colophony resins were detected as sodium adducts. For mastic and colophony resins, occasionally also ions formed during protonation were observed but mainly for peaks present at lower *m/z* values. As described above, the detection of sodium adducts is common with samples with higher content of oxygen and has often been observed in the analysis of natural resin samples. [I] The mass spectra of sandarac and colophony resins consist of clusters (describe the polymerisation/oligomerisation of the compounds) that are in turn composed of sub-clusters (illustrate the oxidation, methylation and demethylation, dehydrogenation, etc. processes). The mass spectrum obtained from mastic resin is rather different from the mass spectra obtained from the other terpenoid resins (see Figure 12a). At the same time, the peaks obtained in this mass spectrum still provide information about the oxidation, (de)methylation, and (de)hydrogenation of the compounds present in mastic resin.

After the analysis of the mass spectra of mastic, sandarac and colophony resins, it was concluded that the used phosphazenes were suitable for the internal calibration of the *m/z* axis of such complex materials because they (1) did not interact with the resin or matrix material during the analysis and (2) they could be included into the calculation of the calibration constant even if they had low intensities or were located close to the peaks corresponding to the resins (see Figure 12).

The impact of the novel internal standards on the *m/z* accuracy of the mass spectra obtained from mastic, sandarac and colophony resins is very good. Overall, the *m/z* errors in case of the mass spectrum of mastic resin were reduced from the range of 11 to 21 ppm to –1.99 to 1.96 ppm. For sandarac resin, the corresponding ranges were 23–58 ppm to –2.07–1.93 ppm, and for colophony resin from 18–53 ppm to –1.98–2.84 ppm (see Tables A3 to A5 in Appendix 1 for more details).

The significant improvement of the *m/z* accuracy is most important during the assignment of the ions (and subsequent identification of the corresponding compounds). For example, the peak with the nominal *m/z* 557 in the mass spectrum of mastic resin is assigned in the case of internal calibration as $C_{30}H_{46}O_8Na^+$. With high probability, this cation corresponds to the oxidised masticadienonic acid or moronic acid (see Figure 1) – identified as main components of the resin. [1, 3, 35] In the mass spectrum with externally calibrated *m/z* axis, the same peak is assigned as $C_{25}H_{49}O_{13}^+$. For sandarac resin, the peak detected at nominal *m/z* 421 in the mass spectrum with internally calibrated *m/z* axis is assigned as $C_{20}H_{30}O_8Na^+$ (see Table 13) but in case of external calibration this peak corresponds to $C_{24}H_{30}O_5Na^+$. The first ion can be identified as an original diterpenoid of the resin, with high probability it is oxidised communic acid that is the main component in this resin. [1, 3, 32, 34] The ion assigned in the mass spectrum of sandarac resin with externally calibrated *m/z* axis is hardly related to the compounds present in the resin. The same risk of misinterpretation is also experienced in the mass spectrum of colophony resin with externally calibrated *m/z* axis. E.g. the peak at nominal

m/z 721 is assigned as $C_{40}H_{58}O_{10}Na^+$ in the mass spectrum with internally calibrated *m/z* axis. With high probability, this peak refers to a dimer of the resin's original diterpenoids, like abietic acid and its derivatives. [1, 3] In the mass spectrum with externally calibrated *m/z* axis, the same peak is assigned as $C_{43}H_{61}O_9^+$ and this ion is not related to the compounds of colophony resin.

4.3.4 2-AA as matrix material and fluorine-rich sulpho-compounds as internal standards for the negative ion mode analysis of natural resins

The negative ion mode mass spectra of all the five resins (dammar, mastic, sandarac, colophony, and shellac resins) chosen for this study were obtained with the help of a new matrix material, 2-AA. In addition, 4 novel internal standards, fluorine-rich sulpho-compounds, were used in order to register mass spectra with the highest *m/z* accuracy possible.

A calibration solution, that contained all the sulpho-compounds, was used for the analysis of the resins. The specific compounds used in the calibration equation for each resin are listed in Table 6. The mass spectrum of shellac resin registered with the novel matrix compound is presented in Figure 13 (along with the results obtained from this resin with DHB and 9-AA). The mass spectra of dammar and mastic resins are presented in Figure 14, the corresponding mass spectra for sandarac and colophony resins are presented in Figure 15. The ion assignments for a selection of characteristic peaks obtained in these mass spectra along with the corresponding *m/z* errors obtained in case of internal and external calibration of the *m/z* axes are summarised in Table 14.

During this stage of the study, it was discovered that DHB failed in ionising the natural resins in the negative ion mode. At the same time, the resins contain many carboxylic acids, so that ionisation in the negative ion mode would be intrinsically suitable. Based on literature suggestion, 9-AA was tested as a substitute for DHB but the results were still not fully satisfactory. Therefore, another member of the aminoacridine family, 2-aminoacridine, was assessed as matrix material.

As can be seen in Figure 13, the mass spectrum of shellac resin obtained with DHB differs greatly from the mass spectra obtained with the help of the aminoacridines. In the mass spectrum acquired with DHB, numerous peaks are visible but the positions and intensities of these peaks are different compared to the peaks present in the mass spectra obtained with 9-AA and 2-AA. The interpretation of the peaks present in the mass spectrum obtained with DHB reveals that most of them can be assigned to the matrix compound itself.

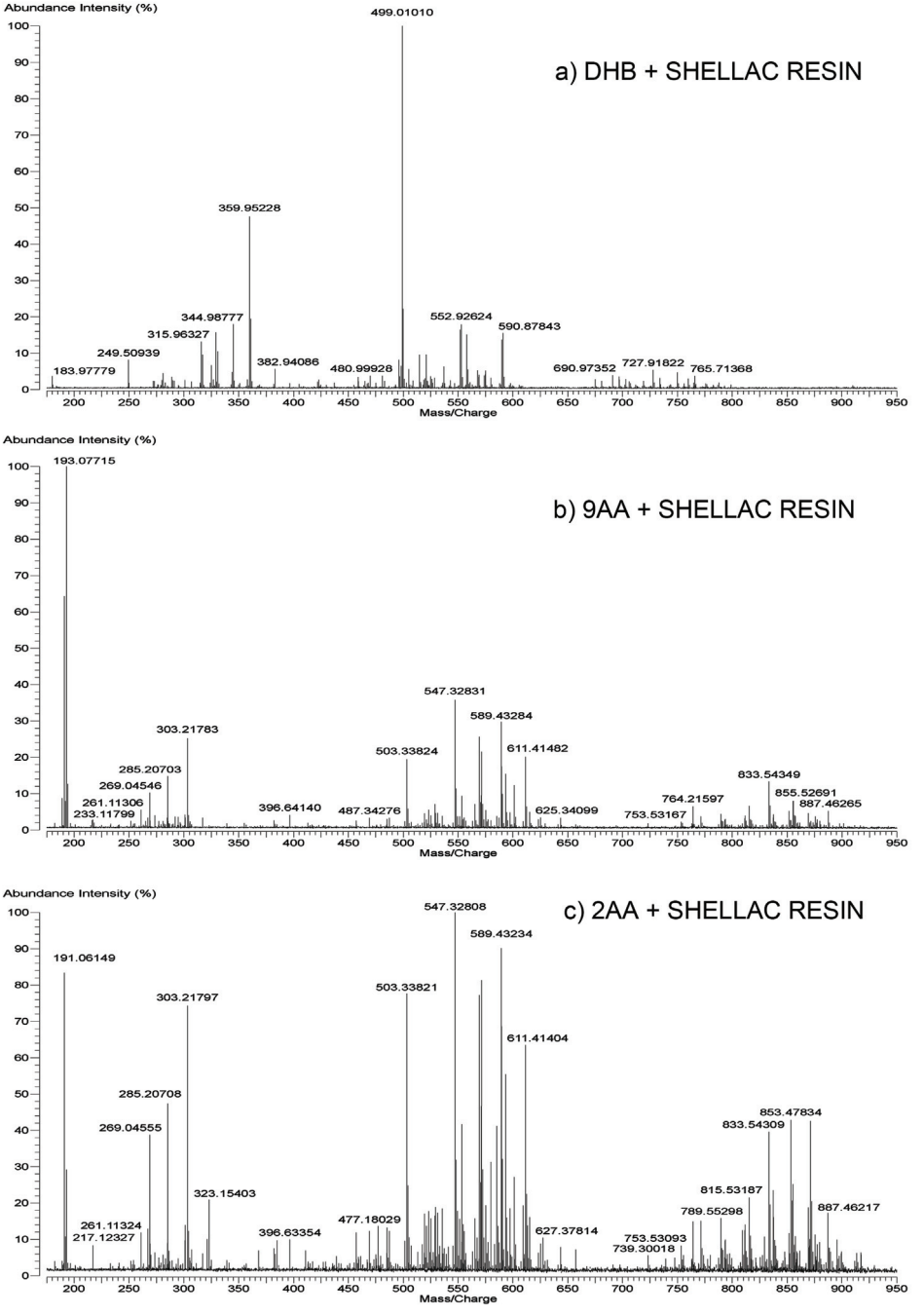

Figure 13. The negative ion mode mass spectra of shellac resin obtained with a) DHB, b) 9-AA, and c) 2-AA.

The most intensive peak in the negative ion mode mass spectrum of shellac resin obtained with 9-AA is found at *m/z* 193.07715. This corresponds to the deprotonated matrix compound. The peaks belonging to shellac resin have considerably lower intensities. In the mass spectrum of shellac resin obtained with 2-AA, the peaks corresponding to the resin are not suppressed by the peaks originating from the matrix compound. Therefore, 2-AA is chosen as a matrix compound for the analysis of resin samples in the negative ion mode.

2-AA was also used for the analysis of the remaining four terpenoid resins and the results obtained demonstrate well the suitability of 2-AA as a matrix material for the analysis of natural resin. It forms very small and homogenous crystals on the MALDI target plate. Mixing the resin sample solution with the matrix solution prior the analysis makes the distribution of the analyte molecules in the matrix even more homogenous. During the MALDI-FT-ICR-MS analysis, no new peaks corresponding to 2-AA were detected in the mass spectra obtained from the resins. This indicates that the recommended matrix compound does not react with the analyte molecules. An important advantage of the new matrix compound is the fact that the mass spectra obtained from resin samples are not over-crowded with peaks belonging to the matrix compound. There are only two peaks originating from 2-AA present in the mass spectra of resinous materials: the deprotonated anion of 2-AA ($[C_{13}H_{10}N_2\text{-}H]^-$) with the exact *m/z* value of 193.07712 and the anion $[C_{13}H_{10}N_2\text{-}3H]^-$ (*m/z* 191.06147). It was observed that the latter anion frequently dominated over the deprotonated ion of 2-AA during the analysis of resinous materials. E.g. for the more acidic resins, such as colophony and shellac the peak at nominal *m/z* 191 was more prominent compared to the peak at *m/z* 193. For the resins with lower acidity, like dammar and mastic, the difference of the intensities of these peaks was not so noticeable. With high probability, the anion at nominal *m/z* 191 has formed by transformation of the initial six-member aromatic ring of the anion into a five-member aromatic (cyclopentadienyl) ring together with the formation of a cyano group (see Appendix 2). This form is more stable than the initially deprotonated ion of 2-AA because of its aromaticity and anion-stabilising power of the cyano group. Therefore, its peak is more intensive.

Nevertheless, the deprotonated ion of 2-AA was always present in the mass spectra obtained from resins. Therefore, the deprotonated ion of 2-AA was a good addition to the list of internal standards enabling to extend the calibration range for the lower part of the *m/z* axis down to *m/z* 190.

The sulpho-compounds applied as internal standards during this study gave good results. The peaks of the calibration compounds were present in the mass spectra of the resins but they did not affect the analysis of the resinous materials in any way.

As Table 14 demonstrates (and Tables A6, A7, A9, and A10 in Appendix 1), the *m/z* errors for dammar, mastic, colophony, and shellac resins were reduced significantly as a result of internal calibration. The overall *m/z* errors for all the peaks corresponding to dammar resin in the mass spectrum with internally calibrated *m/z* axis were in the range of –2.04 to 0.90 ppm, and for the

externally calibrated version the corresponding range was –19 to –14 ppm (see Table A6 in Appendix 1). For mastic resin, the *m/z* errors for the mass spectrum with internally calibrated *m/z* axis were between –1.23 and 1.31 ppm; in case of external calibration the *m/z* errors ranged from –9.95 ppm to –6.51 ppm (see Table A7 in Appendix 1). In case of colophony resin, the *m/z* errors were reduced from the range of 0.6–10.9 ppm to the range of –2.00 to 3.02 ppm (Table A9 in Appendix 1). During the analysis of shellac resin, also an improvement was obtained via internal calibration: the *m/z* errors for the mass spectrum with internally calibrated *m/z* axis ranged from –1.56 to 1.48 ppm, the corresponding values in case of external calibration were in the range of –9.0 to –2.0 ppm (Table A10 in Appendix 1).

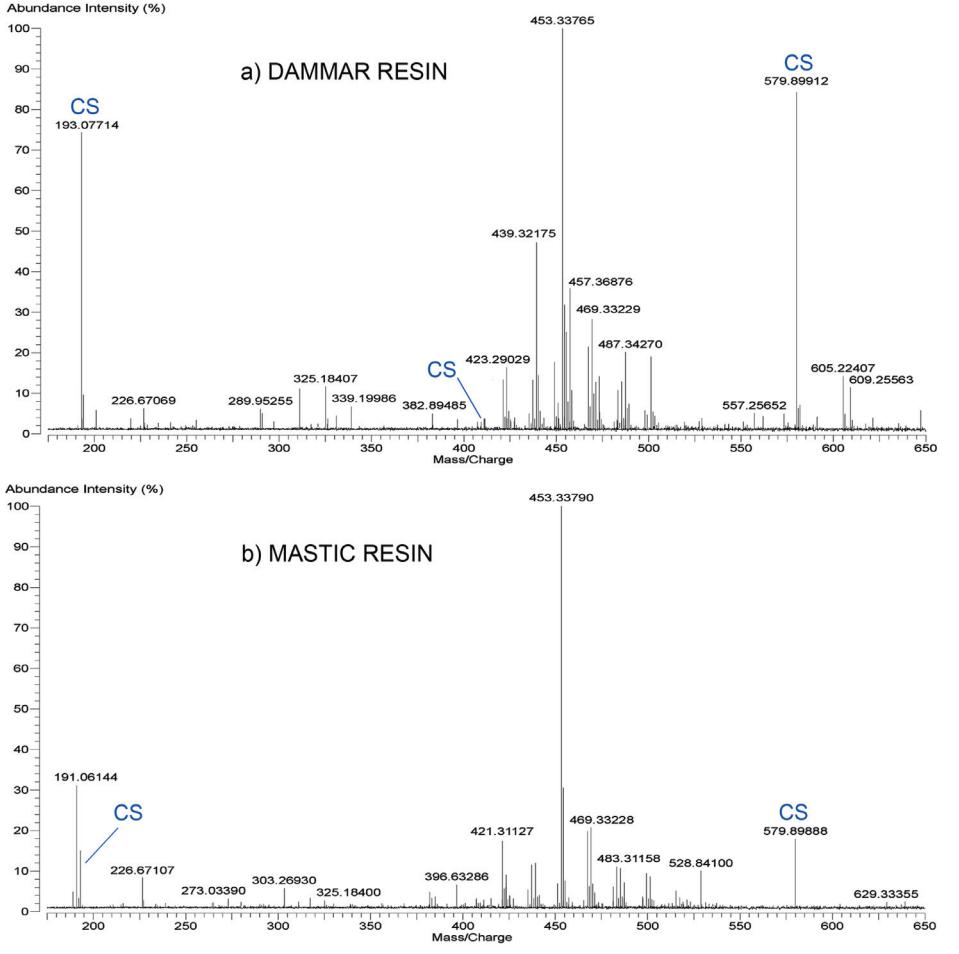

Figure 14. Negative ion mode mass spectra with internally calibrated *m/z* axes of a) dammar resin and b) mastic resin.

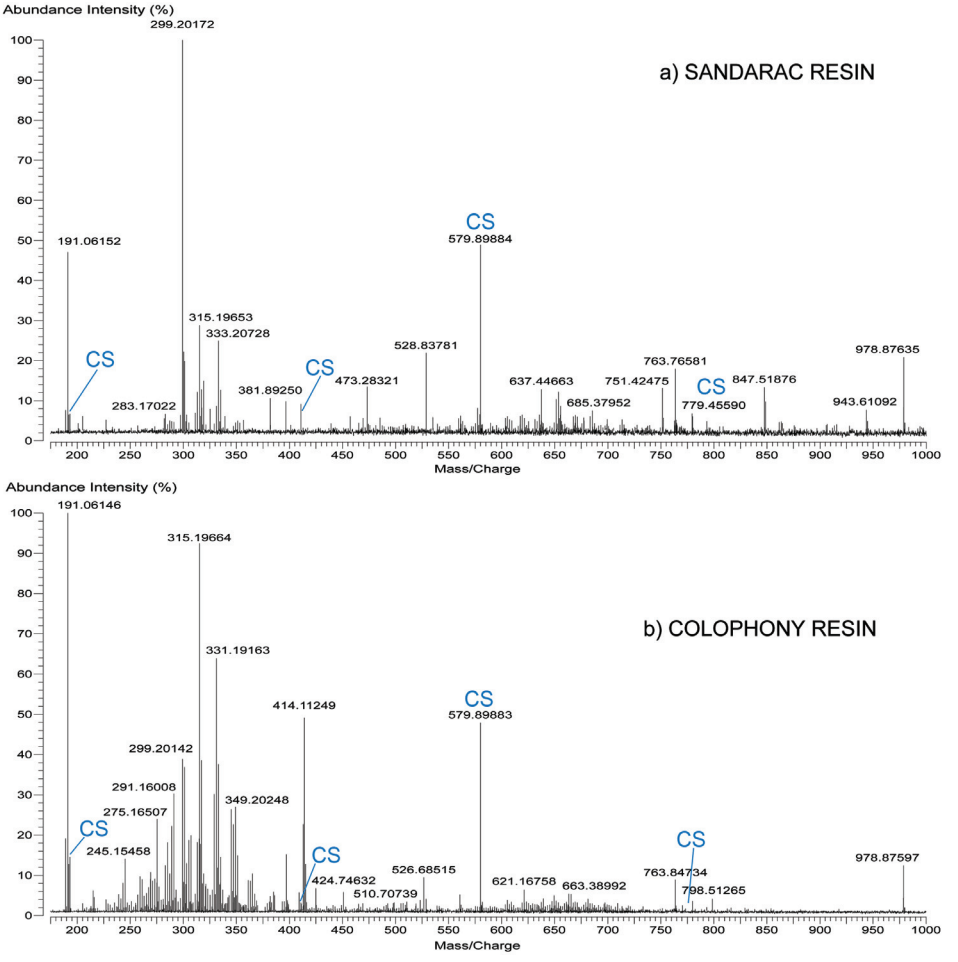

Figure 15. Negative ion mode mass spectra with internally calibrated *m/z* axes of a) sandarac resin and b) colophony resin.

Internal calibration of the *m/z* axis of the mass spectrum obtained from sandarac resin did not influence the accuracy of the *m/z* values markedly, especially for the peaks with lower *m/z* values (≤*m/z* 400); only for the peaks with higher *m/z* values an improvement was obtained (see Table 14 and Table A8 in Appendix 1). The overall *m/z* errors for the mass spectrum of sandarac resin in case of internal calibration were between –1.15 and 1.89 ppm, for external calibration they ranged from 0.03 to 5.25 ppm. With high probability, the smaller difference between the *m/z* errors in the case of sandarac resins is caused by the fact that the overall intensity of the corresponding mass spectrum is very low; thus, better accuracy even in the case of external calibration is obtained. At the same time, the *m/z* errors obtained during the analysis of sandarac resin in the negative ion mode show clear correlation with the *m/z* value – the *m/z* errors are

higher at higher *m/z* values. This illustrates very well the need to have calibration standards distributed across the whole *m/z* range.

During the ion assignment, it was observed that all the peaks that are present in the negative ion mode mass spectra of dammar, mastic, sandarac, colophony and shellac resins are detected as anions formed via deprotonation (see Table 14 and Tables A6–A10 in Appendix 1). It was also observed that the ionisation efficiency of the terpenoid resins was lower compared to the analysis in positive ion mode. The decrease in ionisation efficiency was above all noticeable for the peaks (or the lack of them) corresponding to the polymerised fraction of the terpenoid resins. In the case of triterpenoids (dammar and mastic resins) only the first cluster of peaks (that corresponds to the original compounds and their derivatives) was detected in the mass spectra (see Figure 14). The negative ion mode mass spectra obtained from colophony and sandarac resins both displayed a second cluster of peaks but the intensities of these clusters were very low (see Figure 15). In fact, obtaining a good quality mass spectrum from sandarac resin in the negative ion mode proved to be a very difficult task. This is with high probability related to the fact that sandarac resin is mainly polymeric in its composition. [1, 3, 32, 34] The mass spectrum of shellac resin displays three clusters of peaks similarly to the mass spectrum of this resin obtained in the positive ion mode (see Figure 13c).

Similarly to the mass spectra obtained during the positive ion mode analysis, the clusters present in the negative ion mode mass spectra of the resins are composed of sub-clusters that illustrate the oxidation, (de)methylation, (de)hydrogenation, etc. processes. Compared to the results obtained during the analysis in the positive ion mode, generally compounds with a lower oxygen content were detected during the analysis in the negative ion mode. E.g. in the first cluster of peaks present in the positive ion mode mass spectrum of dammar resin compounds with up to 10 oxygen atoms were obtained. The number of oxygen atoms in case of the mass spectrum registered with the negative ion mode was 6. At the same time, there were numerous compounds present in the resins that would give ions in both polarities, thus, the mass spectra registered from resinous samples in the negative ion mode provided confirmation to the results obtained during the positive ion mode analysis.

Table 14. Summarised assignment of anion formulas corresponding to peaks of the negative ion mode mass spectra of dammar, mastic, sandarac, colophony, and shellac resins and the corresponding *m/z* errors for internal and external calibration.

Resin	Anion	Internal calibration		External calibration	
		Measured *m/z*	*m/z* error (ppm)	Measured *m/z*	*m/z* error (ppm)
Dammar	$C_{28}H_{39}O_3^-$	423.29029	–0.42	423.28415	–14.93
	$C_{29}H_{43}O_3^-$	439.32175	–0.05	439.31514	–15.08
	$C_{30}H_{45}O_3^-$	453.33765	0.51	453.33063	–14.98
	$C_{30}H_{45}O_4^-$	469.33229	–0.09	469.32477	–16.11
	$C_{30}H_{47}O_5^-$	487.34270	–0.41	487.33460	–17.03
	$C_{30}H_{45}O_6^-$	501.32258	0.83	501.31402	–16.25
Mastic	$C_{28}H_{39}O_2^-$	407.29594	0.94	407.29290	–6.51
	$C_{29}H_{41}O_2^-$	421.31127	0.15	421.30804	–7.51
	$C_{29}H_{43}O_3^-$	439.32179	0.05	439.31829	–7.91
	$C_{30}H_{45}O_3^-$	453.33790	1.07	453.33419	–7.12
	$C_{30}H_{45}O_4^-$	469.33228	–0.13	469.32831	–8.57
	$C_{30}H_{43}O_5^-$	483.31158	–0.04	483.30739	–8.71
	$C_{30}H_{43}O_6^-$	499.30636	–0.31	499.30190	–9.24
	$C_{30}H_{43}O_7^-$	515.30142	–0.02	515.29669	–9.21
Sandarac	$C_{19}H_{23}O_2^-$	283.17022	–0.49	283.17040	0.16
	$C_{20}H_{27}O_2^-$	299.20172	0.22	299.20195	0.98
	$C_{20}H_{27}O_3^-$	315.19653	–0.12	315.19681	0.76
	$C_{20}H_{29}O_4^-$	333.20728	0.42	333.20761	1.42
	$C_{30}H_{45}O_5^-$	485.32670	–1.14	485.32770	0.92
	$C_{40}H_{59}O_5^-$	619.43673	–0.11	619.43858	2.88
	$C_{40}H_{61}O_6^-$	637.44663	–1.15	637.44862	1.96
	$C_{40}H_{61}O_7^-$	653.44194	–0.51	653.44406	2.72
	$C_{40}H_{61}O_8^-$	669.43826	1.59	669.44049	4.93
Colophony	$C_{17}H_{23}O_3^-$	275.16507	–0.73	275.16573	1.67
	$C_{17}H_{23}O_4^-$	291.16008	–0.36	291.16085	2.27
	$C_{20}H_{27}O_3^-$	315.19664	0.23	315.19757	3.19
	$C_{20}H_{27}O_4^-$	331.19163	0.43	331.19268	3.62
	$C_{20}H_{29}O_5^-$	349.20248	1.24	349.20369	4.69
	$C_{20}H_{29}O_6^-$	365.19667	–0.81	365.19801	2.87
	$C_{37}H_{51}O_9^-$	639.35258	–2.00	639.35748	5.65
	$C_{40}H_{55}O_8^-$	663.38992	–0.49	663.39523	7.51
	$C_{40}H_{57}O_9^-$	681.40031	–0.73	681.40594	7.52

Table 14. Continued

Resin	Anion	Internal calibration		External calibration	
		Measured *m/z*	*m/z* error (ppm)	Measured *m/z*	*m/z* error (ppm)
Shellac	$C_{16}H_{29}O_4^-$	285.20708	–0.20	285.20626	–3.05
	$C_{16}H_{31}O_5^-$	303.21797	0.88	303.21704	–2.17
	$C_{14}H_{27}O_7^-$	307.17656	1.07	307.17561	–2.01
	$C_{30}H_{47}O_6^-$	503.33821	0.79	503.33565	–4.29
	$C_{31}H_{47}O_8^-$	547.32808	0.79	547.32505	–4.74
	$C_{32}H_{59}O_8^-$	571.42205	0.89	571.41875	–4.89
	$C_{32}H_{61}O_9^-$	589.43234	0.40	589.42883	–5.57
	$C_{46}H_{77}O_{10}^-$	789.55298	0.95	789.54666	–7.05
	$C_{47}H_{75}O_{11}^-$	815.53187	0.46	815.52512	–7.81
	$C_{47}H_{77}O_{12}^-$	833.54309	1.24	833.53604	–7.21

4.3.5 Assessment of the internal calibration process

The resins analysed during this study consist of a variety of compounds with different functionalities, including acidic functionalities. Therefore, these compounds can be analysed both in positive and negative ion modes. Thus, these components present a convenient way to assess the quality of the *m/z* accuracy and consistency of *m/z* axis calibration, and of molecular formula assignment as well.

For evaluating the accuracy obtained during internal calibration, measured *m/z* values were back-calculated to monoisotopic masses of the corresponding neutral species by the subtraction of the mass of H^+ or Na^+ (for positive ion mode) or the addition of mass of H^+ (for negative ion mode). The back-calculated monoisotopic masses of the matching compounds were compared. In Table 15, the information on some of the compounds that were detected in positive and negative ion modes is presented. As can be seen from Table 15, the back-calculated monoisotopic masses of neutral compounds are in very good agreement.

Table 15. Assessment of accuracy of *m/z* axes calibration and molecular formula assignment based on a selection of compounds detected in positive and negative ion mode mass spectra of dammar, mastic, sandarac, colophony and shellac resins.

Positive ion mode			Negative ion mode			Molecular formula	Δ (M_p–M_n)
Cation formula	**Measured *m/z***	**M_p[a]**	**Anion formula**	**Measured *m/z***	**M_n[a]**		
DAMMAR RESIN							
$C_{29}H_{43}O_2^+$	423.32545	422.31818	$C_{29}H_{41}O_2^-$	421.31099	422.31827	$C_{29}H_{42}O_2$	–0.00009
$C_{29}H_{46}O_3Na^+$	465.33398	442.34476	$C_{29}H_{45}O_3^-$	441.33696	442.34424	$C_{29}H_{46}O_3$	0.00052
$C_{29}H_{44}O_4Na^+$	479.31346	456.32424	$C_{29}H_{43}O_4^-$	455.31677	456.32405	$C_{29}H_{44}O_4$	0.00019
$C_{30}H_{50}O_4Na^+$	497.36011	474.37089	$C_{30}H_{49}O_4^-$	473.36335	474.37062	$C_{30}H_{50}O_4$	0.00027
$C_{30}H_{48}O_5Na^+$	511.33919	488.34997	$C_{30}H_{47}O_5^-$	487.34270	488.34997	$C_{30}H_{48}O_5$	0.00000
$C_{30}H_{44}O_6Na^+$	523.30321	500.31399	$C_{30}H_{43}O_6^-$	499.30684	500.31411	$C_{30}H_{44}O_6$	–0.00012
MASTIC RESIN							
$C_{29}H_{42}O_4Na^+$	477.29727	454.30805	$C_{29}H_{41}O_4^-$	453.30115	454.30842	$C_{29}H_{42}O_4$	–0.00037
$C_{29}H_{42}O_5Na^+$	493.29230	470.30308	$C_{29}H_{41}O_5^-$	469.29598	470.30325	$C_{29}H_{42}O_5$	–0.00017
$C_{30}H_{44}O_5Na^+$	507.30799	484.31877	$C_{30}H_{43}O_5^-$	483.31158	484.31886	$C_{30}H_{44}O_5$	–0.00009
$C_{30}H_{48}O_5Na^+$	511.33905	488.34983	$C_{30}H_{47}O_5^-$	487.34276	488.35004	$C_{30}H_{48}O_5$	–0.00021
$C_{30}H_{44}O_7Na^+$	539.29777	516.30855	$C_{30}H_{43}O_7^-$	515.30142	516.30869	$C_{30}H_{44}O_7$	–0.00014
$C_{30}H_{46}O_7Na^+$	541.31332	518.32410	$C_{30}H_{45}O_7^-$	517.31675	518.32402	$C_{30}H_{46}O_7$	0.00008
SANDARAC RESIN							
$C_{20}H_{30}O_4Na^+$	357.20366	334.21444	$C_{20}H_{29}O_4^-$	333.20728	334.21455	$C_{20}H_{30}O_4$	–0.00011
$C_{20}H_{32}O_5Na^+$	375.21444	352.22522	$C_{20}H_{31}O_5^-$	351.21746	352.22474	$C_{20}H_{32}O_5$	0.00048
$C_{30}H_{46}O_5Na^+$	509.32341	486.33419	$C_{30}H_{45}O_5^-$	485.32670	486.33397	$C_{30}H_{46}O_5$	0.00021
$C_{39}H_{58}O_6Na^+$	645.41351	622.42429	$C_{39}H_{57}O_6^-$	621.41667	622.42394	$C_{39}H_{58}O_6$	0.00034
$C_{40}H_{62}O_6Na^+$	661.44281	638.45359	$C_{40}H_{61}O_6^-$	637.44663	638.45390	$C_{40}H_{62}O_6$	–0.00032
$C_{40}H_{64}O_8Na^+$	695.44790	672.45868	$C_{40}H_{63}O_8^-$	671.45411	672.46139	$C_{40}H_{64}O_8$	–0.00271

Table 15. Continued

Positive ion mode			Negative ion mode			Molecular formula	Δ (M_p–M_n)
Cation formula	**Measured *m/z***	**M_p[a]**	**Anion formula**	**Measured *m/z***	**M_n[a]**		
COLOPHONY RESIN							
$C_{20}H_{29}O_2^+$	301.21644	300.20916	$C_{20}H_{27}O_2^-$	299.20142	300.20870	$C_{20}H_{28}O_2$	0.00047
$C_{20}H_{28}O_3Na^+$	339.19326	316.20404	$C_{20}H_{27}O_3^-$	315.19664	316.20392	$C_{20}H_{28}O_3$	0.00012
$C_{20}H_{30}O_4Na^+$	357.20377	334.21455	$C_{20}H_{29}O_4^-$	333.20715	334.21442	$C_{20}H_{30}O_4$	0.00013
$C_{20}H_{30}O_5Na^+$	373.19864	350.20942	$C_{20}H_{29}O_5^-$	349.20248	350.20976	$C_{20}H_{30}O_5$	–0.00033
$C_{20}H_{30}O_6Na^+$	389.19365	366.20443	$C_{20}H_{29}O_6^-$	365.19667	366.20394	$C_{20}H_{30}O_6$	0.00049
$C_{20}H_{30}O_7Na^+$	405.18892	382.19970	$C_{20}H_{29}O_7^-$	381.19151	382.19879	$C_{20}H_{30}O_7$	0.00092
$C_{40}H_{60}O_7Na^+$	675.42267	652.43345	$C_{40}H_{59}O_7^-$	651.42716	652.43443	$C_{40}H_{60}O_7$	–0.00098
SHELLAC RESIN							
$C_{16}H_{30}O_4Na^+$	309.20367	286.21445	$C_{16}H_{29}O_4^-$	285.20708	286.21435	$C_{16}H_{30}O_4$	0.00010
$C_{16}H_{32}O_5Na^+$	327.21422	304.22500	$C_{16}H_{31}O_5^-$	303.21797	304.22524	$C_{16}H_{32}O_5$	0.00024
$C_{31}H_{48}O_7Na^+$	555.32906	532.33984	$C_{31}H_{47}O_7^-$	531.33207	532.33934	$C_{31}H_{48}O_7$	0.00050
$C_{31}H_{48}O_8Na^+$	571.32421	548.33499	$C_{31}H_{47}O_8^-$	547.32808	548.33535	$C_{31}H_{48}O_8$	–0.00036
$C_{46}H_{66}O_{12}Na^+$	833.44467	810.45545	$C_{46}H_{65}O_{12}^-$	809.44899	810.45627	$C_{46}H_{66}O_{12}$	–0.00082
$C_{47}H_{78}O_{12}Na^+$	857.53826	834.54904	$C_{47}H_{77}O_{12}^-$	833.54309	834.55037	$C_{47}H_{78}O_{12}$	–0.00133
$C_{47}H_{80}O_{13}Na^+$	875.54903	852.55981	$C_{47}H_{79}O_{13}^-$	851.55233	852.55961	$C_{47}H_{80}O_{13}$	0.00020

[a] M_p is the monoisotopic mass of neutral species calculated by subtracting the exact mass of H^+ or Na^+ from the measured *m/z* obtained in positive ion mode; M_n is the monoisiotopic mass of neutral species calculated by adding the exact mass of H^+ to the measured *m/z* obtained in negative ion mode.

4.3.6 Main conclusions

During this stage of the study, a MALDI-FT-ICR-MS methodology suitable for the analysis of resinous materials in both, positive and negative ion mode was developed:

- a novel negative ion mode matrix compound, 2-AA and numerous new calibration standards – phosphazenes and sulpho-compounds – for both ionisation modes were successfully added to the MALDI-FT-ICR-MS methodology;
- the sample preparation procedure and set of instrument parameters was thoroughly modified (see Experimental section for more information) in order to incorporate the new materials into the methodology.

The mass spectra of resinous materials obtained with 2-AA have good ion intensities (compared to the results obtained with 9-AA), and lack in the distracting peaks that sometimes are caused by matrix material. 2-AA ionises the components of the resinous materials with satisfactory efficiency, thus, the amount of information obtained from these materials is increased.

The suggested phosphazenes and sulpho-compounds were found to be very suitable for internal calibration of *m/z* axes of positive and negative ion mode mass spectra, respectively. These compounds readily give ions with desired polarity, at the same time, they do not suppress the ionisation of the analyte.

It was noticed during the study that the *m/z* errors in case of positive ion mode mass spectra were generally higher compared to the values obtained during the analysis in the negative ion mode. This is with high probability related to the fact that the intensities of the negative ion mode mass spectra were lower than the intensities of the positive ion mode mass spectra. Thus, the ionisation efficiency of resins is higher in positive ion mode.

During the analysis of resins in the positive ion mode, the ions were mostly identified as sodium adducts, protonated ions were detected rarely. Therefore, more information was obtained about the compounds with higher oxygen content. In addition, also polymerised/oligomerised components of the resins were observed during the positive ion mode analysis. During the analysis of resins in the negative ion mode, all the peaks present in the mass spectra corresponded to deprotonated ions. Compared to the analysis in positive ion mode, generally ions with lower number of oxygen atoms in them were detected.

In conclusion, the new MALDI-FT-ICR-MS methodology is convenient (sample preparation is quick and easy), flexible (the opportunity to performed the analysis in positive and negative ion mode), and provides high accuracy data about resinous materials in both ionisation modes. In addition, all the *m/z* values in the obtained mass spectra of the analysed natural resins that are discussed in this thesis, can be used as reference data for the identification of real-life samples (see section 4.4).

4.4 Application of the modified MALDI-FT-ICR-MS methodology for the analysis of real-life resinous samples

The developed MALDI-FT-ICR-MS methodology was put to the test during the analysis of three real-life resinous samples in order to evaluate the capability and suitability of 2-AA, the novel internal standards and the modified sample preparation procedure.

4.4.1 The analysis of the varnish sample from the drop-leaf sewing table [III]

The drop-leaf sewing table originally belonged to the Kurisoo manor in Aravete, Estonia. The table is made from Brazilian rosewood and decorated with marquetry and carved details. During the 19th century, this kind of tables were common in Estonian manors but very few of them have survived. In the 1920s the table was sold on an auction and for approximately 60 years its location was unknown. In 1985, the table was donated to the Estonian National Museum in the poor state that is demonstrated on Figure 16a.

In 2012/2013, the table underwent conservation (and partial restauration) to preserve the beautiful specimen. The fully restored table can be seen in Figure 16b.

Figure 16. The 19th century drop-leaf sewing table a) before and b) after conservation. Conservation work was done by Indrek Tirrul (wood conservator at Estonian National Museum). The photos are taken by Anu Ansu and Merilyn Suve.

The aim of the varnish analysis was to determine the composition of the varnish.

The varnish sample from the drop-leaf sewing table was analysed with the modified MALDI-FT-ICR-MS methodology in positive and negative ion mode, the corresponding mass spectra are presented in Figure 17a and Figure 17b, respectively. The ion assignments of some of the more prominent peaks detected in the positive and negative ion mode mass spectra are presented in Table 16 (along with the *m/z* errors obtained during internal and external calibration of the *m/z* axes).

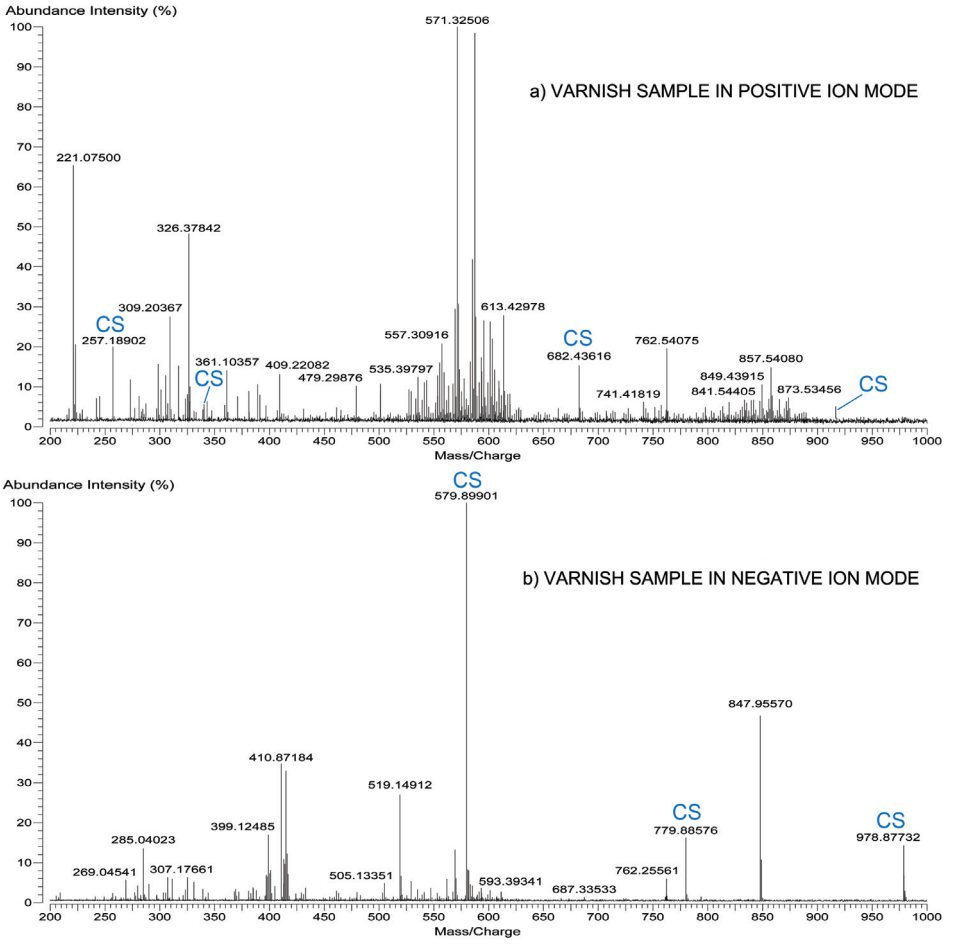

Figure 17. The mass spectra with internally calibrated *m/z* axes of the drop-leaf sewing tables' varnish sample in a) positive ion mode and b) negative ion mode.

The mass spectrum obtained from the tables' varnish sample in the positive ion mode displays three clusters of peaks while the mass spectrum registered in negative ion mode has two clusters. The peaks present in the mass spectrum obtained in the negative ion mode have considerably lower intensities, at the same time, they still present valuable information about the sample (see Table 16).

The ion formulas identified in the mass spectra with internally calibrated *m/z* axes were compared to the corresponding information obtained from the above discussed natural resins. The mass spectra of the varnish sample contain numerous peaks that match the peaks detected in the positive and negative ion mode mass spectra of shellac resin (see Table 16 and Table A2 and Table A10 in Appendix 1). In addition, the peak at *m/z* 325.19854 in the positive ion mode mass spectrum of the varnish sample is assigned as $C_{16}H_{30}O_5Na^+$. This corresponds to the sodium adduct of aleuritic acid ($C_{16}H_{30}O_5$) that is considered as the main compound in shellac resin. [1] The same compound can also be identified in the negative ion mode mass spectrum at *m/z* 303.21783 as a deprotonated molecule.

Table 16. Summarised assignment of ion formulas corresponding to peaks of the positive and negative ion mode mass spectra obtained from the varnish sample of the drop-leaf sewing table.

Assigned ion	Internal calibration		External calibration	
	Measured *m/z*	*m/z* error (ppm)	Measured *m/z*	*m/z* error (ppm)
POSITIVE ION MODE				
$C_{16}H_{30}O_4Na^+$	309.20367	0.12	309.21188	26.69
$C_{16}H_{30}O_5Na^+$	325.19854	–0.03	325.20766	28.03
$C_{31}H_{48}O_7Na^+$	555.33024	1.83	555.35774	51.34
$C_{31}H_{48}O_8Na^+$	571.32506	1.60	571.35419	52.60
$C_{31}H_{48}O_9Na^+$	587.31985	1.35	587.35068	53.84
$C_{32}H_{62}O_9Na^+$	613.42978	1.92	613.46347	56.84
NEGATIVE ION MODE				
$C_{16}H_{31}O_5^-$	303.21783	0.43	303.21481	–9.54
$C_{14}H_{27}O_7^-$	307.17661	1.23	307.17351	–8.85
$C_{14}H_{27}O_8^-$	323.17065	–1.53	323.16726	–12.02
$C_{29}H_{45}O_{11}^-$	569.29834	2.81	569.28862	–14.26
$C_{32}H_{59}O_8^-$	571.42044	–1.94	571.41065	–19.07

As indicated in Table 16, the *m/z* errors obtained during the analysis of the varnish sample from the table were significantly reduced by internal calibration. The improvement was particularly noticeable for the *m/z* errors obtained in the positive ion mode mass spectrum, where the *m/z* errors in the externally calibrated mass spectrum ranged from 27 to 57 ppm (for the peaks presented in Table 16). Internal calibration helped to reduce the *m/z* errors to a range of –0.03 to 1.92 ppm. Thereby, also the risk of misinterpretation was drastically lowered. E.g. in the positive ion mode mass spectrum of the varnish sample, the peak at nominal *m/z* 571 can be assigned in case of internally calibrated *m/z* axis as $C_{31}H_{48}O_8Na^+$. This ion corresponds with high probability to a compound that originates from an ester of an aliphatic acid and a sesquiterpenoid compound,

e.g. the ester of aleuritic and jalaric acids after the loss of H_2O or the oxidised ester of aleuritic acid and laccijalaric acid with the loss of one water molecule, etc. [3] The same peak in the mass spectrum with externally calibrated *m/z* axis corresponds to $C_{39}H_{48}O_2Na^+$ and can hardly be assigned to a resinous compound.

Therefore, it was concluded that the varnish used for the 19th century drop-leaf sewing table contains with high probability shellac resin. The analysis of the varnish sample also demonstrates well the applicability of the developed MALDI-FT-ICR-MS methodology. The high accuracy *m/z* values obtained with the use of novel internals standards reduced the risk of wrong ion assignments. The mass-spectrometric data obtained with the novel matrix compound during the analysis in the negative ion mode enabled to confirm the results gained with positive ion mode MALDI-FT-ICR-MS.

4.4.2 The analysis of the resinous material obtained from the 16th century ship wreck

In the summer of 2015, a wreck of an unknown ship was found near the Island of Naissaar in the Tallinn Bay (part of the Baltic Sea, Northern Estonia) and the object was named "Nargen 1" by the Estonian Maritime Museum. The wreck itself is in a very poor state, the shape and size of the vessel is only predictable: the wooden ship is about 18 m long and 6.5 m wide. Therefore, the dating of the ship is mainly based on the finds that were scattered on the sea bed in and around the wreck.

The site contained numerous ceramic artefacts, mainly common household pottery but also a collection of globular vessels with bungholes and a collection of smaller cylindrical jars (red- and whiteware, also glass) commonly found in connection of Early Modern Age pharmacy equipment (see Figure 18, also Fig. 7 in reference [92]). The key object in determining the time the ship was used is a German tankard that was found on the site (see Fig. 4 in reference [92]). These kinds of tankards were produced in Siegeburg, Germany between the years of 1550 and 1590, and the specific tankard was dated to the 1570s. Combining all the information, it was concluded that with high probability the ship was a *bojer*-type sailing ship with a cargo of pharmaceuticals and pharmacy equipment but unfortunately it sank, probably somewhere in the late 16th century. [92]

The resinous sample analysed during the study was found in one of the smaller jars depicted in Figure 18 (bottom row of jars, the height of the smaller jars is approximately 5 cm). The aim of the analysis was to determine the type of material the ointment jar contained.

On visual inspection, the sample is dark brown but under the optical microscope a more colourful picture emerges (see Figure 19). The sample is partially viscous but has also areas that have crystallised. The sample has a very strong sweet smell that resembles to resins obtained from conifers.

Figure 18. A collection of pharmaceutical artefacts found from the "Nargen 1": four rows of ointment jars (red glaze) and two albarelli (green glaze). Photo taken by Vello Mäss (Estonian Maritime Museum, Tallinn, Estonia).

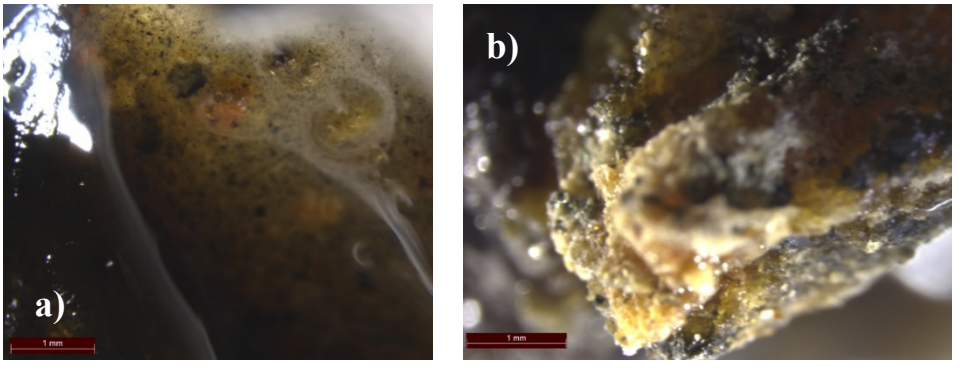

Figure 19. The resinous sample from the ointment jar from the 16th century ship: a) the viscose part of the sample and b) the crystalline part of the sample.

The resinous sample was analysed in positive and negative ion mode with the developed MALDI-FT-ICR-MS methodology and the corresponding mass spectra can be found in Figure 20. The assignment of ions for both ionisation modes is summarised in Table 17, the table also contains information about the *m/z* errors obtained in case of internal and external calibration of the *m/z* axes of the mass spectra.

Table 17. Summarised assignment of ion formulas corresponding to peaks of the positive and negative ion mode mass spectra obtained from the resinous material from the 16th century shipwreck.

Assigned ion	Internal calibration		Externel calibration	
	Measured *m/z*	*m/z* error (ppm)	Measured *m/z*	*m/z* error (ppm)
POSITIVE ION MODE				
$C_{15}H_{15}^+$	195.11674	–0.45	195.12030	17.79
$C_{18}H_{21}^+$	237.16386	0.38	237.16921	22.92
$C_{18}H_{23}^+$	239.17952	0.40	239.18496	23.15
$C_{20}H_{29}O_2^+$	301.21640	0.65	301.22517	29.75
$C_{20}H_{30}O_4Na^+$	357.20374	0.31	357.21618	35.13
$C_{40}H_{58}O_5Na^+$	641.41788	0.36	641.45885	64.24
$C_{40}H_{58}O_6Na^+$	657.41305	0.75	657.45613	66.27
$C_{40}H_{58}O_7Na^+$	673.40824	1.13	673.45346	68.29
$C_{40}H_{58}O_8Na^+$	689.40296	0.83	689.45039	69.62
$C_{40}H_{58}O_9Na^+$	705.39716	–0.21	705.44684	70.22
NEGATIVE ION MODE				
$C_{15}H_{15}O_2^-$	227.10781	0.22	227.11205	18.93
$C_{15}H_{15}O_3^-$	243.10263	–0.19	243.10750	19.86
$C_{18}H_{21}O_2^-$	269.15484	0.49	269.16082	22.70
$C_{20}H_{29}O_2^-$	301.21753	0.74	301.22502	25.63
$C_{20}H_{33}O_2^-$	305.24907	1.51	305.25676	26.73
$C_{20}H_{29}O_3^-$	317.21216	–0.18	317.22048	26.04
$C_{20}H_{29}O_4^-$	333.20710	–0.11	333.21628	27.44

In the positive ion mode mass spectrum of the unknown resinous material (see Figure 20a), a cluster of peaks in the region of *m/z* 625–725 is prominent, the peaks present in this cluster are assigned as terpenoids with 40 carbon atoms in their skeletons (see Table 17). In addition, also diterpenoids are detected in this mass spectrum, e.g. the peak at *m/z* 357.20374 is assigned as $C_{20}H_{30}O_4Na^+$. This implies that the resinous material contains with high probability a diterpenoid resin.

As can be seen from Figure 2, the ion assigned above may refer to several compounds present in diterpenoid resins (like abietic, pimaric, sandaracopimaric and neoabietic acids, also totarol and ferruginol). The key peaks that initially enable the identification of this resinous material are found in the region under *m/z* 300 (see Table 17). The *m/z* values of these peaks (along with other peaks identified in the positive ion mode mass spectrum of the resinous material) were compared to the corresponding values detected in the mass spectra of sandarac and colophony resins (see Tables A4 and A5 in Appendix 1). Similar peaks (assigned to the same ions) were detected also in the mass spectrum of colophony

resin and therefore, it can be concluded that the resinous material is with high probability related to pine resin (or tar).

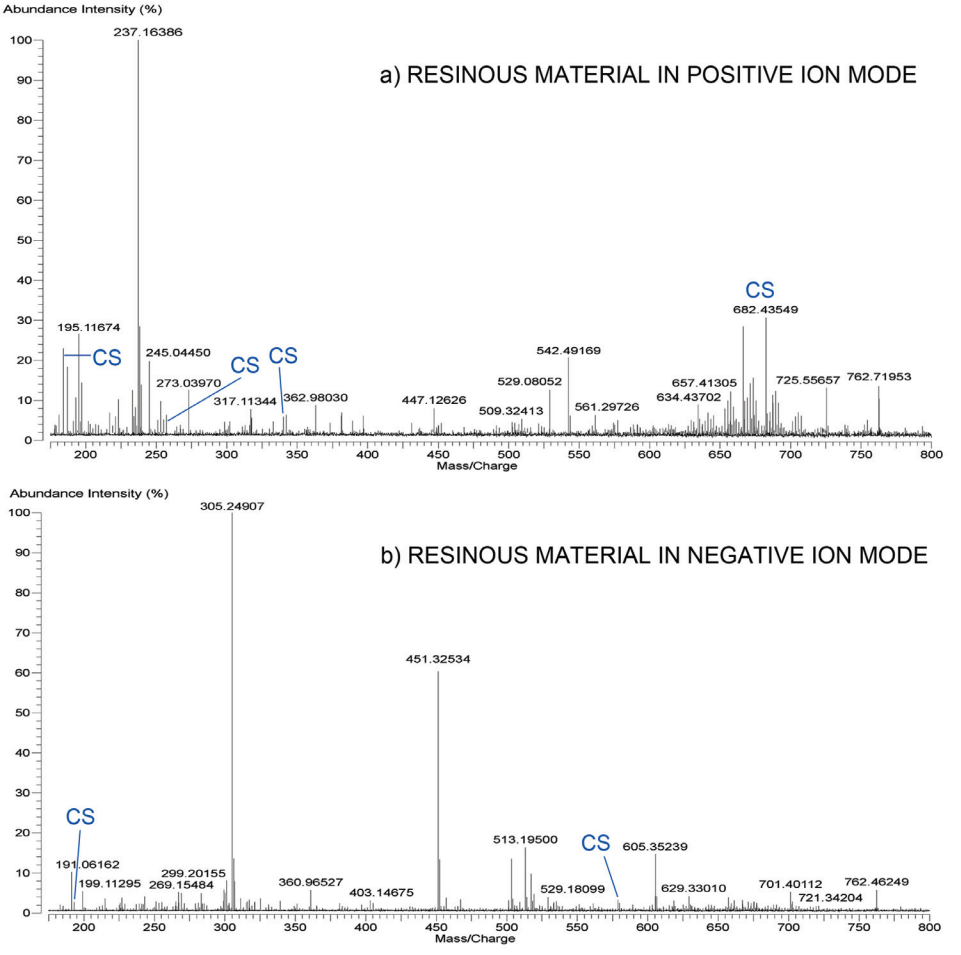

Figure 20. The mass spectra of the resinous material obtained from the 16th century ship a) in positive ion mode and b) in negative ion mode.

The results obtained during the negative ion mode analysis of the resinous material confirmed the assumption that the sample is related to pine resin. Again, peaks corresponding to diterpenoids were detected in the mass spectrum depicted in Figure 20b. E.g. the peak at *m/z* 301.21753 is assigned as $C_{20}H_{29}O_2^-$ and with high probability it corresponds to deprotonated abietic acid.

The identification of this sample relied mostly on the comparison of the *m/z* values present in the mass spectra obtained from the natural resins and from the analysed sample. Therefore, the improvement of *m/z* accuracy obtained with the help of internal standards was very important. As can be seen from Table 17, the *m/z* errors were drastically lowered in the case of internal calibration for the

positive and negative ion mode analysis. Therefore, also the trustworthiness of the results obtained during the analysis of the unknown resinous sample was increased. The opportunity to register the mass spectrum in the negative ion mode provided additional confirmation that the resinous material obtained from the 16th century shipwreck is with high probability a product of pine resin.

4.4.3 The analysis of the varnish sample from the 19th century painting "Dream" [III]

Wilhelm Kotarbiński (1848–1921) was a Polish symbolist painter who is mainly known for fantastical and historical themed paintings but also had a religious (orthodox) period. The painting "Dream" ("Unenägu" in Estonian) is an oil painting on canvas (122 × 56 cm) that is dated to the period 1875–1900.

The painting was brought to the Conservation and Digitization Centre Kanut in 2006 for restoration. The painting was physically damaged (see Figures 21a, 21c and 21d). Extensive yellowing of the varnish layer was revealed during the removal of the varnish (see Figures 21a and 21b). To identify the varnish used for the painting, the sample was analysed with the modified MALDI-FT-ICR-MS methodology.

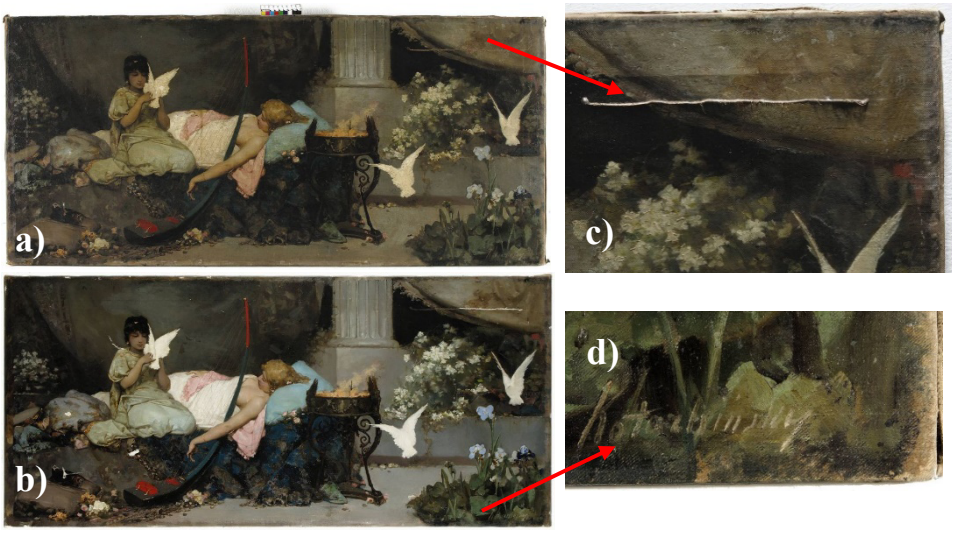

Figure 21. The painting "Dream" a) before the removal of the varnish layer and b) after the removal of the varnish layer, c) an example of the physical damage on the painting and d) the signature of the painter. Photos by Jaanus Heinla (Conservation and Digitization Centre Kanut, Tallinn, Estonia).

The analysis of the varnish sample from the painting "Dream" was carried out only in the positive ion mode and the corresponding mass spectrum is presented in Figure 22. Obtaining a satisfactory mass spectrum from this sample in the

negative ion mode proved to be impossible. With high probability, this is caused by the low ionisation efficiency of the extensively polymerised compounds of the more than 100-year-old sample. In addition, the size of the sample was extremely low: approximately 0.15 mg of the sample was used for the MALDI-FT-ICR-MS analysis.

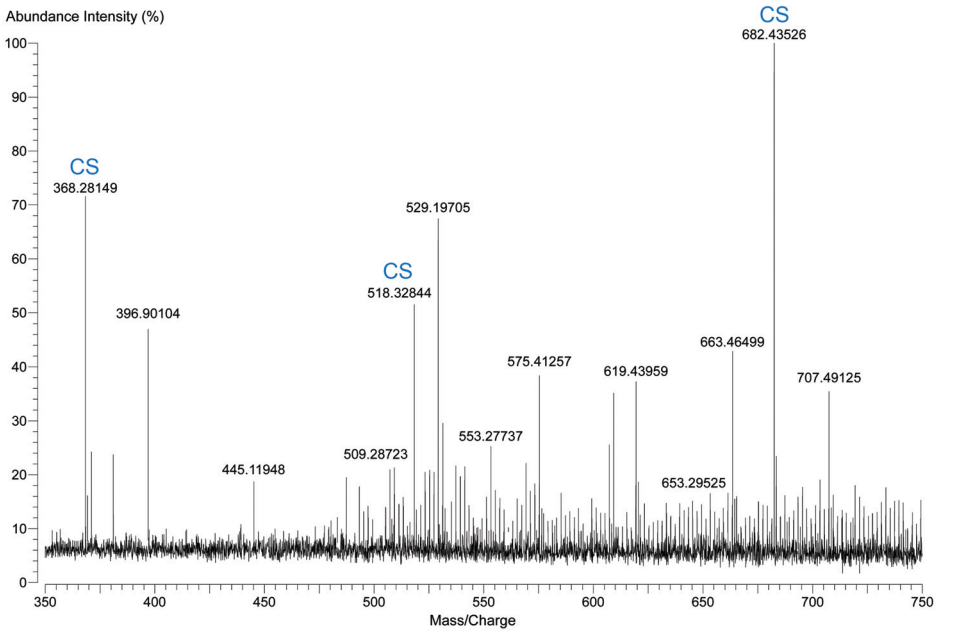

Figure 22. The positive ion mode mass spectrum (with internally calibrated *m/z* axis) of the varnish sample from the painting "Dream".

In Table 18, the ion assignments for some of the more prominent peaks present in the mass spectrum of the varnish sample are presented (along with the corresponding *m/z* errors in case of internal and external calibration).

As can be seen from Table 18, the *m/z* errors were slightly improved during the internal calibration of the *m/z* axis. This can be explained by the low intensity of the mass spectrum obtained from the varnish sample. This in turn may be caused by the amount of sample, also, the ionisation efficiency of aged, thus, highly polymerised materials is low.

The peaks present in the mass spectrum of the varnish sample are detected as sodium adducts but occasionally also protonated ions are observed (see Table 18). A high number of the peaks are identified as ions corresponding to compounds with C_{30} and C_{29} skeletons. This suggests that the resin used for the varnish is a triterpenoid. As mentioned above, there are two triterpenoid resins that give good-quality picture varnishes – mastic and dammar resin. The composition of these two resins is very similar and therefore, reliable discrimination between them purely on the basis of mass spectra is very difficult. Especially in the case where the material has presumably aged for over 100 years.

Table 18. Summarised assignment of ion formulas corresponding to peaks of the positive ion mode mass spectrum obtained from the varnish sample of the painting "Dream".

Assigned cation	Internal calibration		External calibration	
	Measured *m/z*	*m/z* error (ppm)	Measured *m/z*	*m/z* error (ppm)
$C_{29}H_{43}O_2^+$	423.32632	1.33	423.32439	–3.22
$C_{29}H_{41}O_4^+$	453.30054	1.34	453.29838	–3.42
$C_{30}H_{43}O_4^+$	467.31565	0.14	467.31338	–4.72
$C_{29}H_{44}O_5Na^+$	495.30861	1.05	495.30610	–4.03
$C_{30}H_{46}O_6Na^+$	525.31880	0.27	525.31603	–5.01
$C_{30}H_{46}O_7Na^+$	541.31353	–0.08	541.31061	–5.48
$C_{30}H_{46}O_8Na^+$	557.30883	0.61	557.30575	–4.91
$C_{30}H_{44}O_9Na^+$	571.28848	1.26	571.28527	–4.36

Nevertheless, the analysis of this sample demonstrates the capability of the developed MALDI-FT-ICR-MS methodology to obtain high accuracy data even from such problematic and complex materials. All in all, it can be concluded that the varnish used for the painting "Dream" contains a triterpenoid resin.

4.4.4 Main conclusions

The analysis of real-life resinous materials demonstrated the capabilities of the developed MALDI-FT-ICR-MS methodology very well. The methodology enables the investigation of samples that are:

- small in size – mass spectra were obtained from samples as small as 0.15 mg;
- aged and degraded;
- partially insoluble.

With the help of the novel internal standards mass spectra with high accuracy, thus, with a great number of valuable information were obtained. With the new matrix compound negative ion mode mass spectra are obtained that provide additional information about the sample. This data can be used to confirm the results obtained during the positive ion mode analysis.

At the same time, the analysis of aged resinous materials with the negative ion mode MALDI-FT-ICR-MS proved to be one of the challenges during this study. The ionisation efficiency of such materials has decreased, especially the efficiency to give negative ions. During the ageing process, the resinous compounds, terpenoids in particular, oxidise extensively and this leads to compounds that rather give adducts with sodium cations (or other alkali metal cations) than protonated ions. The number of deprotonation centres decreases also during oxidation and therefore, the efficiency to give negative ions drops.

SUMMARY

The aim of this study was to develop a MALDI-FT-ICR-MS methodology for the analysis of somewhat problematic material type – resinous materials.

The development of the methodology included (1) the testing of DHB as a matrix and possible internal calibration compound for the analysis of resinous materials, (2) the incorporation of a new matrix material, 2-aminoacridine, for the analysis of resinous materials in the negative ion mode, (3) use of novel internal standards that allow to obtain more accurate data from resinous materials, (4) the modification of sample preparation procedure, and (5) the acquiring of set of MALDI-FT-ICR-MS parameters most suitable for the analysis of different types of resinous materials.

The suggested matrix material (2-AA) enabled obtaining good-quality negative ion mode mass spectra from resinous samples that provided additional information about these materials. 2-AA helps to ionise the components of the resin with good efficiency. At the same time, the matrix compound itself gives only a small number of peaks in the mass spectra and does not interfere with the analytes (or the calibration standards). As an added value, the peak corresponding to the deprotonated anion of 2-AA can be used for internal calibration, thus, the calibration area for the negative ion mode mass spectra is expanded towards the lower *m/z* region.

The new calibration standards proved to be very useful additions to the MALDI-FT-ICR-MS methodology. In total, 15 phosphazenium cations covering the *m/z* range from *m/z* 257 to *m/z* 916 and 4 fluorine-rich sulpho-compounds yielding anions in the *m/z* range of 410–978 were introduced. These compounds have excellent ionisation efficiencies, thus the amount of internal standards needed for the analysis is very low. At the same time, the novel calibration standards do not hinder the ionisation of the analytes, they do not produce fragments or adduct ions (sodium adducts, etc.) nor do they react with the analyte or matrix molecules/ions. The suggested calibration compounds can be added to the sample or matrix solution to facilitate a more convenient sample preparation procedure.

The capabilities of the developed MALDI-FT-ICR-MS methodology were highlighted during the analysis of three real-life resinous samples: the varnish sample from the 19th century drop-leaf table, the resinous material found on the 16th century shipwreck and the varnish sample from the 19th century painting "Dream" by W. Kotarbiński. The results obtained from the analysis of real-life samples provided mass spectra with high *m/z* accuracy and good resolution. These features in turn helped to identify the materials (or material types) under investigation.

In conclusion, the MALDI-FT-ICR-MS methodology for the analysis of resinous samples developed during this study enabled obtaining a large amount of high-accuracy information from very small samples (approximately 0.15 mg) that were occasionally difficult to dissolve. The work provides a solid basis for

the future investigations of resinous materials with MALDI-FT-ICR-MS thanks to the thorough knowledge about the key aspects regarding the sample preparation and sets of parameters collected during this study. In addition, the high-accuracy mass spectra obtained from the resins are very valuable reference materials for the identification of unknown samples.

KOKKUVÕTE

Metoodika arendus MALDI-FT-ICR-MS rakendamiseks vaiguliste ainete analüüsil

Käesoleva uurimistöö eesmärgiks oli MALDI-FT-ICR-MS metoodika arendus vaiguliste materjalide analüüsimiseks.

Töö hõlmas endas (1) DHB sobivuse hindamist maatriksaine ning sisekalibrandina vaiguliste materjalide analüüsimisel, (2) uue negatiivse režiimi maatriksaine, 2-aminoakridiini, rakendamist vaiguliste materjalide analüüsimiseks, (3) uudsete sisekalibreerimisstandardite kasutusele võtmist, eesmärgiga tõsta vaigulistest materjalidest registreeritud massisspektromeetriliste andmete täpsust, (4) proovi ettevalmistust ja (5) MALDI-FT-ICR-MS mõõtmisparameetrite komplektide modifitseerimist vastavalt uuritud vaigulise aine tüübile.

Uuringu käigus avastatud uus maatriksaine, 2-AA, võimaldas vaigulistest proovidest saada hea kvaliteediga negatiivses režiimis registreeritud massispektreid, mis andsid täiendavat informatsiooni materjali koostise kohta. Leiti, et 2-aminoakridiin ioniseerib hästi vaigu komponente, samas ei põhjusta maatriksaine ise massispektritesse segavaid piike. 2-AA ei reageeri vaiguliste ainete ega sisekalibrantidega ning selle enda piikide arv massispektrites on madal. Siiski detekteeriti kõigis 2-aminoakridiini abiga registreeritud vaiguliste ainete massispektrites maatriksaine deprotoneerunud aniooni piik, mis oli oluliseks abiks sisekalibreerimisel. Tänu sellele piigile oli võimalik laiendada vaiguliste ainete negatiivsete massispektrite kalibreerimisala madalamate *m/z* väärtuste suunas.

Väljapakutud kalibeerimisstandardid osutusid samuti väga kasulikuks täienduseks MALDI-FT-ICR-MS metoodikale. Uurimistöö käigus testiti kokku 15 fosfaseeni, mis annavad katioone *m/z* vahemikus 257–916 ja 4 fluoririkast sulfo-ühendit, mille anioonid katavad *m/z* vahemiku 410–978. Rakendatud sisekalibrante iseloomustab suurepärane ioniseerumisefektiivsus, seega on analüüsiks vaja väga väikest kogust kalibrante. Samal ajal ei põhjusta uued kalibrandid analüüsitava aine signaali mahasurumist. Kalibrandid ei tekita massispektritesse fragmente ega aduktioone, lisaks ei täheldatud, et kalibrandid oleks uuritava materiali või maatriksainega reageerinud.

Väljatöötatud MALDI-FT-ICR-MS metoodika võimekust hinnati reaalsetelt objektidelt pärit vaiguliste proovide analüüsimisel. Uurimisel olid 19. sajandist pärit käsitöölaua lakiproov, 16. sajandist pärit laevavarkilt leitud vaiguline proov ja 19. sajandi lõpust pärit W. Kotarbiński maali "Unenägu" lakiproov. Nende proovide analüüsimisel saadi kõrge *m/z* täpsuse ja hea resolutsiooniga massispektrid, mille abil oli võimalik tuvastada tundmatu koostisega vaiku sisaldavaid materjale (või vaiguliste materjalide tüüp).

Antud uurimistöö raames töötati välja hea võimekusega MALDI-FT-ICR-MS metoodika, mis võimaldab korraga koguda suurel hulgal väga hea *m/z* täpsusega informatsiooni vaiguliste ainete koostisosade kohta. Väljatöötatud metoodika lisaväärtuseks on asjaolu, et sellist informatsiooni on võimalik saada ka

proovidest, mille kogus on väike (umbes 0.15 mg) ning mille lahustuvus on kehv. Uurimistöö käigus saadud praktilised teadmised prooviettevalmistuse ja parameetrikomplektide modifitseerimise kohta annavad tugeva aluse edasisteks MALDI-FT-ICR-MS uuringuteks vaiguliste materjalide alal. Töös puhaste looduslike vaikude kohta kogutud massispektromeetrilised andmed on heaks võrdlusmaterjaliks tundmatu koostisega vaiguliste proovide tuvastamisel.

ACKNOWLEDGMENTS

I would like to thank the Institute of Chemistry and the University of Tartu for offering the possibility and providing the necessary knowledge and facilities in order to successfully enter my journey in the world of science.

My greatest appreciation goes to my supervisors, research fellow Signe Vahur and professor Ivo Leito, for the constant support and guidance offered during the entire project.

I would also like to thank all the co-authors, including my supervisors, of the publications I–III presented in this PhD thesis: Piia Liigand (Burk), Sofja Tshepelevitsh, Tõiv Haljasorg, Ivari Kaljurand, Lauri Toom, Toomas Rodima, Koit Herodes, and Märt Lõkov from the Chair of Analytical Chemistry at the Institute of Chemistry, University of Tartu; Uku Haljasorg from the Institute of Biomedicine, University of Tartu; Werner Bonrath and Thomas Netscher from DSM Nutritional Products (Switzerland); and Aleksander Trummal from the National Institute of Chemical Physics and Biophysics (Estonia).

I am very grateful to all my colleagues at the Chair of Analytical Chemistry. A big thank you to Ester, Pilleriin and Anne Mari for the discussions about MALDI-FT-ICR-MS, and to Ivari, Tõiv and Charly for the technical support on the instrument.

Also, a big thank you to all my former colleagues at the Estonian Health Board Tartu Laboratory for allowing and encouraging me to embark on this journey.

I am thankful to the Estonian National Museum, Estonian Maritime Museum, the Narva Museum, and the Conservation and Digitization Centre Kanut for providing me with such interesting samples and for offering me additional materials, consultations, and support throughout the analysis of them.

My greatest appreciation and thanks goes to my family and friends who patiently listened to my monologues and offered support and help when I was losing track. My deepest and heartfelt thanks belong to my daughter and fiancé. Thank you, Emma, for inspiring me from day to day, thank you, Kristo, for keeping calm and collected.

This work was supported by the Estonian National R & D infrastructure development program of Measure 2.3 ‘Promotion of development activities and innovation’ (Regulation No. 34) funded by the Enterprise Estonia Foundation; by the EU through the European Regional Development Fund (TK141 and TK134); by the Institutional Funding IUT20-14, IUT23-7 and IUT23-9, and by the Personal Research Funding PUT1521 from the Estonian Ministry of Education and Research; by the grant No 8689 from the Estonian Science Foundation; by the UT Centre of Excellence “High-Technology Materials for Sustainable Development” (SLOKT117T) and by the target financing project SF0180061s08 from the Estonian Ministry of Education and Science.

REFERENCES

1. Mills, J.; White, R. *Organic chemistry of museum objects*, 2nd edition; Butterworth-Heinemann: Oxford, UK, 2003.
2. Langenheim, J. H. *Plant resins: chemistry, evolution, ecology, and ethnobotany*; Timber Press, Inc.: Portland, USA, Cambridge, UK, 2003.
3. Colombini, M. P.; Modugno, F. *Organic mass spectrometry in art and archaeology*; John Wiley & Sons, Ltd.: Chichester, UK, 2009.
4. Derrick, M. R.; Stulik, D. C.; Landry, J. M. *Infrared spectroscopy in conservation science. Scientific tools for conservation.*; Getty Publications, 1999.
5. de la Rie, E. R. *Anal. Chem.* **1989**, *61* (21), 1228–1240.
6. Larjavaara, M. *New Phytol.* **2014**, *202* (2), 344–349.
7. Masschelein-Kleiner, L. *Ancient binding media, varnishes and adhesives*; ICCROM: Rome, 1995.
8. van der Doelen, G. A.; van den Berg, K. J.; Boon, J. J.; Shibayama, N.; de la Rie, E. R.; Genuit, W. J. L. *J. Chromatogr. A*. **1998**, *809* (1–2), 21–37.
9. Dietemann, P.; Kälin, M.; Zumbühl, S.; Knochenmuss, R.; Wülfert, S.; Zenobi, R. *Anal. Chem.* **2001**, *73* (9), 2087–2096.
10. Scalarone, D.; Duursma, M. C.; Boon, J. J.; Chiantore, O. *J. Mass Spectrom.* **2005**, *40* (12), 1527–1535.
11. Dietemann, P.; Edelmann, M. J.; Meisterhans, C.; Pfeiffer, C.; Zumbühl, S.; Knochenmuss, R.; Zenobi, R. *Helv. Chim. Acta.* **2000**, *83* (8), 1766–1777.
12. Papageorgiou, V. P.; Bakola-Christianopoulou, M. N.; Apazidou, K. K.; Psarros, E. E. *J. Chromatogr. A.* **1997**, *769* (2), 263–273.
13. Assimopoulou, A. N.; Papageorgiou, V. P. *Biomed. Chromatogr.* **2005**, *19* (4), 285–311.
14. van den Berg, K. J.; van der Horst, J.; Boon, J. J.; Sudeijer, O. O. *Tetrahedron Lett.* **1998**, *39* (17), 2645–2648.
15. Edwards, H. G. M.; Vandenabeele, P. *Analytical archaeometry. Selected topics*; The Royal Society of Chemistry: Cambridge, UK, 2012.
16. Scalarone, D.; Lazzari, M.; Chiantore, O. *J. Anal. Appl. Pyrolysis*. **2003**, *68–69*, 115–136.
17. Horie, C. V. *Materials for conservation: organic consolidants, adhesives and coatings*; Butterworth-Heinemann: Oxford, UK, 2010.
18. Fiebach, K.; Grimm, D. *Resins, natural. Ullmann's encyclopedia of industrial chemistry*; Wiley-VCH Verlag GmbH & Co. KGaA, Weinheim, 2000.
19. Farag, Y. Characterization of different shellac types and development of shellac-coated dosage forms; Hamburg University: Hamburg, Germany, 2010.
20. Unger, A.; Schniewind, A. P.; Unger, W. *Conservation of wood artifacts – a handbook*; Springer-Verlag Berlin Heidelberg: Germany, 2001.
21. Stuart, B. H. *Analytical techniques in materials conservation*; John Wiley & Sons, Ltd.: Chichester, UK, 2007.
22. Vahur, S.; Kriiska, A.; Leito, I. *Estonian Journal of Archaeology*. **2011**, *15* (1), 3–17.
23. Nirgi, T.; Rosentau, A.; Ots, M.; Vahur, S.; Kriiska, A. *Boreas*. **2017**.
24. Golubev, Y. A.; Martirosyan, O. V. *Phys. Chem. Miner.* **2012**, *39* (3), 247–258.
25. Derrick, M. *J. Am. Inst. Conserv.* **1989**, *28* (1), 43–56.
26. Casadio, F.; Toniolo, L. *J. Cult. Herit.* **2001**, *2* (1), 71–78.

27. Prati, S.; Sciutto, G.; Mazzeo, R.; Torri, C.; Fabbri, D. *Anal. Bioanal. Chem.* **2011**, *399* (9), 3081–3091.
28. P.C. Sarkar; A.K. Shrivastava. *Pigment Resin Technol.* **1997**, *26* (6), 378–381.
29. de la Rie, E. R. *Stud. Conserv.* **1988**, *33* (2), 53–70.
30. Font, J.; Salvadó, N.; Butí, S.; Enrich, J. *Anal. Chim. Acta*. **2007**, *598* (1), 119–127.
31. Andreotti, A.; Bonaduce, I.; Colombini, M. P.; Gautier, G.; Modugno, F.; Ribechini, E. *Anal. Chem.* **2006**, *78* (13), 4490–4500.
32. Azemard, C.; Menager, M.; Vieillescazes, C. *Anal. Bioanal. Chem.* **2016**, *408* (24), 6599–6612.
33. Egenberg, I. M.; Aasen, J. A. B.; Holtekjølen, A. K.; Lundanes, E. *J. Anal. Appl. Pyrolysis.* **2002**, *62* (1), 143–155.
34. Steigenberger, G.; Herm, C. *Anal. Bioanal. Chem.* **2011**, *401* (6), 1771.
35. van der Doelen, G. A. Molecular studies of fresh and aged triterpenoid varnishes; University of Amsterdam: Amsterdam, Netherlands, 1999.
36. Colombini, M. P.; Modugno, F.; Ribechini, E. *J. Mass Spectrom.* **2005**, *40* (5), 675–687.
37. Modugno, F.; Ribechini, E.; Colombini, M. P. *Rapid Commun. Mass Spectrom.* **2006**, *20* (11), 1787–1800.
38. Cole, R. B. *Electrospray and MALDI mass spectrometry: fundamentals, instrumentation, practicalities, and biological applications*, 2nd edition; John Wiley & Sons, Inc.: New Jersey, USA, 2010.
39. Hillenkamp, F.; Peter-Katalinic, J. *MALDI MS: a practical guide to instrumentation, methods and applications*; Wiley-VCH Verlag GmbH & Co. KGaA, Weinheim, 2007.
40. de Hoffmann, E.; Stroobant, V. *Mass spectrometry: principles and applications*, 3rd edition; John Wiley & Sons, Ltd.: Chichester, UK, 2007.
41. Matthiesen, R. *Mass Spectrometry: data analysis on proteomics*; Humana Press Inc.: New Jersey, USA, 2007.
42. Karas, M.; Hillenkamp, F. *Anal. Chem.* **1988**, *60* (20), 2299–2301.
43. Tanaka, K.; Waki, H.; Ido, Y.; Akita, S.; Yoshida, Y.; Yoshida, T.; Matsuo, T. *Rapid Commun. Mass Spectrom.* **1988**, *2* (8), 151–153.
44. Fuchs, B.; Schiller, J. *Curr. Org. Chem.* **2009**, *13* (16), 1664–1681.
45. Zenobi, R.; Knochenmuss, R. *Mass Spectrom. Rev.* **1998**, *17* (5), 337–366.
46. Bourcier, S.; Bouchonnet, S.; Hoppilliard, Y. *Int. J. Mass Spectrom.* **2001**, *210–211*, 59–69.
47. Schiller, J.; Süß, R.; Fuchs, B.; Müller, M.; Petković, M.; Zschörnig, O.; Waschipky, H. *Eur. Biophys. J.* **2006**, *36* (4–5), 517–527.
48. Wallace, W. E.; Arnould, M. A.; Knochenmuss, R. *Int. J. Mass Spectrom.* **2005**, *242* (1), 13–22.
49. Strupat, K.; Kampmeier, J.; Horneffer, V. *Int. J. Mass Spectrom. Ion Process.* **1997**, *169*, 43–50.
50. Liu, B.-H.; Charkin, O. P.; Klemenko, N.; Chen, C. W.; Wang, Y.-S. *J. Phys. Chem. B* **2010**, *114* (33), 10853–10859.
51. Ohanessian, G. *Int. J. Mass Spectrom.* **2002**, *219* (3), 577–592.
52. Kampmeier, J.; Dreisewerd, K.; Schurenberg, M.; Strupat, K. *Int. J. Mass Spectrom. Ion Process.* **1997**, *169*, 31–41.
53. Karas, M.; Ehring, H.; Nordhoff, E.; Stahl, B.; Strupat, K.; Hillenkamp, F.; Grehl, M.; Krebs, B. *Org. Mass Spectrom.* **1993**, *28* (12), 1476–1481.

54. Horneffer, V.; Dreisewerd, K.; Lüdemann, H.-C.; Hillenkamp, F.; Läge, M.; Strupat, K. *Int. J. Mass Spectrom.* **1999**, *185–187*, 859–870.
55. Brombacher, S.; Owen, S. J.; Volmer, D. A. *Anal. Bioanal. Chem.* **2003**, *376* (6), 773–779.
56. Strupat, K.; Karas, M.; Hillenkamp, F. *Int. J. Mass Spectrom. Ion Process.* **1991**, *111*, 89–102.
57. Petković, M.; Schiller, J.; Müller, J.; Müller, M.; Arnold, K.; Arnhold, J. *Analyst.* **2001**, *126* (7), 1042–1050.
58. Fremout, W.; Kuckova, S.; Crhova, M.; Sanyova, J.; Saverwyns, S.; Hynek, R.; Kodicek, M.; Vandenabeele, P.; Moens, L. *Rapid Commun. Mass Spectrom.* **2011**, *25* (11), 1631–1640.
59. Tripković, T.; Charvy, C.; Alves, S.; Lolić, A. Đ.; Baošić, R. M.; Nikolić-Mandić, S. D.; Tabet, J. C. *Talanta.* **2013**, *113*, 49–61.
60. Fitzgerald, M. C.; Parr, G. R.; Smith, L. M. *Anal. Chem.* **1993**, *65* (22), 3204–3211.
61. Vermillion-Salsbury, R. L.; Hercules, D. M. *Rapid Commun. Mass Spectrom.* **2002**, *16* (16), 1575–1581.
62. McIver, R. T.; McIver, J. R. *Fourier transform mass spectrometry*; IonSpec Corporation: Lake Forest, CA, 2006.
63. Jing, L.; Amster, I. J. *Eur. J. Mass Spectrom.* **2012**, *18* (3), 269–277.
64. Bruce, J. E.; Anderson, G. A.; Brands, M. D.; Pasa-Tolic, L.; Smith, R. D. *J. Am. Soc. Mass Spectrom.* **2000**, *11* (5), 416–421.
65. Kempka, M. Improved mass accuracy in MALDI-TOF-MS analysis; Royal Institute of Technology: Stockholm, Sweden, 2005.
66. Cornett, D. S.; Frappier, S. L.; Caprioli, R. M. *Anal. Chem.* **2008**, *80* (14), 5648–5653.
67. Harris, W. A.; Janecki, D. J.; Reilly, J. P. *Rapid Commun. Mass Spectrom.* **2002**, *16* (18), 1714–1722.
68. Gross, J. H. *Anal. Bioanal. Chem.* **2016**, *408* (21), 5945–5951.
69. Smith, D. F.; Aizikov, K.; Duursma, M. C.; Giskes, F.; Spaanderman, D.-J.; McDonnell, L. A.; O'Connor, P. B.; Heeren, R. M. A. *J. Am. Soc. Mass Spectrom.* **2011**, *22* (1), 130–137.
70. Burton, R. D.; Matuszak, K. P.; Watson, C. H.; Eyler, J. R. *J. Am. Soc. Mass Spectrom.* **1999**, *10* (12), 1291–1297.
71. Gross, J. H. *Anal. Bioanal. Chem.* **2013**, *405* (26), 8663–8668.
72. Kruegel, A.; Attygalle, A. B. *J. Am. Soc. Mass Spectrom.* **2010**, *21* (1), 112–116.
73. Rodima, T.; Kaljurand, I.; Pihl, A.; Mäemets, V.; Leito, I.; Koppel, I. A. *J. Org. Chem.* **2002**, *67* (6), 1873–1881.
74. Kolomeitsev, A. A.; Koppel, I. A.; Rodima, T.; Barten, J.; Lork, E.; Röschenthaler, G.-V.; Kaljurand, I.; Kütt, A.; Koppel, I.; Mäemets, V.; Leito, I. *J. Am. Chem. Soc.* **2005**, *127* (50), 17656–17666.
75. Rodima, T.; Mäemets, V.; Koppel, I. *J. Chem. Soc. [Perkin 1].* **2000**, No. 16, 2637–2644.
76. Schwesinger, R.; Schlemper, H.; Hasenfratz, C.; Willaredt, J.; Dambacher, T.; Breuer, T.; Ottaway, C.; Fletschinger, M.; Boele, J.; Fritz, H.; Putzas, D.; Rotter, H. W.; Bordwell, F. G.; Satish, A. V.; Ji, G.-Z.; Peters, E.-M.; Peters, K.; von Schnering, H. G.; Walz, L. *Liebigs Ann.* **1996**, No. 7, 1055–1081.
77. Saame, J.; Rodima, T.; Tshepelevitsh, S.; Kütt, A.; Kaljurand, I.; Haljasorg, T.; Koppel, I. A.; Leito, I. *J. Org. Chem.* **2016**, *81* (17), 7349.

78. Eckert-Maksić, M.; Glasovac, Z.; Trošelj, P.; Kütt, A.; Rodima, T.; Koppel, I.; Koppel, I. A. *Eur. J. Org. Chem.* **2008**, *2008* (30), 5176–5184.
79. Netscher, T.; Bonrath, W.; Haas, A.; Hoppmann, E.; Pauling, H. *Chim. Int. J. Chem.* **2004**, *58* (3), 153–155.
80. Bonrath, W.; Haas, A.; Hoppmann, E.; Netscher, T.; Pauling, H.; Schager, F.; Wildermann, A. *Adv. Synth. Catal.* **2002**, *344* (1), 37–39.
81. Ishikawa, T. *Superbases for organic synthesis: guanidines, amidines, phosphazenes and related organocatalysts*; John Wiley & Sons, Ltd.: Chichester, UK, 2009.
82. Burk, P.; Koppel, I. A.; Koppel, I.; Kurg, R.; Gal, J.-F.; Maria, P.-C.; Herreros, M.; Notario, R.; Abboud, J.-L. M.; Anvia, F.; Taft, R. W. *J. Phys. Chem. A.* **2000**, *104* (12), 2824–2833.
83. Leito, I.; Herodes, K.; Huopolainen, M.; Virro, K.; Künnapas, A.; Kruve, A.; Tanner, R. *Rapid Commun. Mass Spectrom.* **2008**, *22* (3), 379–384.
84. van Aarssen, B. G. K.; Cox, H. C.; Hoogendoorn, P.; De Leeuw, J. W. *Geochim. Cosmochim. Acta.* **1990**, *54* (11), 3021–3031.
85. Romero-Noguera, J.; Martín-Sánchez, I.; López-Miras, M. del M.; Ramos-López, J. M.; Bolívar-Galiano, F. *Electron. J. Biotechnol.* **2010**, *13* (3), 6–7.
86. Dietemann, P. Towards more stable natural resin varnishes for paintings; Swiss Federal Institute of Technology: Zurich, Switzerland, 2003.
87. Kruve, A.; Kaupmees, K.; Liigand, J.; Oss, M.; Leito, I. *J. Mass Spectrom.* **2013**, *48* (6), 695–702.
88. Lüdemann, H.-C.; Redmond, R. W.; Hillenkamp, F. *Rapid Commun. Mass Spectrom.* **2002**, *16* (13), 1287–1294.
89. Krishnakumar, V.; Surumbarkuzhali, N. *J. Raman Spectrosc.* **2010**, *41* (4), 473–478.
90. Leito, I.; Raamat, E.; Kütt, A.; Saame, J.; Kipper, K.; Koppel, I. A.; Koppel, I.; Zhang, M.; Mishima, M.; Yagupolskii, L. M.; Garlyauskayte, R. Y.; Filatov, A. A. *J. Phys. Chem. A.* **2009**, *113* (29), 8421–8424.
91. Albert, A. *The acridines: their preparation, physical, chemical, and biological properties and uses*; Richard Clay and Company, Ltd.: Suffolk,UK, 1951.
92. Mäss, V.; Russow, E. *AVE 2015*. **2016**, 211–224.

APPENDIX 1

Hereafter, more comprehensive tables containing ion assignments for the peaks present in the MALDI-FT-ICR mass spectra obtained from dammar, mastic, sandarac, colophony and shellac resins in positive and negative ion mode are presented. The high accuracy *m/z* values obtained in the case of internal calibration are valuable as reference data for the analysis of unknown resinous materials.

Table A1. Assignment of ion formulas corresponding to peaks of the positive ion mode mass spectrum of dammar resin obtained in the first stage of the development of the MALDI-FT-ICR-MS methodology. Additionally, the comparison of *m/z* errors in the case of internal and external calibration is presented. The *m/z* values that have been assigned manually due to the loss of resolving power are highlighted with red. The clusters are outlined with a thick line.

Cation formula	Internal calibration		Externel calibration	
	Measured *m/z*	*m/z* error (ppm)	Measured *m/z*	*m/z* error (ppm)
$C_{30}H_{45}O^+$	421.34632	–0.40	421.34851	4.79
$C_{29}H_{43}O_2^+$	423.32545	–0.73	423.32766	4.49
$C_{30}H_{49}O^+$	425.37706	–1.72	425.37929	3.52
$C_{31}H_{48}ONa^+$	459.35990	0.35	459.36249	5.99
$C_{29}H_{42}O_3Na^+$	461.30258	–0.09	461.30520	5.58
$C_{30}H_{46}O_2Na^+$	461.33888	–0.26	461.34149	5.40
$C_{29}H_{44}O_3Na^+$	463.31829	0.04	463.32093	5.73
$C_{30}H_{48}O_2Na^+$	463.35438	–0.58	463.35702	5.11
$C_{28}H_{42}O_4Na^+$	465.29745	–0.17	465.30011	5.54
$C_{29}H_{46}O_3Na^+$	465.33398	0.13	465.33664	5.84
$C_{27}H_{40}O_5Na^+$	467.27666	–0.30	467.27934	5.43
$C_{28}H_{44}O_4Na^+$	467.31211	–2.29	467.31479	3.45
$C_{29}H_{48}O_3Na^+$	467.34997	0.86	467.35265	6.58
$C_{27}H_{42}O_5Na^+$	469.29262	0.36	469.29532	6.12
$C_{29}H_{40}O_4Na^+$	475.28193	0.11	475.28471	5.94
$C_{30}H_{44}O_3Na^+$	475.31817	–0.21	475.32094	5.61
$C_{29}H_{42}O_4Na^+$	477.29740	–0.27	477.30020	5.59
$C_{30}H_{46}O_3Na^+$	477.33355	–0.78	477.33635	5.09
$C_{29}H_{44}O_4Na^+$	479.31346	0.58	479.31628	6.46
$C_{30}H_{48}O_3Na^+$	479.34973	0.33	479.35255	6.22
$C_{28}H_{42}O_5Na^+$	481.29294	1.02	481.29578	6.92
$C_{29}H_{46}O_4Na^+$	481.32866	–0.35	481.33150	5.55
$C_{30}H_{50}O_3Na^+$	481.36508	–0.29	481.36792	5.61

Table A1. Continued

Cation formula	Internal calibration		Externel calibration	
	Measured *m/z*	*m/z* error (ppm)	Measured *m/z*	*m/z* error (ppm)
$C_{27}H_{40}O_6Na^+$	483.27170	–0.02	483.27456	5.90
$C_{29}H_{48}O_4Na^+$	483.34405	–0.89	483.34691	5.03
$C_{30}H_{52}O_3Na^+$	483.38072	–0.31	483.38359	5.62
$C_{30}H_{42}O_4Na^+$	489.29820	1.37	489.30114	7.38
$C_{29}H_{40}O_5Na^+$	491.27665	–0.31	491.27961	5.72
$C_{30}H_{44}O_4Na^+$	491.31329	0.22	491.31625	6.25
$C_{29}H_{42}O_5Na^+$	493.29260	0.30	493.29558	6.35
$C_{30}H_{46}O_4Na^+$	493.32896	0.26	493.33194	6.31
$C_{29}H_{44}O_5Na^+$	495.30791	–0.38	495.31092	5.69
$C_{30}H_{48}O_4Na^+$	495.34434	–0.28	495.34735	5.79
$C_{28}H_{42}O_6Na^+$	497.28728	–0.16	497.29031	5.93
$C_{29}H_{46}O_5Na^+$	497.32385	0.20	497.32688	6.29
$C_{30}H_{50}O_4Na^+$	497.36011	–0.04	497.36314	6.05
$C_{29}H_{48}O_5Na^+$	499.33941	0.02	499.34247	6.14
$C_{30}H_{52}O_4Na^+$	499.37473	–2.10	499.37779	4.02
$C_{30}H_{42}O_5Na^+$	505.29264	0.38	505.29576	6.56
$C_{29}H_{40}O_6Na^+$	507.27104	–1.32	507.27419	4.88
$C_{30}H_{44}O_5Na^+$	507.30780	–0.59	507.31095	5.62
$C_{29}H_{42}O_6Na^+$	509.28724	–0.24	509.29042	6.00
$C_{30}H_{46}O_5Na^+$	509.32398	0.45	509.32716	6.69
$C_{29}H_{44}O_6Na^+$	511.30292	–0.18	511.30613	6.09
$C_{30}H_{48}O_5Na^+$	511.33919	–0.41	511.34240	5.86
$C_{29}H_{46}O_6Na^+$	513.31873	0.14	513.32195	6.42
$C_{30}H_{50}O_5Na^+$	513.35497	–0.16	513.35820	6.13
$C_{30}H_{42}O_6Na^+$	521.28633	–1.98	521.28966	4.40
$C_{30}H_{44}O_6Na^+$	523.30321	0.38	523.30656	6.79
$C_{31}H_{48}O_5Na^+$	523.34013	1.39	523.34348	7.80
$C_{29}H_{42}O_7Na^+$	525.28170	–1.10	525.28508	5.33
$C_{30}H_{46}O_6Na^+$	525.31815	–0.97	525.32152	5.45
$C_{31}H_{50}O_5Na^+$	525.35449	–1.07	525.35786	5.36
$C_{29}H_{44}O_7Na^+$	527.29791	–0.04	527.30131	6.41
$C_{30}H_{48}O_6Na^+$	527.33444	0.25	527.33785	6.71
$C_{29}H_{46}O_7Na^+$	529.31347	–0.21	529.31690	6.28
$C_{30}H_{50}O_6Na^+$	529.34931	–1.23	529.35274	5.25
$C_{30}H_{42}O_7Na^+$	537.28195	–0.61	537.28548	5.96
$C_{31}H_{46}O_6Na^+$	537.31836	–0.56	537.32189	6.01

Table A1. Continued

Cation formula	Internal calibration		Externel calibration	
	Measured *m/z*	*m/z* error (ppm)	Measured *m/z*	*m/z* error (ppm)
$C_{32}H_{50}O_5Na^+$	537.35525	0.37	537.35878	6.95
$C_{30}H_{44}O_7Na^+$	539.29765	–0.52	539.30121	6.08
$C_{31}H_{48}O_6Na^+$	539.33372	–1.09	539.33728	5.51
$C_{32}H_{52}O_5Na^+$	539.37030	–0.74	539.37386	5.86
$C_{29}H_{42}O_8Na^+$	541.27841	2.25	541.28199	8.87
$C_{30}H_{46}O_7Na^+$	541.31406	0.89	541.31765	7.51
$C_{31}H_{50}O_6Na^+$	541.34992	–0.07	541.35351	6.55
$C_{32}H_{54}O_5Na^+$	541.38646	0.20	541.39005	6.83
$C_{29}H_{44}O_8Na^+$	543.29270	–0.26	543.29631	6.39
$C_{30}H_{48}O_7Na^+$	543.32900	–0.42	543.33261	6.22
$C_{30}H_{50}O_7Na^+$	545.34506	0.33	545.34870	7.00
$C_{30}H_{42}O_8Na^+$	553.27721	0.04	553.28095	6.80
$C_{30}H_{44}O_8Na^+$	555.29330	0.83	555.29707	7.61
$C_{30}H_{46}O_8Na^+$	557.30878	0.52	557.31258	7.34
$C_{30}H_{48}O_8Na^+$	559.32467	0.95	559.32849	7.78
$C_{45}H_{70}O_2Na^+$	665.52763	1.25	665.53302	9.35
$C_{44}H_{68}O_3Na^+$	667.50579	–0.42	667.51122	7.72
$C_{45}H_{72}O_2Na^+$	667.54234	–0.16	667.54776	7.96
$C_{44}H_{70}O_3Na^+$	669.52143	–0.43	669.52689	7.72
$C_{45}H_{74}O_2Na^+$	669.55749	–0.91	669.56295	7.24
$C_{45}H_{68}O_3Na^+$	679.50493	–1.68	679.51055	6.60
$C_{46}H_{72}O_2Na^+$	679.54332	1.28	679.54894	9.55
$C_{44}H_{66}O_4Na^+$	681.48547	0.21	681.49113	8.51
$C_{45}H_{70}O_3Na^+$	681.52145	–0.40	681.52816	9.45
$C_{43}H_{64}O_5Na^+$	683.46382	–1.14	683.46950	7.17
$C_{44}H_{68}O_4Na^+$	683.50154	0.82	683.50723	9.14
$C_{45}H_{72}O_3Na^+$	683.53788	0.75	683.54449	10.42
$C_{45}H_{74}O_3Na^+$	685.55380	1.14	685.56119	11.92
$C_{47}H_{72}O_2Na^+$	691.54195	–0.72	691.54907	9.57
$C_{45}H_{66}O_4Na^+$	693.48590	0.82	693.49250	10.34
$C_{46}H_{70}O_3Na^+$	693.52314	2.05	693.52899	10.49
$C_{44}H_{64}O_5Na^+$	695.46489	0.42	695.47077	8.88
$C_{45}H_{68}O_4Na^+$	695.50146	0.69	695.50734	9.15
$C_{46}H_{72}O_3Na^+$	695.53863	1.81	695.54451	10.27
$C_{44}H_{66}O_5Na^+$	697.48027	0.03	697.48619	8.52
$C_{45}H_{70}O_4Na^+$	697.51698	0.50	697.52291	9.00

Table A1. Continued

Cation formula	Internal calibration		Externel calibration	
	Measured *m/z*	*m/z* error (ppm)	Measured *m/z*	*m/z* error (ppm)
$C_{46}H_{74}O_3Na^+$	697.55345	0.62	697.55937	9.11
$C_{43}H_{64}O_6Na^+$	699.45780	–2.44	699.46357	5.80
$C_{44}H_{68}O_5Na^+$	699.49571	–0.27	699.50167	8.25
$C_{45}H_{72}O_4Na^+$	699.53263	0.50	699.53858	9.01
$C_{44}H_{70}O_5Na^+$	701.51170	0.21	701.51769	8.75
$C_{45}H_{74}O_4Na^+$	701.54812	0.27	701.55411	8.81
$C_{45}H_{66}O_5Na^+$	709.47971	–0.76	709.48583	7.87
$C_{46}H_{70}O_4Na^+$	709.51598	–0.92	709.52210	7.72
$C_{45}H_{68}O_5Na^+$	711.49544	–0.65	711.50107	7.27
$C_{46}H_{72}O_4Na^+$	711.53296	0.96	711.53912	9.61
$C_{44}H_{66}O_6Na^+$	713.47393	–1.72	713.48013	6.96
$C_{45}H_{70}O_5Na^+$	713.51165	0.14	713.51785	8.82
$C_{46}H_{74}O_4Na^+$	713.54885	1.29	713.55505	9.98
$C_{44}H_{48}O_6Na^+$	715.49164	1.16	715.49787	9.86
$C_{45}H_{72}O_5Na^+$	715.52778	0.81	715.53401	9.52
$C_{43}H_{66}O_7Na^+$	717.47205	2.75	717.47831	11.47
$C_{44}H_{70}O_6Na^+$	717.50694	0.67	717.51321	9.40
$C_{45}H_{74}O_5Na^+$	717.54447	2.26	717.55073	10.98
$C_{46}H_{68}O_5Na^+$	723.49473	–1.62	723.50080	6.77
$C_{45}H_{66}O_6Na^+$	725.47471	–0.62	725.48111	8.20
$C_{46}H_{70}O_5Na^+$	725.51123	–0.44	725.51763	8.38
$C_{45}H_{68}O_6Na^+$	727.49171	1.24	727.49815	10.08
$C_{46}H_{72}O_5Na^+$	727.52702	–0.25	727.53346	8.60
$C_{44}H_{66}O_7Na^+$	729.46996	–0.16	729.47643	8.70
$C_{45}H_{70}O_6Na^+$	729.50762	1.59	729.51410	10.47
$C_{46}H_{74}O_5Na^+$	729.54344	0.81	729.54991	9.67
$C_{44}H_{68}O_7Na^+$	731.48624	0.70	731.49274	9.59
$C_{45}H_{72}O_6Na^+$	731.52268	0.78	731.52919	9.68
$C_{44}H_{70}O_7Na^+$	733.50237	1.35	733.50892	10.27
$C_{45}H_{74}O_6Na^+$	733.53844	0.93	733.54498	9.84
$C_{45}H_{66}O_7Na^+$	741.47178	2.29	741.47847	11.31
$C_{44}H_{64}O_8Na^+$	743.45139	2.76	743.45811	11.80
$C_{45}H_{68}O_7Na^+$	743.48609	0.48	743.49281	9.53
$C_{46}H_{72}O_6Na^+$	743.52403	2.58	743.53075	11.61
$C_{44}H_{66}O_8Na^+$	745.46602	1.38	745.47278	10.45
$C_{45}H_{70}O_7Na^+$	745.50164	0.35	745.50840	9.42

Table A1. Continued

Cation formula	Internal calibration		Externel calibration	
	Measured *m/z*	*m/z* error (ppm)	Measured *m/z*	*m/z* error (ppm)
$C_{44}H_{68}O_8Na^+$	747.48040	–0.32	747.48719	8.77
$C_{45}H_{72}O_7Na^+$	747.51727	0.32	747.52406	9.40
$C_{44}H_{70}O_8Na^+$	749.49627	–0.03	749.50310	9.08
$C_{45}H_{74}O_7Na^+$	749.53235	–0.44	749.53918	8.67
$C_{45}H_{66}O_8Na^+$	757.46491	–0.11	757.47188	9.10
$C_{45}H_{68}O_8Na^+$	759.48008	–0.74	759.48709	8.49
$C_{45}H_{70}O_8Na^+$	761.49553	–1.00	761.50257	8.25
$C_{45}H_{72}O_8Na^+$	763.51162	–0.42	763.51871	8.86
$C_{45}H_{66}O_9Na^+$	773.46010	0.25	773.46737	9.64
$C_{45}H_{68}O_9Na^+$	775.47503	–0.68	775.48233	8.74
$C_{45}H_{70}O_9Na^+$	777.49065	–0.72	777.49952	10.69
$C_{45}H_{72}O_9Na^+$	779.50613	–0.94	779.51351	8.53
$C_{45}H_{70}O_{10}Na^+$	793.48568	–0.55	793.49225	7.72
$C_{60}H_{94}O_2Na^+$	869.71538	0.90	869.72455	11.44
$C_{60}H_{96}O_2Na^+$	871.73070	0.52	871.73990	11.07
$C_{60}H_{98}O_2Na^+$	873.74642	0.60	873.75568	11.20
$C_{61}H_{96}O_2Na^+$	883.72980	–0.51	883.73930	10.24
$C_{60}H_{94}O_3Na^+$	885.70855	–1.10	885.71805	9.63
$C_{60}H_{96}O_3Na^+$	887.72405	–1.26	887.73365	9.55
$C_{60}H_{98}O_3Na^+$	889.74175	1.05	889.75105	11.50
$C_{61}H_{94}O_3Na^+$	897.70906	–0.51	897.71883	10.37
$C_{61}H_{96}O_3Na^+$	899.72525	0.09	899.73505	10.98
$C_{60}H_{94}O_4Na^+$	901.70415	–0.31	901.71400	10.61
$C_{61}H_{98}O_3Na^+$	901.74020	–0.69	901.75005	10.24
$C_{60}H_{96}O_4Na^+$	903.72080	0.80	903.73070	11.75
$C_{60}H_{98}O_4Na^+$	905.73512	–0.67	905.74507	10.31
$C_{59}H_{96}O_5Na^+$	907.71418	–0.90	907.72417	10.10
$C_{60}H_{90}O_5Na^+$	913.66685	–1.31	913.67690	9.69
$C_{61}H_{94}O_4Na^+$	913.70375	–0.74	913.71384	10.30
$C_{60}H_{92}O_5Na^+$	915.68520	1.64	915.69530	12.67
$C_{61}H_{98}O_4Na^+$	917.73500	–0.80	917.74520	10.32
$C_{60}H_{96}O_5Na^+$	919.71875	4.08	919.72895	15.17
$C_{60}H_{98}O_5Na^+$	921.72685	–4.12	921.73720	7.11
$C_{60}H_{100}O_5Na^+$	923.74311	–3.45	923.75350	7.79
$C_{60}H_{90}O_6Na^+$	929.66180	–1.25	929.67225	9.99
$C_{60}H_{92}O_6Na^+$	931.68204	3.68	931.69256	14.97

Table A1. Continued

Cation formula	Internal calibration		Externel calibration	
	Measured *m/z*	*m/z* error (ppm)	Measured *m/z*	*m/z* error (ppm)
$C_{60}H_{94}O_6Na^+$	933.69276	–1.61	933.70332	9.70
$C_{60}H_{96}O_6Na^+$	935.71095	1.11	935.72155	12.44
$C_{60}H_{98}O_6Na^+$	937.72675	1.27	937.73745	12.68
$C_{60}H_{90}O_7Na^+$	945.65550	–2.52	945.66630	8.90
$C_{60}H_{92}O_7Na^+$	947.67279	–0.78	947.68367	10.70
$C_{60}H_{94}O_7Na^+$	949.68832	–0.91	949.69924	10.60
$C_{60}H_{96}O_7Na^+$	951.70610	1.33	951.71705	12.84
$C_{60}H_{98}O_7Na^+$	953.71905	–1.50	953.73010	10.09
$C_{60}H_{88}O_8Na^+$	959.63725	0.11	959.64840	11.73
$C_{60}H_{90}O_8Na^+$	961.65081	–2.06	961.66205	9.63
$C_{60}H_{92}O_8Na^+$	963.67126	2.93	963.68250	14.59
$C_{60}H_{94}O_8Na^+$	965.68383	–0.27	965.69512	11.42
$C_{60}H_{96}O_8Na^+$	967.69340	–6.55	967.70515	5.59
$C_{60}H_{98}O_8Na^+$	969.71530	–0.09	969.72680	11.77
$C_{60}H_{88}O_9Na^+$	975.63173	–0.34	975.64325	11.47
$C_{60}H_{90}O_9Na^+$	977.64530	–2.47	977.65690	9.40
$C_{60}H_{92}O_9Na^+$	979.66703	3.75	979.67860	15.56
$C_{60}H_{94}O_9Na^+$	981.68025	1.26	981.69190	13.13
$C_{60}H_{96}O_9Na^+$	983.69317	–1.51	983.70490	10.41
$C_{60}H_{98}O_9Na^+$	985.70578	–4.60	985.71755	7.34
$C_{60}H_{88}O_{10}Na^+$	991.62735	0.38	991.63930	12.43
$C_{60}H_{90}O_{10}Na^+$	993.64558	2.98	993.65753	15.01
$C_{60}H_{92}O_{10}Na^+$	995.65687	–1.41	995.66887	10.64
$C_{60}H_{94}O_{10}Na^+$	997.67342	–0.50	997.68550	11.61
$C_{60}H_{96}O_{10}Na^+$	999.69033	0.76	999.70245	12.88
$C_{60}H_{92}O_{11}Na^+$	1011.65277	–0.42	1011.66516	11.83
$C_{60}H_{94}O_{11}Na^+$	1013.66750	–1.32	1013.67760	8.64
$C_{75}H_{118}O_2Na^+$	1073.89955	–2.65	1073.91303	9.89
$C_{75}H_{120}O_2Na^+$	1075.91337	–4.35	1075.92738	8.67
$C_{74}H_{119}O_5^+$	1087.90721	1.85	1087.92153	15.01
$C_{75}H_{118}O_3Na^+$	1089.89910	1.63	1089.91347	14.82
$C_{76}H_{118}O_3Na^+$	1101.89328	–3.67	1101.90796	9.66
$C_{74}H_{121}O_6^+$	1105.92420	–4.0	1105.92933	12.26
$C_{75}H_{120}O_4Na^+$	1107.90406	–3.45	1107.91890	9.95
$C_{75}H_{122}O_4Na^+$	1109.92010	–3.09	1109.93423	9.64
$C_{75}H_{119}O_6^+$	1115.90612	5.38	1115.92118	18.87

Table A1. Continued

Cation formula	Internal calibration		Externel calibration	
	Measured *m/z*	*m/z* error (ppm)	Measured *m/z*	*m/z* error (ppm)
$C_{74}H_{117}O_7^+$	1117.88243	2.73	1117.89754	16.24
$C_{75}H_{116}O_5Na^+$	1119.88144	8.88	1119.89660	22.41
$C_{74}H_{121}O_7^+$	1121.91087	0.17	1121.92608	13.73
$C_{75}H_{120}O_5Na^+$	1123.90209	–0.63	1123.91736	12.95
$C_{75}H_{122}O_5Na^+$	1125.91515	–2.93	1125.92534	6.12
$C_{75}H_{124}O_5Na^+$	1127.93318	–0.82	1127.94856	12.82
$C_{75}H_{118}O_6Na^+$	1137.88773	4.98	1137.90338	18.74
$C_{75}H_{120}O_6Na^+$	1139.89212	–4.90	1139.90783	8.88
$C_{75}H_{122}O_6Na^+$	1141.91495	1.39	1141.92475	9.98
$C_{75}H_{124}O_6Na^+$	1143.92734	–1.46	1143.94316	12.37
$C_{75}H_{116}O_7Na^+$	1151.86977	7.33	1151.88581	21.25
$C_{75}H_{118}O_7Na^+$	1153.87739	0.36	1153.89348	14.30
$C_{75}H_{120}O_7Na^+$	1155.89237	–0.22	1155.90852	13.74
$C_{75}H_{122}O_7Na^+$	1157.90487	–2.94	1157.92107	11.04
$C_{75}H_{114}O_8Na^+$	1165.84799	6.35	1165.86442	20.44
$C_{75}H_{116}O_8Na^+$	1167.86515	7.63	1167.88163	21.74
$C_{75}H_{118}O_8Na^+$	1169.87100	–0.76	1169.88754	13.37
$C_{75}H_{120}O_8Na^+$	1171.88591	–1.39	1171.90250	12.77
$C_{75}H_{122}O_8Na^+$	1173.89772	–4.66	1173.91437	9.52
$C_{75}H_{116}O_9Na^+$	1183.85156	0.34	1183.86850	14.64
$C_{75}H_{118}O_9Na^+$	1185.85893	–6.64	1185.87592	7.68
$C_{75}H_{120}O_9Na^+$	1187.87246	–8.42	1187.88951	5.93
$C_{75}H_{116}O_{10}Na^+$	1199.84376	–1.93	1199.86115	12.57
$C_{90}H_{142}O_2Na^+$	1278.08826	–1.52	1278.10798	13.91
$C_{90}H_{144}O_2Na^+$	1280.10818	1.83	1280.12796	17.28
$C_{90}H_{146}O_2Na^+$	1282.12363	1.66	1282.14348	17.14
$C_{90}H_{148}O_2Na^+$	1284.13710	–0.04	1284.15701	15.47
$C_{91}H_{144}O_2Na^+$	1292.10932	2.69	1292.12947	18.28
$C_{90}H_{142}O_3Na^+$	1294.08190	–2.49	1294.10211	13.13
$C_{90}H_{144}O_3Na^+$	1296.10154	0.59	1296.12182	16.24
$C_{90}H_{146}O_3Na^+$	1298.11923	2.18	1298.13957	17.85
$C_{90}H_{148}O_3Na^+$	1300.13182	–0.19	1300.15222	15.50
$C_{91}H_{142}O_3Na^+$	1306.08459	–0.41	1306.10518	15.36
$C_{91}H_{144}O_3Na^+$	1308.10501	3.24	1308.12566	19.03
$C_{91}H_{146}O_3Na^+$	1310.11993	2.68	1310.14064	18.49
$C_{90}H_{146}O_4Na^+$	1314.11233	0.76	1314.13317	16.62

Table A1. Continued

Cation formula	Internal calibration		Externel calibration	
	Measured *m/z*	*m/z* error (ppm)	Measured *m/z*	*m/z* error (ppm)
$C_{90}H_{148}O_4Na^+$	1316.12567	–1.00	1316.14658	14.89
$C_{91}H_{146}O_4Na^+$	1326.11609	3.59	1326.13731	19.59
$C_{90}H_{146}O_5Na^+$	1330.10484	–1.06	1330.12619	14.99
$C_{90}H_{148}O_5Na^+$	1332.12064	–0.95	1332.14206	15.13
$C_{90}H_{144}O_6Na^+$	1344.07576	–7.25	1344.09756	8.97
$C_{90}H_{146}O_6Na^+$	1346.10110	–0.04	1346.12296	16.20
$C_{90}H_{148}O_6Na^+$	1348.11634	–0.35	1348.13827	15.92
$C_{90}H_{144}O_9Na^+$	1392.06565	–3.31	1392.08903	13.48
$C_{105}H_{166}O_2Na^+$	1482.27813	0.09	1482.30462	17.96
$C_{105}H_{168}O_2Na^+$	1484.29890	3.54	1484.32547	21.43
$C_{105}H_{170}O_2Na^+$	1486.31676	5.02	1486.34339	22.94
$C_{105}H_{168}O_3Na^+$	1500.29522	4.43	1500.32235	22.52
$C_{105}H_{170}O_3Na^+$	1502.31289	5.77	1502.34010	23.88
$C_{105}H_{172}O_3Na^+$	1504.32115	0.85	1504.34843	18.98
$C_{106}H_{166}O_3Na^+$	1510.27935	4.26	1510.30685	22.46
$C_{106}H_{168}O_3Na^+$	1512.29314	3.02	1512.32071	21.25
$C_{106}H_{170}O_3Na^+$	1514.30840	2.76	1514.34155	24.65
$C_{106}H_{172}O_3Na^+$	1516.32647	4.35	1516.35419	22.64
$C_{105}H_{170}O_4Na^+$	1518.30326	2.72	1518.33105	21.02
$C_{105}H_{172}O_4Na^+$	1520.31839	2.37	1520.34626	20.70
$C_{105}H_{170}O_5Na^+$	1534.29470	0.42	1534.32307	18.92
$C_{105}H_{172}O_5Na^+$	1536.30891	–0.51	1536.33736	18.00
$C_{103}H_{174}O_7Na^+$	1546.31393	–0.81	1546.34275	17.83
$C_{105}H_{170}O_6Na^+$	1550.28772	–0.80	1550.31669	17.89
$C_{105}H_{172}O_6Na^+$	1552.30898	2.82	1552.33802	21.52
$C_{120}H_{192}O_2Na^+$	1688.48554	2.42	1688.51988	22.76
$C_{120}H_{192}O_3Na^+$	1704.47382	–1.50	1704.50881	19.03
$C_{120}H_{194}O_3Na^+$	1706.49295	0.54	1706.52803	21.10
$C_{121}H_{192}O_3Na^+$	1716.47843	1.20	1716.51391	21.87
$C_{121}H_{194}O_3Na^+$	1718.49489	1.67	1718.53046	22.37
$C_{120}H_{194}O_4Na^+$	1722.49026	1.93	1722.52600	22.68
$C_{120}H_{196}O_4Na^+$	1724.50355	0.56	1724.53937	21.33
$C_{121}H_{194}O_4Na^+$	1734.49019	1.88	1734.52642	22.77
$C_{120}H_{192}O_5Na^+$	1736.48338	9.89	1736.51970	30.81
$C_{120}H_{194}O_5Na^+$	1738.47991	–1.12	1738.51630	19.82
$C_{120}H_{196}O_5Na^+$	1740.49547	–1.17	1740.53195	19.80

Table A1. Continued

Cation formula	Internal calibration		Externel calibration	
	Measured *m/z*	*m/z* error (ppm)	Measured *m/z*	*m/z* error (ppm)
$C_{119}H_{198}O_6Na^+$	1746.50371	–2.49	1746.54044	18.54
$C_{121}H_{194}O_5Na^+$	1750.47891	–1.68	1750.51581	19.40
$C_{120}H_{194}O_6Na^+$	1754.47780	0.59	1754.51486	21.72
$C_{120}H_{196}O_6Na^+$	1756.48555	–3.91	1756.52270	17.24
$C_{120}H_{198}O_6Na^+$	1758.50005	–4.55	1758.53728	16.62
$C_{120}H_{195}O_8^+$	1764.48969	2.86	1764.52718	24.10
$C_{121}H_{194}O_6Na^+$	1766.48238	3.18	1766.51996	24.45
$C_{120}H_{192}O_7Na^+$	1768.46779	6.65	1768.50545	27.95
$C_{136}H_{216}O_3Na^+$	1920.66602	0.96	1920.71041	24.08
$C_{136}H_{218}O_3Na^+$	1922.68081	0.51	1922.72530	23.65
$C_{136}H_{220}O_3Na^+$	1924.69102	–2.31	1924.73560	20.85
$C_{135}H_{218}O_4Na^+$	1926.67784	1.61	1926.72251	24.80
$C_{135}H_{220}O_4Na^+$	1928.68118	–4.77	1928.72594	18.44
$C_{136}H_{218}O_4Na^+$	1938.67311	–0.84	1938.71834	22.49
$C_{134}H_{219}O_7^+$	1940.67278	–2.45	1940.71811	20.91
$C_{135}H_{218}O_5Na^+$	1942.67044	0.41	1942.71585	23.78
$C_{135}H_{220}O_5Na^+$	1944.67490	–5.35	1944.72040	18.05
$C_{136}H_{218}O_5Na^+$	1954.66820	–0.74	1954.71418	22.78
$C_{134}H_{219}O_8^+$	1956.66874	–1.90	1956.71481	21.65
$C_{135}H_{218}O_6Na^+$	1958.66098	–1.83	1958.70715	21.74
$C_{135}H_{220}O_6Na^+$	1960.67651	–1.89	1960.72276	21.70
$C_{134}H_{217}O_9^+$	1970.65578	2.07	1970.70251	25.78
$C_{134}H_{219}O_9^+$	1972.67032	1.50	1972.71714	25.23
$C_{149}H_{243}O_7^+$	2144.85745	–3.67	2144.91278	22.12
$C_{150}H_{242}O_5Na^+$	2146.85925	0.84	2146.91468	26.66
$C_{149}H_{243}O_9^+$	2176.85490	–0.12	2176.91188	26.06

Table A2. Assignment of ion formulas corresponding to peaks of the positive ion mode mass spectrum of shellac resin obtained in the second stage of the development of the MALDI-FT-ICR-MS methodology and the comparison of *m/z* errors in the case of internal and external calibration. The clusters are outlined with a thick line.

Cation formula	Internal calibration		Externel calibration	
	Measured *m/z*	*m/z* error (ppm)	Measured *m/z*	*m/z* error (ppm)
$C_{15}H_{18}O_4Na^+$	285.10987	0.50	285.10929	–1.56
$C_{16}H_{28}O_3Na^+$	291.19311	0.16	291.19251	–1.91
$C_{16}H_{30}O_4Na^+$	309.20369	0.19	309.20305	–1.88
$C_{16}H_{32}O_5Na^+$	327.21425	0.17	327.21357	–1.92
$C_{30}H_{48}O_6Na^+$	527.33433	0.03	527.33315	–2.20
$C_{31}H_{44}O_6Na^+$	535.30318	0.31	535.30198	–1.92
$C_{30}H_{56}O_6Na^+$	535.39649	–0.79	535.39529	–3.03
$C_{31}H_{46}O_6Na^+$	537.31844	–0.41	537.31731	–2.51
$C_{31}H_{48}O_6Na^+$	539.33360	–1.33	539.33239	–3.56
$C_{30}H_{48}O_7Na^+$	543.32959	0.67	543.32837	–1.57
$C_{31}H_{46}O_7Na^+$	553.31382	0.44	553.31258	–1.80
$C_{30}H_{58}O_7Na^+$	553.40767	0.34	553.40642	–1.90
$C_{31}H_{48}O_7Na^+$	555.32906	–0.30	555.32789	–2.41
$C_{31}H_{46}O_8Na^+$	569.30892	0.76	569.30764	–1.50
$C_{31}H_{48}O_8Na^+$	571.32421	0.12	571.32300	–2.00
$C_{32}H_{58}O_7Na^+$	577.40755	0.12	577.40624	–2.14
$C_{32}H_{60}O_7Na^+$	579.42370	0.99	579.42238	–1.28
$C_{31}H_{46}O_9Na^+$	585.30404	1.10	585.30271	–1.18
$C_{31}H_{48}O_9Na^+$	587.31937	0.53	587.31803	–1.74
$C_{31}H_{50}O_9Na^+$	589.33477	0.10	589.33343	–2.17
$C_{32}H_{60}O_8Na^+$	595.41825	0.35	595.41689	–1.92
$C_{32}H_{62}O_8Na^+$	597.43373	0.06	597.43237	–2.22
$C_{33}H_{52}O_8Na^+$	599.35565	0.35	599.35428	–1.93
$C_{31}H_{46}O_{10}Na^+$	601.29867	0.58	601.29730	–1.70
$C_{31}H_{50}O_{10}Na^+$	605.33065	1.71	605.32927	–0.58
$C_{32}H_{60}O_9Na^+$	611.41259	–0.59	611.41119	–2.88
$C_{33}H_{50}O_9Na^+$	613.33463	–0.13	613.33322	–2.42
$C_{32}H_{62}O_9Na^+$	613.42857	–0.06	613.42726	–2.20
$C_{33}H_{54}O_9Na^+$	617.36641	0.65	617.36499	–1.65
$C_{33}H_{52}O_{10}Na^+$	631.34619	1.45	631.34473	–0.85
$C_{45}H_{74}O_{10}Na^+$	797.51752	0.13	797.51560	–2.29
$C_{46}H_{64}O_{10}Na^+$	799.43949	0.40	799.43771	–1.82

Table A2. Continued

Cation formula	Internal calibration		Externel calibration	
	Measured *m/z*	*m/z* error (ppm)	Measured *m/z*	*m/z* error (ppm)
$C_{46}H_{64}O_{11}Na^+$	815.43381	–0.34	815.43199	–2.56
$C_{46}H_{66}O_{11}Na^+$	817.45065	1.11	817.44866	–1.32
$C_{46}H_{66}O_{12}Na^+$	833.44467	0.02	833.44280	–2.22
$C_{47}H_{76}O_{11}Na^+$	839.52788	–0.13	839.52583	–2.57
$C_{47}H_{78}O_{11}Na^+$	841.54480	1.38	841.54273	–1.07
$C_{46}H_{68}O_{13}Na^+$	851.45390	–1.55	851.45181	–4.00
$C_{47}H_{78}O_{12}Na^+$	857.53826	–0.34	857.53634	–2.58
$C_{47}H_{80}O_{12}Na^+$	859.55528	1.25	859.55316	–1.21
$C_{47}H_{80}O_{13}Na^+$	875.54903	–0.10	875.54706	–2.35

Table A3. Assignment of ion formulas corresponding to peaks of the positive ion mode mass spectrum of mastic resin obtained with the modified MALDI-FT-ICR-MS methodology and the comparison of *m/z* errors in the case of internal and external calibration.

Cation formula	Internal calibration		Externel calibration	
	Measured *m/z*	*m/z* error (ppm)	Measured *m/z*	*m/z* error (ppm)
$C_{29}H_{43}O_2^+$	423.32568	–0.19	423.33059	11.41
$C_{24}H_{38}O_5Na^+$	429.26084	–0.71	429.26590	11.08
$C_{22}H_{32}O_7Na^+$	431.20403	0.02	431.20915	11.88
$C_{23}H_{36}O_6Na^+$	431.24070	0.68	431.24582	12.54
$C_{22}H_{34}O_7Na^+$	433.21954	–0.32	433.22470	11.61
$C_{29}H_{41}O_3^+$	437.30573	1.62	437.31100	13.68
$C_{24}H_{32}O_6Na^+$	439.20960	1.11	439.21492	13.23
$C_{25}H_{36}O_5Na^+$	439.24521	–0.66	439.25053	11.46
$C_{29}H_{43}O_3^+$	439.32032	–0.79	439.32565	11.33
$C_{24}H_{34}O_6Na^+$	441.22532	1.28	441.23070	13.46
$C_{25}H_{38}O_5Na^+$	441.26151	0.84	441.26689	13.02
$C_{23}H_{32}O_7Na^+$	443.20449	1.04	443.20991	13.29
$C_{24}H_{36}O_6Na^+$	443.24064	0.52	443.24607	12.77
$C_{25}H_{40}O_5Na^+$	443.27704	0.56	443.28247	12.81
$C_{23}H_{34}O_7Na^+$	445.21964	–0.07	445.22512	12.24
$C_{24}H_{38}O_6Na^+$	445.25638	0.71	445.26186	13.02
$C_{22}H_{32}O_8Na^+$	447.19903	0.21	447.20457	12.58
$C_{23}H_{36}O_7Na^+$	447.23545	0.28	447.24099	12.66
$C_{26}H_{36}O_5Na^+$	451.24541	–0.19	451.25105	12.31
$C_{27}H_{40}O_4Na^+$	451.28264	1.68	451.28828	14.19

Table A3. Continued

Cation formula	Internal calibration		Externel calibration	
	Measured *m/z*	*m/z* error (ppm)	Measured *m/z*	*m/z* error (ppm)
$C_{30}H_{43}O_3^+$	451.32047	–0.44	451.32612	12.07
$C_{25}H_{34}O_6Na^+$	453.22557	1.79	453.23127	14.36
$C_{26}H_{38}O_5Na^+$	453.26200	1.89	453.26770	14.46
$C_{27}H_{42}O_4Na^+$	453.29790	0.82	453.30360	13.39
$C_{30}H_{45}O_3^+$	453.33665	0.73	453.34235	13.30
$C_{24}H_{32}O_7Na^+$	455.20417	0.32	455.20992	12.95
$C_{25}H_{36}O_6Na^+$	455.24076	0.76	455.24651	13.40
$C_{26}H_{40}O_5Na^+$	455.27722	0.93	455.28297	13.56
$C_{24}H_{34}O_7Na^+$	457.21996	0.63	457.22577	13.33
$C_{25}H_{38}O_6Na^+$	457.25613	0.14	457.26193	12.84
$C_{26}H_{42}O_5Na^+$	457.29232	–0.27	457.29813	12.43
$C_{23}H_{32}O_8Na^+$	459.19827	–1.45	459.20413	11.31
$C_{24}H_{36}O_7Na^+$	459.23552	0.41	459.24138	13.18
$C_{25}H_{40}O_6Na^+$	459.27119	–1.12	459.27706	11.64
$C_{23}H_{34}O_8Na^+$	461.21502	0.94	461.22094	13.77
$C_{24}H_{38}O_7Na^+$	461.25103	0.12	461.25695	12.95
$C_{28}H_{38}O_4Na^+$	461.26647	0.52	461.27239	13.35
$C_{29}H_{42}O_3Na^+$	461.30232	–0.64	461.30824	12.19
$C_{28}H_{40}O_4Na^+$	463.28242	1.17	463.28840	14.06
$C_{27}H_{38}O_5Na^+$	465.26196	1.74	465.26798	14.70
$C_{26}H_{36}O_6Na^+$	467.24096	1.17	467.24704	14.19
$C_{27}H_{40}O_5Na^+$	467.27708	0.61	467.28316	13.63
$C_{30}H_{43}O_4^+$	467.31534	–0.53	467.32142	12.49
$C_{25}H_{34}O_7Na^+$	469.21976	0.19	469.22590	13.27
$C_{26}H_{38}O_6Na^+$	469.25629	0.49	469.26243	13.57
$C_{27}H_{42}O_5Na^+$	469.29302	1.22	469.29916	14.31
$C_{30}H_{45}O_4^+$	469.33074	–1.05	469.33688	12.04
$C_{25}H_{36}O_7Na^+$	471.23565	0.69	471.24185	13.84
$C_{26}H_{40}O_6Na^+$	471.27224	1.12	471.27844	14.28
$C_{27}H_{44}O_5Na^+$	471.30901	1.95	471.31521	15.10
$C_{24}H_{34}O_8Na^+$	473.21490	0.65	473.22115	13.86
$C_{25}H_{38}O_7Na^+$	473.25107	0.20	473.25733	13.42
$C_{26}H_{42}O_6Na^+$	473.28765	0.61	473.29391	13.83
$C_{24}H_{36}O_8Na^+$	475.23048	0.51	475.23679	13.79
$C_{29}H_{40}O_4Na^+$	475.28189	0.03	475.28821	13.32
$C_{24}H_{38}O_8Na^+$	477.24585	–0.08	477.25222	13.27

Table A3. Continued

Cation formula	Internal calibration		Externel calibration	
	Measured *m/z*	*m/z* error (ppm)	Measured *m/z*	*m/z* error (ppm)
$C_{28}H_{38}O_5Na^+$	477.26072	–0.88	477.26709	12.46
$C_{29}H_{42}O_4Na^+$	477.29727	–0.54	477.30364	12.81
$C_{27}H_{36}O_6Na^+$	479.24063	0.46	479.24706	13.87
$C_{28}H_{40}O_5Na^+$	479.27702	0.48	479.28345	13.89
$C_{29}H_{44}O_4Na^+$	479.31315	–0.06	479.31958	13.35
$C_{27}H_{38}O_6Na^+$	481.25635	0.60	481.26283	14.07
$C_{29}H_{46}O_4Na^+$	481.32934	1.06	481.33583	14.54
$C_{26}H_{36}O_7Na^+$	483.23615	1.71	483.24270	15.25
$C_{27}H_{40}O_6Na^+$	483.27163	–0.16	483.27818	13.38
$C_{30}H_{43}O_5^+$	483.30989	–1.26	483.31644	12.29
$C_{26}H_{38}O_7Na^+$	485.25121	0.48	485.25781	14.08
$C_{27}H_{42}O_6Na^+$	485.28761	0.51	485.29421	14.12
$C_{25}H_{36}O_8Na^+$	487.22999	–0.51	487.23665	13.16
$C_{26}H_{40}O_7Na^+$	487.26670	0.15	487.27336	13.82
$C_{27}H_{44}O_6Na^+$	487.30301	0.00	487.30967	13.68
$C_{25}H_{38}O_8Na^+$	489.24628	0.79	489.25300	14.52
$C_{26}H_{42}O_7Na^+$	489.28263	0.73	489.28935	14.46
$C_{30}H_{42}O_4Na^+$	489.29739	–0.30	489.30411	13.44
$C_{24}H_{36}O_9Na^+$	491.22488	–0.55	491.23166	13.24
$C_{29}H_{40}O_5Na^+$	491.27696	0.34	491.28374	14.13
$C_{30}H_{44}O_4Na^+$	491.31326	0.16	491.32004	13.96
$C_{28}H_{38}O_6Na^+$	493.25639	0.67	493.26323	14.54
$C_{29}H_{42}O_5Na^+$	493.29230	–0.29	493.29914	13.57
$C_{30}H_{46}O_4Na^+$	493.32870	–0.26	493.33554	13.61
$C_{27}H_{36}O_7Na^+$	495.23558	0.51	495.24248	14.44
$C_{28}H_{40}O_6Na^+$	495.27215	0.89	495.27905	14.82
$C_{29}H_{44}O_5Na^+$	495.30830	0.42	495.31520	14.35
$C_{30}H_{48}O_4Na^+$	495.34465	0.34	495.35155	14.27
$C_{27}H_{38}O_7Na^+$	497.25110	0.26	497.25806	14.25
$C_{28}H_{42}O_6Na^+$	497.28774	0.77	497.29470	14.76
$C_{29}H_{46}O_5Na^+$	497.32376	0.03	497.33072	14.03
$C_{30}H_{50}O_4Na^+$	497.36023	0.20	497.36719	14.19
$C_{26}H_{36}O_8Na^+$	499.23105	1.62	499.23807	15.68
$C_{27}H_{40}O_7Na^+$	499.26728	1.32	499.27430	15.37
$C_{28}H_{44}O_6Na^+$	499.30375	1.49	499.31077	15.55
$C_{29}H_{48}O_5Na^+$	499.33912	–0.56	499.34614	13.50

Table A3. Continued

Cation formula	Internal calibration		Externel calibration	
	Measured *m/z*	*m/z* error (ppm)	Measured *m/z*	*m/z* error (ppm)
$C_{30}H_{52}O_4Na^+$	499.37544	–0.68	499.38247	13.39
$C_{26}H_{38}O_8Na^+$	501.24617	0.56	501.25325	14.68
$C_{27}H_{42}O_7Na^+$	501.28320	1.84	501.29028	15.96
$C_{28}H_{46}O_6Na^+$	501.31847	–0.37	501.32556	13.75
$C_{29}H_{50}O_5Na^+$	501.35567	1.25	501.36275	15.37
$C_{25}H_{36}O_9Na^+$	503.22567	1.02	503.23281	15.21
$C_{26}H_{40}O_8Na^+$	503.26222	1.35	503.26936	15.53
$C_{30}H_{40}O_5Na^+$	503.27724	0.88	503.28438	15.07
$C_{27}H_{44}O_7Na^+$	503.29786	–0.12	503.30500	14.07
$C_{26}H_{42}O_8Na^+$	505.27719	0.00	505.28439	14.25
$C_{30}H_{42}O_5Na^+$	505.29241	–0.06	505.29962	14.19
$C_{29}H_{40}O_6Na^+$	507.27230	1.17	507.27957	15.48
$C_{30}H_{44}O_5Na^+$	507.30799	–0.21	507.31525	14.11
$C_{28}H_{38}O_7Na^+$	509.25082	–0.31	509.25814	14.07
$C_{29}H_{42}O_6Na^+$	509.28767	0.61	509.29499	14.99
$C_{30}H_{46}O_5Na^+$	509.32370	–0.09	509.33103	14.30
$C_{28}H_{40}O_7Na^+$	511.26692	0.57	511.27430	15.02
$C_{29}H_{44}O_6Na^+$	511.30326	0.49	511.31065	14.93
$C_{30}H_{48}O_5Na^+$	511.33905	–0.68	511.34644	13.77
$C_{27}H_{38}O_8Na^+$	513.24537	–1.02	513.25281	13.49
$C_{28}H_{42}O_7Na^+$	513.28282	1.06	513.29027	15.57
$C_{29}H_{46}O_6Na^+$	513.31837	–0.56	513.32582	13.95
$C_{30}H_{50}O_5Na^+$	513.35438	–1.29	513.36183	13.22
$C_{26}H_{36}O_9Na^+$	515.22516	0.02	515.23267	14.59
$C_{27}H_{40}O_8Na^+$	515.26200	0.89	515.26951	15.47
$C_{28}H_{44}O_7Na^+$	515.29842	0.96	515.30593	15.53
$C_{29}H_{48}O_6Na^+$	515.33489	1.13	515.34240	15.70
$C_{30}H_{52}O_5Na^+$	515.37027	–0.82	515.37779	13.76
$C_{26}H_{38}O_9Na^+$	517.24095	0.27	517.24852	14.91
$C_{27}H_{42}O_8Na^+$	517.27778	1.14	517.28535	15.78
$C_{28}H_{46}O_7Na^+$	517.31395	0.73	517.32153	15.37
$C_{30}H_{54}O_5Na^+$	517.38561	–1.42	517.39318	13.22
$C_{26}H_{40}O_9Na^+$	519.25698	1.02	519.26462	15.72
$C_{30}H_{40}O_6Na^+$	519.27236	1.24	519.27999	15.95
$C_{27}H_{44}O_8Na^+$	519.29278	–0.11	519.30042	14.60
$C_{29}H_{38}O_7Na^+$	521.25144	0.89	521.25914	15.66

Table A3. Continued

Cation formula	Internal calibration		Externel calibration	
	Measured *m/z*	*m/z* error (ppm)	Measured *m/z*	*m/z* error (ppm)
$C_{30}H_{42}O_6Na^+$	521.28758	0.42	521.29528	15.19
$C_{31}H_{46}O_5Na^+$	521.32432	1.10	521.33202	15.87
$C_{29}H_{40}O_7Na^+$	523.26731	1.31	523.27507	16.15
$C_{30}H_{44}O_6Na^+$	523.30278	–0.44	523.31054	14.39
$C_{31}H_{48}O_5Na^+$	523.33971	0.59	523.34747	15.43
$C_{29}H_{42}O_7Na^+$	525.28270	0.82	525.29053	15.72
$C_{30}H_{46}O_6Na^+$	525.31813	–1.01	525.32595	13.88
$C_{28}H_{40}O_8Na^+$	527.26180	0.50	527.26969	15.46
$C_{29}H_{44}O_7Na^+$	527.29825	0.62	527.30614	15.58
$C_{30}H_{48}O_6Na^+$	527.33404	–0.52	527.34193	14.45
$C_{28}H_{42}O_8Na^+$	529.27778	1.12	529.28574	16.15
$C_{29}H_{46}O_7Na^+$	529.31384	0.51	529.32180	15.54
$C_{30}H_{50}O_6Na^+$	529.34952	–0.82	529.35748	14.21
$C_{27}H_{40}O_9Na^+$	531.25572	–1.38	531.26374	13.72
$C_{28}H_{44}O_8Na^+$	531.29314	0.56	531.30116	15.65
$C_{29}H_{48}O_7Na^+$	531.32837	–1.61	531.33639	13.48
$C_{30}H_{52}O_6Na^+$	531.36508	–1.00	531.37310	14.09
$C_{27}H_{42}O_9Na^+$	533.27208	–0.04	533.28017	15.12
$C_{28}H_{46}O_8Na^+$	533.30795	–1.02	533.31603	14.14
$C_{30}H_{54}O_6Na^+$	533.38079	–0.87	533.38888	14.29
$C_{30}H_{40}O_7Na^+$	535.26674	0.22	535.27489	15.44
$C_{31}H_{44}O_6Na^+$	535.30272	–0.55	535.31087	14.68
$C_{32}H_{48}O_5Na^+$	535.34006	1.24	535.34821	16.47
$C_{30}H_{42}O_7Na^+$	537.28196	–0.58	537.29017	14.70
$C_{31}H_{46}O_6Na^+$	537.31839	–0.51	537.32660	14.78
$C_{29}H_{40}O_8Na^+$	539.26170	0.30	539.26998	15.65
$C_{30}H_{44}O_7Na^+$	539.29777	–0.29	539.30605	15.06
$C_{31}H_{48}O_6Na^+$	539.33324	–1.99	539.34152	13.37
$C_{29}H_{42}O_8Na^+$	541.27755	0.67	541.28590	16.08
$C_{30}H_{46}O_7Na^+$	541.31332	–0.46	541.32167	14.95
$C_{31}H_{50}O_6Na^+$	541.34925	–1.32	541.35759	14.10
$C_{28}H_{40}O_9Na^+$	543.25564	–1.50	543.26405	13.98
$C_{29}H_{44}O_8Na^+$	543.29307	0.42	543.30148	15.90
$C_{30}H_{48}O_7Na^+$	543.32868	–1.01	543.33709	14.47
$C_{28}H_{42}O_9Na^+$	545.27266	1.02	545.28114	16.56
$C_{32}H_{42}O_6Na^+$	545.28645	–1.67	545.29493	13.88

Table A3. Continued

Cation formula	Internal calibration		Externel calibration	
	Measured *m/z*	*m/z* error (ppm)	Measured *m/z*	*m/z* error (ppm)
$C_{29}H_{46}O_8Na^+$	545.30908	1.09	545.31756	16.63
$C_{30}H_{50}O_7Na^+$	545.34461	–0.48	545.35309	15.07
$C_{27}H_{40}O_{10}Na^+$	547.25194	1.04	547.26048	16.65
$C_{28}H_{44}O_9Na^+$	547.28816	0.73	547.29670	16.35
$C_{29}H_{48}O_8Na^+$	547.32315	–1.81	547.33169	13.80
$C_{30}H_{52}O_7Na^+$	547.36015	–0.69	547.36869	14.92
$C_{31}H_{42}O_7Na^+$	549.28252	0.44	549.29113	16.12
$C_{32}H_{46}O_6Na^+$	549.31904	0.70	549.32765	16.37
$C_{30}H_{40}O_8Na^+$	551.26127	–0.49	551.26994	15.25
$C_{31}H_{44}O_7Na^+$	551.29820	0.50	551.30688	16.24
$C_{32}H_{48}O_6Na^+$	551.33418	–0.23	551.34286	15.51
$C_{30}H_{42}O_8Na^+$	553.27722	0.06	553.28597	15.87
$C_{31}H_{46}O_7Na^+$	553.31380	0.40	553.32254	16.20
$C_{32}H_{50}O_6Na^+$	553.35038	0.76	553.35913	16.56
$C_{29}H_{40}O_9Na^+$	555.25732	1.56	555.26613	17.42
$C_{30}H_{44}O_8Na^+$	555.29303	0.35	555.30184	16.21
$C_{31}H_{48}O_7Na^+$	555.32928	0.10	555.33810	15.97
$C_{31}H_{41}O_9^+$	557.27376	–1.34	557.28264	14.59
$C_{30}H_{46}O_8Na^+$	557.30880	0.56	557.31768	16.49
$C_{31}H_{43}O_9^+$	559.28953	–1.13	559.29848	14.87
$C_{30}H_{48}O_8Na^+$	559.32426	0.21	559.33321	16.21
$C_{29}H_{46}O_9Na^+$	561.30351	0.19	561.31253	16.25
$C_{30}H_{50}O_8Na^+$	561.33977	–0.03	561.34879	16.03
$C_{32}H_{44}O_7Na^+$	563.29776	–0.30	563.30684	15.83
$C_{30}H_{52}O_8Na^+$	563.35460	–1.50	563.36368	14.63
$C_{30}H_{40}O_9Na^+$	567.25610	–0.63	567.26532	15.63
$C_{31H44}O_8Na^+$	567.29291	0.13	567.30213	16.38
$C_{32}H_{48}O_7Na^+$	567.32920	–0.05	567.33842	16.21
$C_{30}H_{42}O_9Na^+$	569.27266	0.97	569.28195	17.30
$C_{31}H_{46}O_8Na^+$	569.30880	0.54	569.31809	16.86
$C_{32}H_{50}O_7Na^+$	569.34412	–1.32	569.35342	15.00
$C_{30}H_{44}O_9Na^+$	571.28810	0.60	571.29746	16.98
$C_{31}H_{48}O_8Na^+$	571.32433	0.34	571.33369	16.72
$C_{32}H_{52}O_7Na^+$	571.36115	1.10	571.37052	17.49
$C_{31}H_{41}O_{10}^+$	573.26854	–1.54	573.27797	14.91
$C_{30}H_{46}O_9Na^+$	573.30385	0.78	573.31328	17.23

Table A3. Continued

Cation formula	Internal calibration		Externel calibration	
	Measured *m/z*	*m/z* error (ppm)	Measured *m/z*	*m/z* error (ppm)
$C_{31}H_{50}O_8Na^+$	573.33945	–0.60	573.34888	15.85
$C_{29}H_{44}O_{10}Na^+$	575.28366	1.73	575.29316	18.24
$C_{30}H_{48}O_9Na^+$	575.31936	0.54	575.32887	17.05
$C_{31}H_{52}O_8Na^+$	575.35550	0.11	575.36501	16.63
$C_{30}H_{50}O_9Na^+$	577.33477	0.12	577.34435	16.71
$C_{32}H_{44}O_8Na^+$	579.29209	–1.29	579.30173	15.35
$C_{33}H_{48}O_7Na^+$	579.33018	1.64	579.33982	18.29
$C_{32}H_{46}O_8Na^+$	581.30866	0.29	581.31837	17.00
$C_{33}H_{50}O_7Na^+$	581.34490	0.05	581.35462	16.76
$C_{31}H_{44}O_9Na^+$	583.28872	1.65	583.29850	18.42
$C_{32}H_{48}O_8Na^+$	583.32529	1.96	583.33507	18.74
$C_{33}H_{52}O_7Na^+$	583.36057	0.08	583.37036	16.85
$C_{31}H_{46}O_9Na^+$	585.30411	1.20	585.31396	18.04
$C_{32}H_{50}O_8Na^+$	585.34075	1.64	585.35061	18.48
$C_{31}H_{48}O_9Na^+$	587.31797	–1.85	587.32790	15.06
$C_{32}H_{52}O_8Na^+$	587.35651	1.83	587.36644	18.73
$C_{29}H_{42}O_{11}Na^+$	589.26293	1.70	589.27293	18.66
$C_{32}H_{45}O_{10}^+$	589.30147	1.26	589.31147	18.23
$C_{33}H_{46}O_8Na^+$	593.30767	–1.38	593.31782	15.72
$C_{32}H_{44}O_9Na^+$	595.28709	–1.12	595.29731	16.04
$C_{33}H_{48}O_8Na^+$	595.32451	0.62	595.33473	17.78
$C_{32}H_{46}O_9Na^+$	597.30388	0.80	597.31417	18.02
$C_{32}H_{48}O_9Na^+$	599.31916	0.17	599.32952	17.46
$C_{33}H_{52}O_8Na^+$	599.35578	0.57	599.36615	17.86
$C_{33}H_{45}O_{10}^+$	601.30031	–0.69	601.31075	16.67
$C_{32}H_{50}O_9Na^+$	601.33427	–0.73	601.34471	16.63
$C_{33}H_{47}O_{10}^+$	603.31521	–1.93	603.32572	15.49
$C_{34}H_{46}O_8Na^+$	605.30793	–0.93	605.31851	16.56
$C_{34}H_{48}O_8Na^+$	607.32442	0.46	607.33508	18.01
$C_{33}H_{46}O_9Na^+$	609.30387	0.76	609.31460	18.38
$C_{34}H_{50}O_8Na^+$	609.33972	–0.12	609.35045	17.50
$C_{33}H_{48}O_9Na^+$	611.31890	–0.26	611.32971	17.42
$C_{34}H_{52}O_8Na^+$	611.35534	–0.17	611.36615	17.51
$C_{32}H_{46}O_{10}Na^+$	613.29951	1.93	613.31039	19.68
$C_{32}H_{48}O_{10}Na^+$	615.31405	0.13	615.32501	17.94
$C_{33}H_{52}O_9Na^+$	615.35074	0.63	615.36187	18.71

Table A3. Continued

Cation formula	Internal calibration		Externel calibration	
	Measured *m/z*	*m/z* error (ppm)	Measured *m/z*	*m/z* error (ppm)
$C_{34}H_{48}O_9Na^+$	623.31860	–0.73	623.32986	17.34
$C_{34}H_{50}O_9Na^+$	625.33529	0.94	625.34663	19.08
$C_{34}H_{52}O_9Na^+$	627.35145	1.75	627.36287	19.94
$C_{34}H_{54}O_9Na^+$	629.36708	1.71	629.37858	19.98
$C_{35}H_{48}O_9Na^+$	635.31871	–0.54	635.33044	17.91
$C_{36}H_{52}O_8Na^+$	635.35592	0.75	635.36765	19.21
$C_{36}H_{54}O_8Na^+$	637.37178	1.09	637.38359	19.61
$C_{35}H_{52}O_9Na^+$	639.35049	0.20	639.36237	18.79
$C_{36}H_{56}O_8Na^+$	639.38692	0.29	639.39881	18.87
$C_{34}H_{50}O_{10}Na^+$	641.33028	1.03	641.34224	19.68
$C_{34}H_{52}O_{10}Na^+$	643.34606	1.23	643.35810	19.95
$C_{38}H_{56}O_7Na^+$	647.39055	–1.98	647.40275	16.87
$C_{36}H_{50}O_9Na^+$	649.33446	–0.38	649.34674	18.53
$C_{38}H_{58}O_7Na^+$	649.40623	–1.92	649.41851	16.99
$C_{36}H_{54}O_9Na^+$	653.36696	1.47	653.37940	20.51
$C_{35}H_{52}O_{10}Na^+$	655.34512	–0.22	655.35764	18.88

Table A4. Assignment of ion formulas corresponding to peaks of the positive ion mode mass spectrum of sandarac resin obtained with the modified MALDI-FT-ICR-MS methodology and the comparison of *m/z* errors in the case of internal and external calibration. The clusters are outlined with a thick line.

Cation formula	Internal calibration		Externel calibration	
	Measured *m/z*	*m/z* error (ppm)	Measured *m/z*	*m/z* error (ppm)
$C_{20}H_{29}O_2^+$	301.21631	0.35	301.223185	23.17
$C_{19}H_{26}O_5Na^+$	357.16729	0.12	357.177054	27.46
$C_{20}H_{30}O_4Na^+$	357.20366	0.07	357.213423	27.42
$C_{19}H_{28}O_5Na^+$	359.18317	0.76	359.193048	28.27
$C_{20}H_{32}O_4Na^+$	359.21986	1.61	359.229738	29.11
$C_{20}H_{28}O_5Na^+$	371.18296	0.18	371.193530	28.65
$C_{19}H_{26}O_6Na^+$	373.16225	0.24	373.172935	28.87
$C_{20}H_{30}O_5Na^+$	373.19883	0.75	373.209512	29.39
$C_{19}H_{28}O_6Na^+$	375.17826	1.19	375.189060	29.99
$C_{20}H_{32}O_5Na^+$	375.21444	0.66	375.225248	29.46
$C_{20}H_{34}O_5Na^+$	377.23035	1.34	377.241276	30.30
$C_{20}H_{26}O_6Na^+$	385.16239	0.61	385.173795	30.21
$C_{20}H_{28}O_6Na^+$	387.17808	0.69	387.189601	30.45

Table A4. Continued

Cation formula	Internal calibration		Externel calibration	
	Measured *m/z*	*m/z* error (ppm)	Measured *m/z*	*m/z* error (ppm)
$C_{20}H_{30}O_6Na^+$	389.19370	0.61	389.205343	30.53
$C_{19}H_{28}O_7Na^+$	391.17268	–0.12	391.184446	29.96
$C_{20}H_{32}O_6Na^+$	391.20934	0.60	391.221113	30.68
$C_{20}H_{34}O_6Na^+$	393.22484	0.20	393.236732	30.45
$C_{20}H_{26}O_7Na^+$	401.15749	1.03	401.169882	31.93
$C_{20}H_{28}O_7Na^+$	403.17289	0.42	403.185413	31.47
$C_{20}H_{30}O_7Na^+$	405.18863	0.63	405.201277	31.84
$C_{20}H_{32}O_7Na^+$	407.20437	0.85	407.217151	32.23
$C_{20}H_{34}O_7Na^+$	409.21976	0.20	409.232664	31.74
$C_{21}H_{30}O_7Na^+$	417.18829	–0.21	417.201715	31.98
$C_{20}H_{28}O_8Na^+$	419.16817	1.25	419.181723	33.60
$C_{20}H_{30}O_8Na^+$	421.18347	0.43	421.197164	32.94
$C_{20}H_{32}O_8Na^+$	423.19964	1.64	423.213461	34.31
$C_{20}H_{28}O_9Na^+$	435.16331	1.73	435.177942	35.36
$C_{29}H_{40}O_5Na^+$	491.27689	0.20	491.295640	38.36
$C_{30}H_{44}O_4Na^+$	491.31367	1.00	491.332422	39.16
$C_{28}H_{38}O_6Na^+$	493.25542	–1.29	493.274326	37.03
$C_{29}H_{42}O_5Na^+$	493.29238	–0.12	493.311290	38.20
$C_{30}H_{46}O_4Na^+$	493.32921	0.77	493.348118	39.10
$C_{27}H_{36}O_7Na^+$	495.23582	1.01	495.254881	39.49
$C_{28}H_{40}O_6Na^+$	495.27227	1.12	495.291326	39.61
$C_{29}H_{44}O_5Na^+$	495.30772	–0.77	495.326779	37.72
$C_{30}H_{48}O_4Na^+$	495.34482	0.69	495.363888	39.18
$C_{27}H_{38}O_7Na^+$	497.25111	0.27	497.270323	38.91
$C_{28}H_{42}O_6Na^+$	497.28787	1.03	497.307091	39.68
$C_{29}H_{46}O_5Na^+$	497.32405	0.62	497.343274	39.27
$C_{27}H_{40}O_7Na^+$	499.26670	0.14	499.286073	38.95
$C_{27}H_{42}O_7Na^+$	501.28287	1.18	501.302402	40.15
$C_{29}H_{40}O_6Na^+$	507.27193	0.44	507.291946	39.89
$C_{30}H_{44}O_5Na^+$	507.30793	–0.32	507.327949	39.14
$C_{27}H_{34}O_8Na^+$	509.21417	–0.82	509.234344	38.79
$C_{28}H_{38}O_7Na^+$	509.25196	1.93	509.272129	41.54
$C_{29}H_{42}O_6Na^+$	509.28756	0.38	509.307731	40.00
$C_{30}H_{46}O_5Na^+$	509.32341	–0.67	509.343585	38.95
$C_{27}H_{36}O_8Na^+$	511.23056	0.63	511.250895	40.40
$C_{28}H_{40}O_7Na^+$	511.26700	0.73	511.287335	40.51

Table A4. Continued

Cation formula	Internal calibration		Externel calibration	
	Measured *m/z*	*m/z* error (ppm)	Measured *m/z*	*m/z* error (ppm)
$C_{29}H_{44}O_6Na^+$	511.30305	0.07	511.323386	39.85
$C_{30}H_{48}O_5Na^+$	511.33887	–1.02	511.359214	38.76
$C_{27}H_{38}O_8Na^+$	513.24634	0.87	513.266834	40.81
$C_{28}H_{42}O_7Na^+$	513.28287	1.16	513.303367	41.09
$C_{29}H_{46}O_6Na^+$	513.31912	0.90	513.339623	40.84
$C_{27}H_{40}O_8Na^+$	515.26239	1.64	515.283047	41.74
$C_{28}H_{44}O_7Na^+$	515.29752	–0.78	515.318185	39.32
$C_{27}H_{42}O_8Na^+$	517.27771	1.00	517.298531	41.26
$C_{30}H_{42}O_6Na^+$	521.28771	0.68	521.308869	41.26
$C_{30}H_{44}O_6Na^+$	523.30291	–0.19	523.324235	40.56
$C_{28}H_{38}O_8Na^+$	525.24544	–0.85	525.266926	40.05
$C_{29}H_{42}O_7Na^+$	525.28270	0.81	525.304190	41.72
$C_{30}H_{46}O_6Na^+$	525.31830	–0.68	525.339793	40.23
$C_{29}H_{44}O_7Na^+$	527.29854	1.17	527.320197	42.24
$C_{30}H_{48}O_6Na^+$	527.33405	–0.50	527.355707	40.58
$C_{27}H_{38}O_9Na^+$	529.24109	0.54	529.262911	41.77
$C_{29}H_{46}O_7Na^+$	529.31409	0.97	529.335913	42.20
$C_{30}H_{50}O_6Na^+$	529.34958	–0.72	529.371405	40.51
$C_{30}H_{40}O_7Na^+$	535.26654	–0.17	535.288864	41.55
$C_{30}H_{42}O_7Na^+$	537.28266	0.71	537.305154	42.58
$C_{31}H_{46}O_6Na^+$	537.31827	–0.72	537.340774	41.16
$C_{29}H_{40}O_8Na^+$	539.26179	0.46	539.284454	42.49
$C_{30}H_{44}O_7Na^+$	539.29773	–0.37	539.320399	41.67
$C_{29}H_{42}O_8Na^+$	541.27752	0.61	541.300361	42.81
$C_{30}H_{46}O_7Na^+$	541.31327	–0.56	541.336117	41.64
$C_{29}H_{44}O_8Na^+$	543.29343	1.08	543.316440	43.44
$C_{30}H_{50}O_7Na^+$	545.34469	–0.34	545.367880	42.18
$C_{31}H_{44}O_7Na^+$	551.29899	1.93	551.322699	44.94
$C_{30}H_{42}O_8Na^+$	553.27749	0.54	553.301371	43.71
$C_{31}H_{46}O_7Na^+$	553.31325	–0.59	553.337133	42.58
$C_{29}H_{40}O_9Na^+$	555.25695	0.90	555.281009	44.22
$C_{30}H_{44}O_8Na^+$	555.29284	0.00	555.316901	43.33
$C_{31}H_{48}O_7Na^+$	555.32906	–0.30	555.353122	43.03
$C_{29}H_{42}O_9Na^+$	557.27268	1.03	557.296915	44.52
$C_{30}H_{46}O_8Na^+$	557.30805	–0.78	557.332291	42.71
$C_{30}H_{48}O_8Na^+$	559.32394	–0.35	559.348360	43.30

Table A4. Continued

Cation formula	Internal calibration		Externel calibration	
	Measured *m/z*	*m/z* error (ppm)	Measured *m/z*	*m/z* error (ppm)
$C_{32}H46O7Na^+$	565.31377	0.34	565.338721	44.48
$C_{31}H_{44}O_8Na^+$	567.29314	0.53	567.318268	44.82
$C_{30}H_{42}O_9Na^+$	569.27220	0.17	569.297507	44.62
$C_{31}H_{46}O_8Na^+$	569.30814	–0.62	569.333448	43.84
$C_{31}H_{48}O_8Na^+$	571.32459	0.78	571.350081	45.41
$C_{31}H_{44}O_9Na^+$	583.28840	1.10	583.314985	46.68
$C_{32}H_{48}O_8Na^+$	583.32509	1.62	583.351681	47.21
$C_{30}H_{44}O_{10}Na^+$	587.28333	1.12	587.310291	47.03
$C_{32}H_{45}O_{10}^+$	589.30115	0.72	589.328299	46.79
$C_{38}H_{54}O_6Na^+$	629.38144	0.28	629.412471	49.59
$C_{37}H_{54}O_7Na^+$	633.37733	1.83	633.408766	51.46
$C_{38}H_{53}O_8^+$	637.37338	–0.17	637.405222	49.78
$C_{39}H_{56}O_6Na^+$	643.39635	–0.86	643.428805	49.57
$C_{40}H_{60}O_5Na^+$	643.43405	1.17	643.466504	51.61
$C_{38}H_{54}O_7Na^+$	645.37693	1.17	645.409584	51.77
$C_{39}H_{58}O_6Na^+$	645.41351	1.47	645.446166	52.07
$C_{37}H_{52}O_8Na^+$	647.35667	1.90	647.389531	52.66
$C_{38}H_{56}O_7Na^+$	647.39281	1.52	647.425669	52.28
$C_{39}H_{60}O_6Na^+$	647.42888	1.03	647.461742	51.79
$C_{38}H_{58}O_7Na^+$	649.40810	0.96	649.441167	51.88
$C_{39}H_{62}O_6Na^+$	649.44444	0.89	649.477514	51.82
$C_{38}H_{51}O_9^+$	651.35306	0.47	651.386334	51.55
$C_{38}H_{53}O_9^+$	653.36760	–1.24	653.401081	50.00
$C_{39}H_{54}O_7Na^+$	657.37578	–0.61	657.409674	50.96
$C_{40}H_{58}O_6Na^+$	657.41146	–1.67	657.445364	49.90
$C_{39}H_{56}O_7Na^+$	659.39185	0.04	659.425964	51.77
$C_{40}H_{60}O_6Na^+$	659.42902	1.22	659.463130	52.95
$C_{39}H_{58}O_7Na^+$	661.40697	–0.77	661.441288	51.12
$C_{40}H_{62}O_6Na^+$	661.44281	–1.59	661.477134	50.31
$C_{38}H_{56}O_8Na^+$	663.38706	0.49	663.421593	52.54
$C_{39}H_{60}O_7Na^+$	663.42363	0.77	663.458167	52.82
$C_{37}H_{54}O_9Na^+$	665.36638	0.56	665.401118	52.77
$C_{40}H_{57}O_8^+$	665.40378	–1.53	665.438520	50.68
$C_{39}H_{62}O_7Na^+$	665.43848	–0.44	665.473230	51.78
$C_{40}H_{60}O_7Na^+$	675.42408	1.41	675.459889	54.43
$C_{40}H_{62}O_7Na^+$	677.43994	1.72	677.475970	54.91

Table A4. Continued

Cation formula	Internal calibration		Externel calibration	
	Measured *m/z*	*m/z* error (ppm)	Measured *m/z*	*m/z* error (ppm)
$C_{37}H_{52}O_{10}Na^+$	679.34556	0.43	679.381718	53.65
$C_{38}H_{56}O_9Na^+$	679.38133	–0.48	679.417566	52.86
$C_{39}H_{60}O_8Na^+$	679.41823	0.27	679.454468	53.62
$C_{39}H_{54}O_9Na^+$	689.36645	0.65	689.403780	54.80
$C_{39}H_{56}O_9Na^+$	691.38299	1.93	691.420540	56.24
$C_{41}H_{57}O_9^+$	693.39876	–1.37	693.436529	53.10
$C_{40}H_{62}O_8Na^+$	693.43237	–1.90	693.470149	52.58
$C_{41}H_{59}O_9^+$	695.41517	–0.27	695.453166	54.36
$C_{40}H_{64}O_8Na^+$	695.44790	–2.07	695.485890	52.56
$C_{41}H_{61}O_9^+$	697.43073	–0.41	697.468944	54.39
$C_{40}H_{56}O_9Na^+$	703.38257	1.30	703.421451	56.58
$C_{40}H_{58}O_9Na^+$	705.39715	–0.22	705.436261	55.23
$C_{40}H_{60}O_9Na^+$	707.41200	–1.35	707.451333	54.25
$C_{39}H_{60}O_{10}Na^+$	711.40766	–0.30	711.447444	55.63
$C_{40}H_{56}O_{10}Na^+$	719.37791	1.86	719.418601	58.43
$C_{40}H_{58}O_{10}Na^+$	721.39307	1.17	721.433993	57.91
$C_{39}H_{56}O_{11}Na^+$	723.37206	0.79	723.413214	57.69
$C_{40}H_{60}O_{10}Na^+$	723.40793	0.08	723.449085	56.97
$C_{40}H_{62}O_{10}Na^+$	725.42326	–0.37	725.464645	56.69
$C_{40}H_{64}O_{10}Na^+$	727.43969	0.72	727.481318	57.94
$C_{40}H_{66}O_{10}Na^+$	729.45384	–1.34	729.495697	56.04

Table A5. Assignment of ion formulas corresponding to peaks of the positive ion mode mass spectrum of colophony resin obtained with the modified MALDI-FT-ICR-MS methodology and the comparison of *m/z* errors in the case of internal and external calibration. The clusters are outlined with a thick line.

Cation formula	Internal calibration		Externel calibration	
	Measured *m/z*	*m/z* error (ppm)	Measured *m/z*	*m/z* error (ppm)
$C_{15}H_{15}^+$	195.11645	–1.93	195.12031	17.84
$C_{15}H_{17}^+$	197.13215	–1.64	197.13607	18.24
$C_{15}H_{19}^+$	199.14783	–1.47	199.15182	18.53
$C_{15}H_{21}^+$	201.16346	–1.58	201.16750	18.53
$C_{16}H_{17}^+$	209.13216	–1.52	209.13646	19.06
$C_{16}H_{19}^+$	211.14781	–1.49	211.15218	19.20
$C_{15}H_{17}O^+$	213.12700	–1.82	213.13144	18.98
$C_{16}H_{21}^+$	213.16348	–1.38	213.16792	19.43

Table A5. Continued

Cation formula	Internal calibration		Externel calibration	
	Measured *m/z*	*m/z* error (ppm)	Measured *m/z*	*m/z* error (ppm)
$C_{15}H_{19}O^+$	215.14263	–1.91	215.14713	19.01
$C_{17}H_{19}^+$	223.14775	–1.69	223.15252	19.69
$C_{17}H_{21}^+$	225.16354	–1.06	225.16838	20.44
$C_{17}H_{23}^+$	227.17924	–0.83	227.18415	20.79
$C_{18}H_{19}^+$	235.14822	0.39	235.15341	22.47
$C_{18}H_{21}^+$	237.16336	–1.77	237.16862	20.42
$C_{18}H_{23}^+$	239.17941	–0.07	239.18474	22.24
$C_{18}H_{25}^+$	241.19495	–0.52	241.20036	21.91
$C_{19}H_{23}^+$	251.17934	–0.33	251.18512	22.67
$C_{18}H_{21}O^+$	253.15822	–1.86	253.16407	21.26
$C_{19}H_{25}^+$	253.19500	–0.28	253.20086	22.83
$C_{19}H_{27}^+$	255.21062	–0.40	255.21655	22.84
$C_{19}H_{29}^+$	257.22599	–1.50	257.23199	21.84
$C_{19}H_{23}O^+$	267.17433	–0.05	267.18072	23.88
$C_{19}H_{25}O^+$	269.19017	0.65	269.19664	24.69
$C_{19}H_{27}O^+$	271.20568	0.13	271.21223	24.29
$C_{19}H_{23}O_2^+$	283.16943	0.63	283.17647	25.48
$C_{19}H_{25}O_2^+$	285.18510	0.69	285.19222	25.66
$C_{19}H_{27}O_2^+$	287.20067	0.38	287.20787	25.46
$C_{20}H_{25}O_2^+$	297.18494	0.11	297.19256	25.77
$C_{16}H_{20}O_4Na^+$	299.12532	–0.21	299.13303	25.56
$C_{20}H_{29}O_2^+$	301.21644	0.78	301.22424	26.67
$C_{19}H_{27}O_3^+$	303.19515	–1.05	303.20304	24.95
$C_{19}H_{26}O_2Na^+$	309.18255	0.17	309.19070	26.52
$C_{17}H_{20}O_4Na^+$	311.12499	–1.25	311.13322	25.21
$C_{19}H_{28}O_2Na^+$	311.19792	–0.73	311.20616	25.74
$C_{17}C_{22}O_4Na^+$	313.14124	0.67	313.14956	27.25
$C_{20}H_{25}O_3^+$	313.18021	1.24	313.18853	27.82
$C_{21}H_{29}O_2^+$	313.21648	0.87	313.22480	27.45
$C_{17}C_{24}O_4Na^+$	315.15615	–1.68	315.16456	25.01
$C_{20}H_{27}O_3^+$	315.19588	1.30	315.20430	28.00
$C_{21}H_{31}O_2^+$	315.23153	–1.02	315.23995	25.67
$C_{20}H_{29}O_3^+$	317.21151	1.24	317.22002	28.05
$C_{20}H_{26}O_2Na^+$	321.18312	1.92	321.19180	28.96
$C_{20}H_{28}O_2Na^+$	323.19824	0.27	323.20701	27.42
$C_{19}H_{26}O_3Na^+$	325.17778	1.11	325.18665	28.38

Table A5. Continued

Cation formula	Internal calibration		Externel calibration	
	Measured *m/z*	*m/z* error (ppm)	Measured *m/z*	*m/z* error (ppm)
$C_{17}C_{20}O_5Na^+$	327.12057	0.85	327.12953	28.24
$C_{19}H_{28}O_3Na^+$	327.19319	0.38	327.20215	27.76
$C_{17}C_{22}O_5Na^+$	329.13624	0.89	329.14529	28.39
$C_{20}C_{25}O_4^+$	329.17515	1.25	329.18420	28.75
$C_{17}C_{24}O_5Na^+$	331.15189	0.88	331.16103	28.50
$C_{20}H_{27}O_4^+$	331.19069	0.91	331.19983	28.53
$C_{20}H_{29}O_4^+$	333.20543	–1.82	333.21467	25.92
$C_{20}H_{26}O_3Na^+$	337.17776	1.04	337.18719	29.00
$C_{19}H_{24}O_4Na^+$	339.15723	1.62	339.16676	29.71
$C_{20}H_{28}O_3Na^+$	339.19326	0.56	339.20278	28.64
$C_{19}H_{26}O_4Na^+$	341.17285	1.54	341.18247	29.73
$C_{20}H_{30}O_3Na^+$	341.20938	1.95	341.21900	30.15
$C_{18}H_{24}O_5Na^+$	343.15226	1.93	343.16197	30.24
$C_{19}H_{28}O_4Na^+$	343.18843	1.31	343.19815	29.62
$C_{17}C_{22}O_6Na^+$	345.13152	1.90	345.14133	30.32
$C_{18}H_{26}O_5Na^+$	345.16789	1.87	345.17770	30.29
$C_{19}H_{30}O_4Na^+$	345.20297	–1.91	345.21278	26.51
$C_{17}C_{24}O_6Na^+$	347.14683	0.92	347.15674	29.46
$C_{20}C_{24}O_4Na^+$	351.15675	0.20	351.16685	28.97
$C_{20}H_{26}O_4Na^+$	353.17273	1.12	353.18293	30.01
$C_{19}H_{24}O_5Na^+$	355.15197	1.06	355.16227	30.06
$C_{20}H_{28}O_4Na^+$	355.18810	0.35	355.19841	29.35
$C_{19}H_{26}O_5Na^+$	357.16818	2.62	357.17858	31.73
$C_{20}H_{30}O_4Na^+$	357.20377	0.39	357.21417	29.51
$C_{18}H_{24}O_6Na^+$	359.14587	–1.78	359.15637	27.45
$C_{19}H_{28}O_5Na^+$	359.18364	2.08	359.19414	31.32
$C_{17}C_{22}O_7Na^+$	361.12598	0.57	361.13658	29.92
$C_{18}H_{26}O_6Na^+$	361.16162	–1.49	361.17222	27.86
$C_{19}H_{30}O_5Na^+$	361.19915	1.66	361.20975	31.02
$C_{17}C_{24}O_7Na^+$	363.14125	–0.50	363.15194	28.97
$C_{18}H_{28}O_6Na^+$	363.17709	–1.98	363.18779	27.49
$C_{20}C_{24}O_5Na^+$	367.15217	1.57	367.16308	31.27
$C_{20}H_{26}O_5Na^+$	369.16772	1.28	369.17872	31.09
$C_{19}H_{24}O_6Na^+$	371.14638	–0.34	371.15749	29.58
$C_{20}H_{28}O_5Na^+$	371.18308	0.51	371.19419	30.44
$C_{19}H_{26}O_6Na^+$	373.16322	2.84	373.17443	32.88

Table A5. Continued

Cation formula	Internal calibration		Externel calibration	
	Measured *m/z*	*m/z* error (ppm)	Measured *m/z*	*m/z* error (ppm)
$C_{20}H_{30}O_5Na^+$	373.19864	0.26	373.20985	30.30
$C_{20}H_{32}O_5Na^+$	375.21470	1.34	375.22601	31.50
$C_{19}H_{30}O_6Na^+$	377.19342	–0.12	377.20483	30.15
$C_{20}C_{24}O_6Na^+$	383.14670	0.48	383.15843	31.10
$C_{20}H_{26}O_6Na^+$	385.16283	1.73	385.17466	32.46
$C_{21}H_{30}O_5Na^+$	385.19890	0.91	385.21074	31.65
$C_{20}H_{28}O_6Na^+$	387.17820	1.02	387.19015	31.87
$C_{19}H_{26}O_7Na^+$	389.15785	1.98	389.16990	32.95
$C_{20}H_{30}O_6Na^+$	389.19365	0.50	389.20571	31.47
$C_{20}H_{32}O_6Na^+$	391.20979	1.74	391.22195	32.83
$C_{19}H_{30}O_7Na^+$	393.18861	0.60	393.20088	31.79
$C_{21}H_{30}O_6Na^+$	401.19418	1.80	401.20689	33.46
$C_{20}H_{28}O_7Na^+$	403.17342	1.73	403.18623	33.51
$C_{21}H_{32}O_6Na^+$	403.20894	–0.43	403.22175	31.34
$C_{20}H_{30}O_7Na^+$	405.18892	1.35	405.20184	33.24
$C_{19}H_{30}O_8Na^+$	409.18268	–1.50	409.19582	30.62
$C_{20}H_{26}O_8Na^+$	417.15223	0.57	417.16582	33.15
$C_{21}H_{30}O_7Na^+$	417.18799	–0.93	417.20158	31.65
$C_{20}H_{28}O_8Na^+$	419.16851	2.08	419.18278	36.11
$C_{21}H_{32}O_7Na^+$	419.20325	–1.84	419.21696	30.86
$C_{20}H_{28}O_9Na^+$	435.16171	–1.93	435.17634	31.69
$C_{37}H_{48}O_6Na^+$	611.33412	–0.31	611.36089	43.48
$C_{37}H_{50}O_6Na^+$	613.34903	–1.52	613.37596	42.39
$C_{37}H_{49}O_8^+$	621.34127	–1.49	621.36883	42.87
$C_{37}H_{50}O_7Na^+$	629.34416	–1.14	629.37237	43.69
$C_{37}H_{52}O_7Na^+$	631.35958	–1.50	631.38796	43.45
$C_{37}H_{46}O_8Na^+$	641.30784	–1.02	641.33703	44.50
$C_{37}H_{48}O_8Na^+$	643.32363	–0.80	643.35299	44.84
$C_{37}H_{50}O_8Na^+$	645.33887	–1.43	645.36839	44.32
$C_{37}H_{52}O_8Na^+$	647.35514	–0.47	647.38483	45.40
$C_{37}H_{54}O_8Na^+$	649.37092	–0.27	649.40078	45.72
$C_{40}H_{56}O_6Na^+$	655.39598	–1.41	655.42635	44.92
$C_{39}H_{54}O_7Na^+$	657.37533	–1.28	657.40586	45.16
$C_{40}H_{51}O_8^+$	659.35662	–1.86	659.38732	44.70
$C_{40}H_{60}O_6Na^+$	659.42706	–1.75	659.45777	44.82
$C_{38}H_{54}O_8Na^+$	661.37061	–0.73	661.40148	45.95

Table A5. Continued

Cation formula	Internal calibration		Externel calibration	
	Measured *m/z*	*m/z* error (ppm)	Measured *m/z*	*m/z* error (ppm)
$C_{39}H_{58}O_7Na^+$	661.40735	–0.19	661.43823	46.49
$C_{37}H_{52}O_9Na^+$	663.34966	–1.05	663.38070	45.74
$C_{39}H_{52}O_8Na^+$	671.35575	0.47	671.38748	47.72
$C_{42}H_{55}O_7^+$	671.39416	–0.10	671.42589	47.16
$C_{37}H_{46}O_{10}Na^+$	673.29838	0.08	673.33027	47.45
$C_{38}H_{50}O_9Na^+$	673.33442	–0.42	673.36632	46.95
$C_{37}H_{48}O_{10}Na^+$	675.31398	0.01	675.34604	47.49
$C_{38}H_{52}O_9Na^+$	675.35140	1.54	675.38347	49.03
$C_{39}H_{56}O_8Na^+$	675.38572	–1.51	675.41779	45.97
$C_{40}H_{60}O_7Na^+$	675.42267	–0.67	675.45475	46.82
$C_{37}H_{50}O_{10}Na^+$	677.32857	–1.55	677.36081	46.05
$C_{40}H_{53}O_9^+$	677.36758	–1.22	677.39983	46.38
$C_{39}H_{58}O_8Na^+$	677.40117	–1.81	677.43341	45.80
$C_{37}H_{52}O_{10}Na^+$	679.34603	1.12	679.37844	48.83
$C_{39}H_{50}O_9Na^+$	685.33553	1.21	685.36847	49.27
$C_{42}H_{55}O_8^+$	687.38917	0.04	687.42229	48.22
$C_{40}H_{49}O_{10}^+$	689.33192	–0.15	689.36521	48.14
$C_{37}H_{48}O_{11}Na^+$	691.30871	–0.25	691.34218	48.16
$C_{38}H_{52}O_{10}Na^+$	691.34599	1.04	691.37946	49.45
$C_{39}H_{56}O_9Na^+$	691.38195	0.43	691.41542	48.84
$C_{39}H_{49}O_{11}^+$	693.32745	0.73	693.36109	49.25
$C_{40}H_{53}O_{10}^+$	693.36390	0.82	693.39754	49.35
$C_{39}H_{58}O_9Na^+$	693.39778	0.69	693.43143	49.21
$C_{40}H_{50}O_9Na^+$	697.33377	–1.34	697.36777	47.41
$C_{40}H_{52}O_9Na^+$	699.35061	0.36	699.38479	49.24
$C_{42}H_{57}O_9^+$	705.39948	–0.33	705.43420	48.89
$C_{41}H_{55}O_{10}^+$	707.37885	–0.18	707.41375	49.15
$C_{37}H_{50}O_{12}Na^+$	709.32028	1.17	709.35516	50.35
$C_{39}H_{58}O_{10}Na^+$	709.39147	–1.06	709.42655	48.39
$C_{37}H_{52}O_{12}Na^+$	711.33428	–1.15	711.36954	48.41
$C_{40}H_{50}O_{10}Na^+$	713.33028	0.93	713.36572	50.60
$C_{40}H_{52}O_{10}Na^+$	715.34586	0.83	715.38148	50.62
$C_{41}H_{56}O_9Na^+$	715.38085	–1.13	715.41647	48.67
$C_{39}H_{54}O_{11}Na^+$	721.35551	–0.44	721.39168	49.70
$C_{42}H_{57}O_{10}^+$	721.39553	1.25	721.43170	51.40
$C_{40}H_{62}O_{10}Na^+$	725.42247	–1.45	725.45901	48.92

Table A5. Continued

Cation formula	Internal calibration		Externel calibration	
	Measured *m/z*	*m/z* error (ppm)	Measured *m/z*	*m/z* error (ppm)
$C_{40}H_{52}O_{11}Na^+$	731.34164	1.99	731.37873	52.71
$C_{39}H_{55}O_{13}^+$	731.36313	–0.81	731.40022	49.91
$C_{40}H_{54}O_{11}Na^+$	733.35503	–1.09	733.39231	49.74
$C_{40}H_{60}O_{11}Na^+$	739.40136	–1.93	739.43920	49.25
$C_{39}H_{57}O_{14}^+$	749.37502	0.97	749.41380	52.73
$C_{40}H_{56}O_{12}Na^+$	751.36689	0.65	751.40586	52.52
$C_{40}H_{58}O_{12}Na^+$	753.38086	–1.59	753.42002	50.40

Table A6. Assignment of ion formulas corresponding to peaks of the negative ion mode mass spectrum of dammar resin and the corresponding *m/z* errors for internal and external calibration.

Anion formula	Internal calibration		Externel calibration	
	Measured *m/z*	*m/z* error (ppm)	Measured *m/z*	*m/z* error (ppm)
$C_{28}H_{43}O_2^-$	411.32636	–1.21	411.32055	–15.33
$C_{29}H_{41}O_2^-$	421.31099	–0.51	421.30490	–14.96
$C_{28}H_{39}O_3^-$	423.29029	–0.42	423.28415	–14.93
$C_{29}H_{43}O_2^-$	423.32655	–0.73	423.32040	–15.24
$C_{28}H_{41}O_3^-$	425.30528	–1.97	425.29908	–16.55
$C_{29}H_{45}O_2^-$	425.34207	–1.01	425.33587	–15.59
$C_{28}H_{43}O_3^-$	427.32211	0.78	427.31585	–13.86
$C_{29}H_{47}O_2^-$	427.35769	–1.10	427.35143	–15.75
$C_{29}H_{39}O_3^-$	435.29025	–0.50	435.28376	–15.41
$C_{29}H_{41}O_3^-$	437.30574	–0.87	437.29919	–15.84
$C_{28}H_{39}O_4^-$	439.28497	–0.96	439.27836	–15.99
$C_{29}H_{43}O_3^-$	439.32175	–0.05	439.31514	–15.08
$C_{28}H_{41}O_4^-$	441.30087	–0.39	441.29420	–15.49
$C_{29}H_{45}O_3^-$	441.33696	–1.04	441.33030	–16.14
$C_{29}H_{47}O_3^-$	443.35339	0.72	443.34666	–14.45
$C_{29}H_{39}O_4^-$	451.28453	–1.91	451.27756	–17.34
$C_{30}H_{43}O_3^-$	451.32085	–2.04	451.31342	–18.50
$C_{29}H_{41}O_4^-$	453.30101	–0.07	453.29398	–15.56
$C_{30}H_{45}O_3^-$	453.33765	0.51	453.33063	–14.98
$C_{29}H_{43}O_4^-$	455.31677	0.19	455.30969	–15.37
$C_{30}H_{47}O_3^-$	455.35229	–1.72	455.34520	–17.29
$C_{29}H_{45}O_4^-$	457.33215	–0.41	457.32500	–16.04
$C_{30}H_{49}O_3^-$	457.36876	0.09	457.36162	–15.53

Table A6. Continued

Anion formula	Internal calibration		Externel calibration	
	Measured *m/z*	*m/z* error (ppm)	Measured *m/z*	*m/z* error (ppm)
$C_{29}H_{47}O_4^-$	459.34797	–0.03	459.34076	–15.72
$C_{30}H_{43}O_4^-$	467.31663	–0.11	467.30918	–16.07
$C_{29}H_{41}O_5^-$	469.29584	–0.23	469.28833	–16.25
$C_{30}H_{45}O_4^-$	469.33229	–0.09	469.32477	–16.11
$C_{29}H_{43}O_5^-$	471.31137	–0.49	471.30379	–16.58
$C_{30}H_{47}O_4^-$	471.34790	–0.19	471.34031	–16.28
$C_{30}H_{49}O_4^-$	473.36335	–0.61	473.35570	–16.77
$C_{30}H_{41}O_5^-$	481.29515	–1.67	481.28725	–18.08
$C_{30}H_{43}O_5^-$	483.31140	–0.42	483.30343	–16.91
$C_{29}H_{41}O_6^-$	485.29130	0.90	485.28327	–15.65
$C_{30}H_{45}O_5^-$	485.32711	–0.30	485.31908	–16.84
$C_{29}H_{43}O_6^-$	487.30605	–0.96	487.29795	–17.57
$C_{30}H_{47}O_5^-$	487.34270	–0.41	487.33460	–17.03
$C_{30}H_{49}O_5^-$	489.35825	–0.62	489.35009	–17.29
$C_{30}H_{43}O_6^-$	499.30684	0.65	499.29835	–16.36
$C_{30}H_{45}O_6^-$	501.32258	0.83	501.31402	–16.25
$C_{30}H_{47}O_6^-$	503.33765	–0.32	503.32903	–17.46

Table A7. Assignment of ion formulas corresponding to peaks of the negative ion mode mass spectrum of mastic resin and the corresponding *m/z* errors for internal and external calibration.

Anion formula	Internal calibration		Externel calibration	
	Measured *m/z*	*m/z* error (ppm)	Measured *m/z*	*m/z* error (ppm)
$C_{27}H_{35}O_3^-$	407.25924	0.17	407.25621	–7.28
$C_{28}H_{39}O_2^-$	407.29594	0.94	407.29290	–6.51
$C_{27}H_{39}O_3^-$	411.29029	–0.44	411.28720	–7.95
$C_{28}H_{37}O_3^-$	421.27492	0.23	421.27168	–7.44
$C_{29}H_{41}O_2^-$	421.31127	0.15	421.30804	–7.51
$C_{27}H_{35}O_4^-$	423.25428	0.46	423.25102	–7.24
$C_{28}H_{39}O_3^-$	423.29066	0.45	423.28740	–7.26
$C_{29}H_{43}O_2^-$	423.32664	–0.50	423.32338	–8.21
$C_{28}H_{41}O_3^-$	425.30654	0.98	425.30325	–6.76
$C_{29}H_{45}O_2^-$	425.34233	–0.40	425.33904	–8.14
$C_{27}H_{39}O_4^-$	427.28545	0.14	427.28213	–7.63
$C_{28}H_{43}O_3^-$	427.32180	0.07	427.31848	–7.70
$C_{29}H_{39}O_3^-$	435.29027	–0.45	435.28683	–8.35

Table A7. Continued

Anion formula	Internal calibration		Externel calibration	
	Measured *m/z*	*m/z* error (ppm)	Measured *m/z*	*m/z* error (ppm)
$C_{28}H_{37}O_4^-$	437.26993	0.46	437.26647	–7.47
$C_{29}H_{41}O_3^-$	437.30587	–0.57	437.30240	–8.50
$C_{28}H_{39}O_4^-$	439.28508	–0.69	439.28159	–8.65
$C_{29}H_{43}O_3^-$	439.32179	0.05	439.31829	–7.91
$C_{28}H_{41}O_4^-$	441.30103	–0.02	441.29750	–8.02
$C_{29}H_{45}O_3^-$	441.33710	–0.73	441.33357	–8.72
$C_{29}H_{39}O_4^-$	451.28505	–0.74	451.28137	–8.89
$C_{30}H_{43}O_3^-$	451.32179	0.05	451.31811	–8.11
$C_{28}H_{37}O_5^-$	453.26482	0.37	453.26111	–7.82
$C_{29}H_{41}O_4^-$	453.30115	0.24	453.29743	–7.94
$C_{30}H_{45}O_3^-$	453.33790	1.07	453.33419	–7.12
$C_{28}H_{39}O_5^-$	455.28064	0.75	455.27690	–7.47
$C_{29}H_{43}O_4^-$	455.31662	–0.14	455.31288	–8.36
$C_{29}H_{45}O_4^-$	457.33224	–0.21	457.32847	–8.46
$C_{30}H_{41}O_4^-$	465.30075	–0.61	465.29685	–8.99
$C_{29}H_{39}O_5^-$	467.28044	0.31	467.27651	–8.10
$C_{30}H_{43}O_4^-$	467.31672	0.07	467.31279	–8.34
$C_{29}H_{41}O_5^-$	469.29598	0.06	469.29201	–8.39
$C_{30}H_{45}O_4^-$	469.33228	–0.13	469.32831	–8.57
$C_{29}H_{43}O_5^-$	471.31219	1.26	471.30820	–7.22
$C_{30}H_{47}O_4^-$	471.34741	–1.23	471.34341	–9.71
$C_{29}H_{37}O_6^-$	481.26020	1.31	481.25604	–7.32
$C_{30}H_{41}O_5^-$	481.29606	0.23	481.29188	–8.45
$C_{29}H_{39}O_6^-$	483.27554	0.67	483.27135	–8.00
$C_{30}H_{43}O_5^-$	483.31158	–0.04	483.30739	–8.71
$C_{29}H_{41}O_6^-$	485.29098	0.23	485.28676	–8.47
$C_{30}H_{45}O_5^-$	485.32692	–0.67	485.32270	–9.38
$C_{29}H_{43}O_6^-$	487.30677	0.52	487.30251	–8.22
$C_{30}H_{47}O_5^-$	487.34276	–0.28	487.33851	–9.01
$C_{30}H_{41}O_6^-$	497.29034	–1.05	497.28592	–9.95
$C_{32}H_{49}O_4^-$	497.36346	–0.35	497.35904	–9.24
$C_{30}H_{43}O_6^-$	499.30636	–0.31	499.30190	–9.24
$C_{30}H_{45}O_6^-$	501.32190	–0.52	501.31741	–9.49
$C_{30}H_{43}O_7^-$	515.30142	–0.02	515.29669	–9.21
$C_{30}H_{45}O_7^-$	517.31675	–0.65	517.31198	–9.87

Table A8. Assignment of ion formulas corresponding to peaks of the negative ion mode mass spectrum of sandarac resin and the corresponding *m/z* errors for internal and external calibration. The clusters are separated with a thick line.

Anion formula	Internal calibration		Externel calibration	
	Measured *m/z*	*m/z* error (ppm)	Measured *m/z*	*m/z* error (ppm)
$C_{13}H_{17}O_2^-$	205.12346	0.26	205.12348	0.37
$C_{15}H_{15}O_2^-$	227.10785	0.44	227.10791	0.69
$C_{19}H_{23}O_2^-$	283.17022	–0.49	283.17040	0.16
$C_{19}H_{27}O_2^-$	287.20169	0.11	287.20188	0.79
$C_{18}H_{25}O_3^-$	289.18107	0.50	289.18127	1.20
$C_{18}H_{27}O_3^-$	291.19666	0.32	291.19687	1.02
$C_{20}H_{25}O_2^-$	297.18598	–0.09	297.18620	0.65
$C_{19}H_{23}O_3^-$	299.16517	–0.32	299.16540	0.44
$C_{20}H_{27}O_2^-$	299.20172	0.22	299.20195	0.98
$C_{20}H_{29}O_2^-$	301.21740	0.31	301.21763	1.09
$C_{19}H_{27}O_3^-$	303.19690	1.09	303.19714	1.88
$C_{18}H_{25}O_4^-$	305.17613	0.97	305.17638	1.78
$C_{20}H_{25}O_3^-$	313.18091	–0.02	313.18118	0.84
$C_{20}H_{27}O_3^-$	315.19653	–0.12	315.19681	0.76
$C_{20}H_{29}O_3^-$	317.21218	–0.13	317.21246	0.76
$C_{19}H_{27}O_4^-$	319.19132	–0.53	319.19160	0.37
$C_{20}H_{31}O_3^-$	319.22772	–0.46	319.22801	0.44
$C_{20}H_{27}O_4^-$	331.19170	0.65	331.19203	1.64
$C_{20}H_{29}O_4^-$	333.20728	0.42	333.20761	1.42
$C_{20}H_{31}O_4^-$	335.22246	–0.98	335.22280	0.03
$C_{20}H_{31}O_5^-$	351.21746	–0.67	351.21786	0.45
$C_{20}H_{33}O_5^-$	353.23356	0.59	353.23396	1.73
$C_{30}H_{45}O_5^-$	485.32670	–1.14	485.32770	0.92
$C_{39}H_{57}O_5^-$	605.42050	–1.07	605.42226	1.83
$C_{40}H_{57}O_5^-$	617.42148	0.53	617.42332	3.51
$C_{40}H_{59}O_5^-$	619.43673	–0.11	619.43858	2.88
$C_{39}H_{57}O_6^-$	621.41667	0.97	621.41854	3.98
$C_{40}H_{59}O_6^-$	635.43161	–0.17	635.43358	2.93
$C_{40}H_{61}O_6^-$	637.44663	–1.15	637.44862	1.96
$C_{40}H_{59}O_7^-$	651.42670	0.11	651.42880	3.33
$C_{40}H_{61}O_7^-$	653.44194	–0.51	653.44406	2.72
$C_{40}H_{63}O_7^-$	655.45887	1.44	655.46100	4.68
$C_{40}H_{61}O_8^-$	669.43826	1.59	669.44049	4.93
$C_{40}H_{63}O_8^-$	671.45411	1.89	671.45637	5.25
$C_{40}H_{59}O_9^-$	683.41599	–0.69	683.41834	2.75

Table A9. Assignment of ion formulas corresponding to peaks of the negative ion mode mass spectrum of colophony resin and the corresponding *m/z* errors for internal and external calibration. The clusters are separated with a thick line.

Anion formula	Internal calibration		Externel calibration	
	Measured *m/z*	*m/z* error (ppm)	Measured *m/z*	*m/z* error (ppm)
$C_{15}H_{15}O_2^-$	227.10773	–0.13	227.10811	1.56
$C_{16}H_{19}O^-$	227.14406	–0.35	227.14444	1.34
$C_{15}H_{17}O_2^-$	229.12321	–0.84	229.12361	0.87
$C_{15}H_{19}O_2^-$	231.13908	0.13	231.13949	1.87
$C_{16}H_{17}O_2^-$	241.12341	0.01	241.12386	1.90
$C_{15}H_{15}O_3^-$	243.10263	–0.15	243.10310	1.76
$C_{16}H_{19}O_2^-$	243.13891	–0.59	243.13938	1.33
$C_{15}H_{17}O_3^-$	245.11802	–1.24	245.11849	0.71
$C_{16}H_{21}O_2^-$	245.15458	–0.51	245.15506	1.44
$C_{15}H_{19}O_3^-$	247.13379	–0.75	247.13427	1.23
$C_{15}H_{21}O_3^-$	249.14969	0.27	249.15019	2.27
$C_{14}H_{19}O_4^-$	251.12854	–1.37	251.12905	0.66
$C_{17}H_{19}O_2^-$	255.13867	–1.50	255.13921	0.60
$C_{18}H_{23}O^-$	255.17519	–0.98	255.17572	1.11
$C_{16}H_{17}O_3^-$	257.11809	–0.89	257.11864	1.23
$C_{17}H_{21}O_2^-$	257.15456	–0.55	257.15511	1.57
$C_{18}H_{25}O^-$	257.19083	–1.03	257.19137	1.09
$C_{15}H_{15}O_4^-$	259.09737	–0.82	259.09793	1.33
$C_{16}H_{19}O_3^-$	259.13379	–0.68	259.13435	1.47
$C_{17}H_{23}O_2^-$	259.17005	–1.18	259.17061	0.97
$C_{16}H_{21}O_3^-$	261.14964	0.06	261.15021	2.24
$C_{15}H_{19}O_4^-$	263.12883	–0.20	263.12941	2.01
$C_{16}H_{23}O_3^-$	263.16527	0.00	263.16585	2.21
$C_{15}H_{21}O_4^-$	265.14434	–0.75	265.14493	1.48
$C_{18}H_{19}O_2^-$	267.13910	0.16	267.13970	2.43
$C_{19}H_{23}O^-$	267.17526	–0.68	267.17587	1.59
$C_{18}H_{21}O_2^-$	269.15467	–0.14	269.15528	2.15
$C_{19}H_{25}O^-$	269.19109	0.01	269.19171	2.31
$C_{17}H_{19}O_3^-$	271.13364	–1.22	271.13427	1.11
$C_{18}H_{23}O_2^-$	271.17019	–0.60	271.17082	1.72
$C_{19}H_{27}O^-$	271.20653	–0.77	271.20716	1.56
$C_{16}H_{17}O_4^-$	273.11317	–0.22	273.11382	2.13
$C_{17}H_{21}O_3^-$	273.14966	0.16	273.15031	2.51

Table A9. Continued

Anion formula	Internal calibration		Externel calibration	
	Measured *m/z*	*m/z* error (ppm)	Measured *m/z*	*m/z* error (ppm)
$C_{18}H_{25}O_2^-$	273.18594	–0.25	273.18658	2.10
$C_{16}H_{19}O_4^-$	275.12874	–0.53	275.12939	1.85
$C_{17}H_{23}O_3^-$	275.16507	–0.73	275.16573	1.67
$C_{16}H_{21}O_4^-$	277.14447	–0.23	277.14514	2.18
$C_{15}H_{19}O_5^-$	279.12330	–1.81	279.12398	0.63
$C_{16}H_{23}O_4^-$	279.15977	–1.49	279.16045	0.96
$C_{15}H_{21}O_5^-$	281.13925	–0.71	281.13994	1.76
$C_{19}H_{21}O_2^-$	281.15461	–0.35	281.15530	2.13
$C_{18}H_{19}O_3^-$	283.13360	–1.30	283.13431	1.20
$C_{19}H_{23}O_2^-$	283.17019	–0.59	283.17089	1.90
$C_{18}H_{21}O_3^-$	285.14934	–1.00	285.15006	1.53
$C_{19}H_{25}O_2^-$	285.18587	–0.48	285.18659	2.04
$C_{17}H_{19}O_4^-$	287.12889	0.01	287.12962	2.57
$C_{18}H_{23}O_3^-$	287.16520	–0.25	287.16593	2.31
$C_{19}H_{27}O_2^-$	287.20162	–0.12	287.20235	2.43
$C_{17}H_{21}O_4^-$	289.14433	–0.70	289.14508	1.89
$C_{18}H_{25}O_3^-$	289.18071	–0.74	289.18145	1.84
$C_{16}H_{19}O_5^-$	291.12367	–0.46	291.12443	2.15
$C_{17}H_{23}O_4^-$	291.16008	–0.36	291.16085	2.27
$C_{18}H_{27}O_3^-$	291.19654	–0.11	291.19730	2.50
$C_{16}H_{21}O_5^-$	293.13955	0.34	293.14032	2.98
$C_{17}H_{25}O_4^-$	293.17579	–0.17	293.17656	2.47
$C_{16}H_{23}O_5^-$	295.15512	0.07	295.15591	2.74
$C_{19}H_{21}O_3^-$	297.14972	0.33	297.15052	3.03
$C_{20}H_{25}O_2^-$	297.18563	–1.25	297.18644	1.45
$C_{18}H_{19}O_4^-$	299.12839	–1.67	299.12920	1.06
$C_{19}H_{23}O_3^-$	299.16496	–1.04	299.16578	1.69
$C_{20}H_{27}O_2^-$	299.20142	–0.78	299.20224	1.95
$C_{18}H_{21}O_4^-$	301.14451	–0.08	301.14534	2.67
$C_{19}H_{25}O_3^-$	301.18095	0.09	301.18178	2.85
$C_{20}H_{29}O_2^-$	301.21736	0.19	301.21819	2.95
$C_{17}H_{19}O_5^-$	303.12395	0.48	303.12479	3.27
$C_{18}H_{23}O_4^-$	303.16051	1.08	303.16136	3.87
$C_{19}H_{27}O_3^-$	303.19674	0.55	303.19758	3.34
$C_{17}H_{21}O_5^-$	305.13973	0.91	305.14059	3.72
$C_{18}H_{25}O_4^-$	305.17604	0.66	305.17690	3.48

Table A9. Continued

Anion formula	Internal calibration		Externel calibration	
	Measured *m/z*	*m/z* error (ppm)	Measured *m/z*	*m/z* error (ppm)
$C_{19}H_{29}O_3^-$	305.21243	0.67	305.21328	3.49
$C_{16}H_{19}O_6^-$	307.11860	–0.36	307.11948	2.48
$C_{18}H_{27}O_4^-$	307.19144	–0.14	307.19232	2.70
$C_{16}H_{21}O_6^-$	309.13435	–0.05	309.13524	2.82
$C_{19}H_{21}O_4^-$	313.14440	–0.43	313.14532	2.50
$C_{20}H_{25}O_3^-$	313.18092	0.01	313.18184	2.94
$C_{19}H_{23}O_4^-$	315.16021	0.08	315.16114	3.04
$C_{20}H_{27}O_3^-$	315.19664	0.23	315.19757	3.19
$C_{18}H_{21}O_5^-$	317.13939	–0.18	317.14034	2.81
$C_{19}H_{25}O_4^-$	317.17566	–0.55	317.17661	2.44
$C_{20}H_{29}O_3^-$	317.21206	–0.52	317.21300	2.47
$C_{17}H_{19}O_6^-$	319.11840	–0.99	319.11936	2.03
$C_{18}H_{23}O_5^-$	319.15501	–0.27	319.15598	2.75
$C_{19}H_{27}O_4^-$	319.19121	–0.86	319.19217	2.16
$C_{17}H_{21}O_6^-$	321.13444	0.24	321.13542	3.29
$C_{18}H_{25}O_5^-$	321.17082	0.21	321.17180	3.26
$C_{19}H_{29}O_4^-$	321.20707	–0.21	321.20805	2.84
$C_{17}H_{23}O_6^-$	323.15006	0.13	323.15105	3.21
$C_{18}H_{27}O_5^-$	323.18615	–0.78	323.18714	2.30
$C_{20}H_{23}O_4^-$	327.16037	0.58	327.16140	3.71
$C_{19}H_{21}O_5^-$	329.14007	1.88	329.14111	5.05
$C_{20}H_{25}O_4^-$	329.17607	0.71	329.17711	3.87
$C_{19}H_{23}O_5^-$	331.15522	0.37	331.15628	3.57
$C_{20}H_{27}O_4^-$	331.19163	0.43	331.19268	3.62
$C_{19}H_{25}O_5^-$	333.17071	–0.11	333.17179	3.11
$C_{20}H_{29}O_4^-$	333.20715	0.03	333.20822	3.25
$C_{19}H_{27}O_5^-$	335.18597	–1.27	335.18706	1.98
$C_{20}H_{31}O_4^-$	335.22237	–1.23	335.22346	2.02
$C_{19}H_{29}O_5^-$	337.20167	–1.13	337.20278	2.15
$C_{17}H_{23}O_7^-$	339.14520	0.79	339.14632	4.10
$C_{20}H_{23}O_5^-$	343.15500	–0.29	343.15616	3.08
$C_{20}H_{25}O_5^-$	345.17045	–0.88	345.17162	2.51
$C_{19}H_{23}O_6^-$	347.15002	0.03	347.15121	3.45
$C_{20}H_{27}O_5^-$	347.18619	–0.60	347.18738	2.83
$C_{21}H_{31}O_4^-$	347.22230	–1.40	347.22349	2.03
$C_{19}H_{25}O_6^-$	349.16569	0.06	349.16689	3.51

Table A9. Continued

Anion formula	Internal calibration		Externel calibration	
	Measured *m/z*	*m/z* error (ppm)	Measured *m/z*	*m/z* error (ppm)
$C_{20}H_{29}O_5^-$	349.20248	1.24	349.20369	4.69
$C_{21}H_{33}O_4^-$	349.23840	–0.09	349.23961	3.36
$C_{19}H_{27}O_6^-$	351.18093	–1.10	351.18215	2.38
$C_{20}H_{31}O_5^-$	351.21747	–0.66	351.21869	2.82
$C_{19}H_{29}O_6^-$	353.19636	–1.71	353.19760	1.80
$C_{20}H_{23}O_6^-$	359.14979	–0.64	359.15108	2.96
$C_{20}H_{25}O_6^-$	361.16596	0.81	361.16727	4.43
$C_{20}H_{27}O_6^-$	363.18134	0.07	363.18267	3.73
$C_{20}H_{29}O_6^-$	365.19667	–0.81	365.19801	2.87
$C_{20}H_{31}O_6^-$	367.21229	–0.89	367.21365	2.83
$C_{20}H_{25}O_7^-$	377.16067	0.24	377.16213	4.10
$C_{20}H_{27}O_7^-$	379.17602	–0.56	379.17749	3.33
$C_{20}H_{29}O_7^-$	381.19151	–0.97	381.19300	2.94
$C_{20}H_{31}O_7^-$	383.20805	1.35	383.20956	5.29
$C_{20}H_{27}O_8^-$	395.17078	–0.93	395.17241	3.19
$C_{20}H_{29}O_8^-$	397.18700	0.51	397.18864	4.66
$C_{20}H_{31}O_8^-$	399.20187	–1.44	399.20354	2.73
$C_{37}H_{49}O_7^-$	605.34825	–0.21	605.35258	6.94
$C_{36}H_{49}O_8^-$	609.34369	0.64	609.34808	7.86
$C_{37}H_{49}O_8^-$	621.34409	1.28	621.34868	8.67
$C_{37}H_{51}O_8^-$	623.35818	–1.23	623.36280	6.19
$C_{37}H_{53}O_8^-$	625.37517	0.91	625.37982	8.36
$C_{37}H_{49}O_9^-$	637.33717	–1.64	637.34202	5.98
$C_{37}H_{51}O_9^-$	639.35258	–2.00	639.35748	5.65
$C_{40}H_{55}O_7^-$	647.39614	1.25	647.40117	9.02
$C_{40}H_{57}O_7^-$	649.41093	–0.08	649.41599	7.72
$C_{40}H_{59}O_7^-$	651.42716	0.81	651.43225	8.63
$C_{38}H_{53}O_9^-$	653.37148	3.02	653.37661	10.87
$C_{40}H_{55}O_8^-$	663.38992	–0.49	663.39523	7.51
$C_{40}H_{57}O_8^-$	665.40595	0.08	665.41129	8.11
$C_{40}H_{59}O_8^-$	667.42294	2.09	667.42832	10.15
$C_{38}H_{53}O_{10}^-$	669.36579	2.04	669.37120	10.12
$C_{40}H_{55}O_9^-$	679.38423	–1.37	679.38982	6.86
$C_{40}H_{57}O_9^-$	681.40031	–0.73	681.40594	7.52
$C_{40}H_{57}O_{10}^-$	697.39641	0.98	697.40233	9.47

Table A10. Assignment of ion formulas corresponding to peaks of the negative ion mode mass spectrum of shellac resin and the corresponding *m/z* errors for internal and external calibration. The clusters are separated with a thick line.

Anion formula	Internal calibration		Externel calibration	
	Measured *m/z*	*m/z* error (ppm)	Measured *m/z*	*m/z* error (ppm)
$C_{16}H_{27}O_3^-$	267.19645	–0.44	267.19574	–3.12
$C_{16}H_{29}O_3^-$	269.21227	0.19	269.21155	–2.50
$C_{16}H_{27}O_4^-$	283.19148	–0.02	283.19068	–2.86
$C_{16}H_{29}O_4^-$	285.20708	–0.20	285.20626	–3.05
$C_{16}H_{31}O_4^-$	287.22286	0.25	287.22203	–2.63
$C_{16}H_{29}O_5^-$	301.20210	0.17	301.20119	–2.85
$C_{16}H_{31}O_5^-$	303.21797	0.88	303.21704	–2.17
$C_{14}H_{27}O_7^-$	307.17656	1.07	307.17561	–2.01
$C_{29}H_{45}O_4^-$	457.33178	–1.21	457.32967	–5.82
$C_{28}H_{43}O_5^-$	459.31112	–1.06	459.30899	–5.69
$C_{29}H_{45}O_5^-$	473.32795	1.48	473.32569	–3.30
$C_{29}H_{47}O_5^-$	475.34286	–0.09	475.34058	–4.89
$C_{30}H_{45}O_5^-$	485.32721	–0.08	485.32483	–4.99
$C_{30}H_{47}O_5^-$	487.34269	–0.44	487.34029	–5.36
$C_{30}H_{45}O_6^-$	501.32210	–0.13	501.31956	–5.20
$C_{30}H_{47}O_6^-$	503.33821	0.79	503.33565	–4.29
$C_{30}H_{49}O_6^-$	505.35268	–1.56	505.35010	–6.66
$C_{31}H_{45}O_6^-$	513.32192	–0.48	513.31926	–5.67
$C_{32}H_{53}O_5^-$	517.38917	–1.31	517.38647	–6.54
$C_{30}H_{47}O_7^-$	519.33234	–0.75	519.32961	–6.00
$C_{30}H_{49}O_7^-$	521.34813	–0.47	521.34539	–5.74
$C_{30}H_{55}O_7^-$	527.39510	–0.45	527.39228	–5.78
$C_{31}H_{45}O_7^-$	529.31683	–0.47	529.31400	–5.82
$C_{30}H_{57}O_7^-$	529.41049	–0.92	529.40766	–6.27
$C_{31}H_{47}O_7^-$	531.33207	–1.25	531.32922	–6.62
$C_{32}H_{51}O_6^-$	531.36882	–0.56	531.36596	–5.93
$C_{32}H_{57}O_6^-$	537.41614	0.13	537.41322	–5.30
$C_{31}H_{45}O_8^-$	545.31193	–0.12	545.30892	–5.63
$C_{30}H_{57}O_8^-$	545.40544	–0.84	545.40243	–6.35
$C_{31}H_{47}O_8^-$	547.32808	0.79	547.32505	–4.74
$C_{32}H_{53}O_7^-$	549.37976	0.15	549.37671	–5.41
$C_{32}H_{57}O_7^-$	553.41133	0.62	553.40823	–4.97

Table A10. Continued

Anion formula	Internal calibration		Externel calibration	
	Measured *m/z*	*m/z* error (ppm)	Measured *m/z*	*m/z* error (ppm)
$C_{31}H_{47}O_9^-$	563.32257	0.01	563.31936	–5.68
$C_{31}H_{49}O_9^-$	565.33837	0.29	565.33514	–5.43
$C_{32}H_{57}O_8^-$	569.40509	–1.41	569.40181	–7.17
$C_{32}H_{59}O_8^-$	571.42205	0.89	571.41875	–4.89
$C_{32}H_{59}O_9^-$	587.41588	–0.98	587.41239	–6.93
$C_{32}H_{61}O_9^-$	589.43234	0.40	589.42883	–5.57
$C_{46}H_{73}O_8^-$	753.53093	–0.21	753.52518	–7.85
$C_{46}H_{75}O_8^-$	755.54649	–0.34	755.54070	–8.00
$C_{46}H_{75}O_9^-$	771.54135	–0.40	771.53532	–8.22
$C_{46}H_{77}O_9^-$	773.55789	0.75	773.55182	–7.10
$C_{46}H_{75}O_{10}^-$	787.53729	0.90	787.53100	–7.08
$C_{46}H_{77}O_{10}^-$	789.55298	0.95	789.54666	–7.05
$C_{46}H_{63}O_{11}^-$	791.43821	0.78	791.43186	–7.25
$C_{47}H_{73}O_{10}^-$	797.52202	1.38	797.51557	–6.71
$C_{47}H_{75}O_{10}^-$	799.53684	0.33	799.53035	–7.78
$C_{46}H_{65}O_{12}^-$	809.44899	1.04	809.44235	–7.17
$C_{47}H_{75}O_{11}^-$	815.53187	0.46	815.52512	–7.81
$C_{47}H_{71}O_{12}^-$	827.49620	1.32	827.48925	–7.07
$C_{47}H_{75}O_{12}^-$	831.52608	–0.40	831.51906	–8.83
$C_{47}H_{77}O_{12}^-$	833.54309	1.24	833.53604	–7.21
$C_{47}H_{79}O_{13}^-$	851.55233	–0.34	851.54497	–8.98
$C_{48}H_{89}O_{12}^-$	857.63625	0.34	857.62879	–8.35

APPENDIX 2

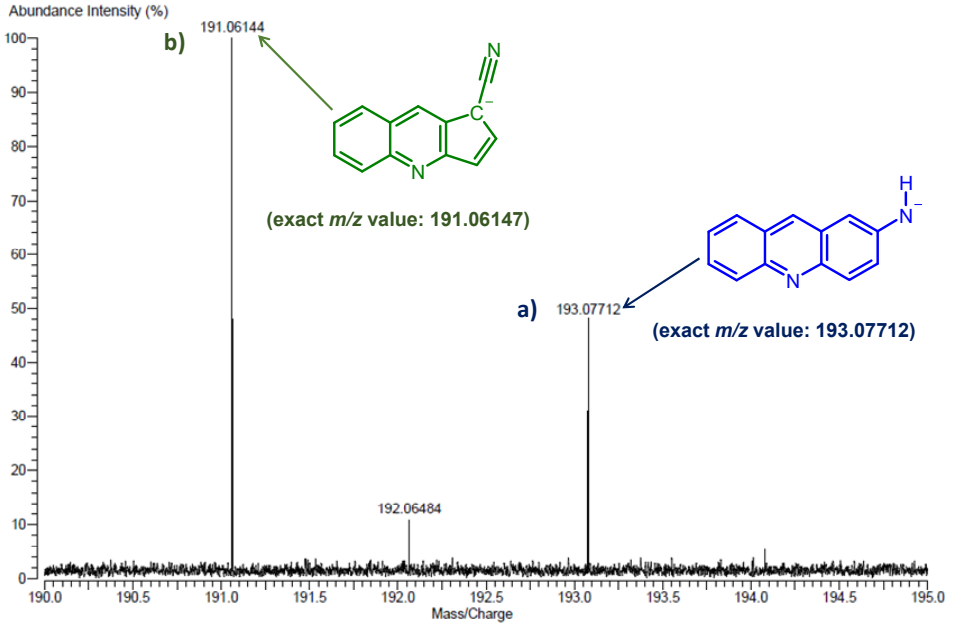

Figure A1. The ion structures (along with the corresponding exact *m/z* values) of a) $[C_{13}H_{10}N_2\text{-}H]^-$ and b) $[C_{13}H_{10}N_2\text{-}3H]^-$ anions. The structures are presented as canonical structures. In reality, the negative charge is delocalised across the whole aromatic structures. The mass spectrum is obtained during the analysis of mastic resin (see Figure 14b).

APPENDIX 3

Table A11. The exact *m/z* values of doubly and triply charged radical ions corresponding to phosphazenes and sulpho-compounds used during this study (see Figure 5 and Table 2).

No	**Phosphazene salt**	**$[M+H]^+$ formula**	**Exact *m/z***	
			z=2	**z=3**
1	$HP_1(pyrr)\cdot HBF_4$	$C_{12}H_{26}N_4P^+$	128.59420	85.72929
2	$H_2NP_1(pyrr)\cdot HBPh_4$	$C_{12}H_{27}N_5P^+$	136.09965	90.73292
3	$2\text{-Cl-}C_6H_4\text{-}P_1(dma)\cdot HBPh_4$	$C_{12}H_{23}N_4ClP^+$	144.56689	96.37775
4	$EtP_2(dma)\cdot HBPh4$	$C_{12}H_{36}N_7P_2^+$	170.12482	113.41636
5	$4\text{-MeO-Ph}P_1(pyrr)\cdot HBF_4$	$C_{19}H_{32}N_4OP^+$	181.61514	121.07657
6	$t\text{-Bu-}P_2(dma)\cdot HBF_4$	$C_{14}H_{40}N_7P_2^+$	184.14047	122.76013
7	$4\text{-Br-}C_6H_4\text{-}P_1(pyrr)\cdot HBPh_4$	$C_{18}H_{29}N_4BrP^+$	205.56511	137.04322
8	$PhP_2(pyrr)\cdot HBPh_4$	$C_{26}H_{46}N_7P_2^+$	259.16395	172.77578
9	$2\text{-Cl-}C_6H_4\text{-}P_2(pyrr)\cdot HBPh_4$	$C_{26}H_{45}N_7ClP_2^+$	276.14446	184.09612
10	$4\text{-}CF_3\text{-}C_6H_4\text{-}P_2(pyrr)\cdot HBPh_4$	$C_{27}H_{45}N_7F_3P_2^+$	293.15764	195.43824
11	$4\text{-Br-}C_6H_4\text{-}P_2(pyrr)\cdot HBPh_4$	$C_{26}H_{45}N_7BrP_2^+$	298.11920	198.74595
12	$t\text{-Bu}P_4(dma)\cdot HBF_4$	$C_{22}H_{64}N_{13}P_4^+$	317.21736	211.47805
13	$Ph\text{-Et}P_4(dma)\cdot HBF_4$	$C_{26}H_{64}N_{13}P_4^+$	341.21736	227.47805
14	$Ph\text{-}P_4(pyrr)\cdot HBF_4$	$C_{42}H_{78}N_{13}P_4^+$	444.27213	296.18124
15	$Ph\text{-Et}P_4(pyrr)\cdot HBF_4$	$C_{44}H_{82}N_{13}P_4^+$	458.28778	305.52500
No	**Sulpho-compound**	**$[M-H]^-$ formula**	**z=2**	**z=3**
16	$(CF_3SO_2)_3CH$	$C_4F_9O_6S_3^-$	205.43622	136.95766
17	$[CF_3(CF_2)_3SO_2]_2NH$	$C_8F_{18}NO_4S_2^-$	289.94962	193.29993
18	$[CF_3(CF_2)_3SO_2]NH[CF_3(CF_2)_7SO_2]$	$C_{12}F_{26}NO_4S_2^-$	389.94323	259.96234
19	$[CF_3(CF_2)_7SO_2]_2CH$	$C_{17}HF_{34}O_4S_2^-$	489.43922	326.29299

PUBLICATIONS

CURRICULUM VITAE

Name:	Anu Teearu
Date of birth:	June 21, 1985, Türi, Estonia
Citizenship:	Estonian
Contact details:	University of Tartu, Institute of chemistry Ravila 14a, 50411, Tartu, Estonia
Phone:	+372 56 568 216
E-mail:	anu.teearu@ut.ee

Education

Sept 2011 – …	PhD student at Institute of Chemistry, University of Tartu
Sept 2007 – June 2009	Master of Science in Engineering (Chemical Technology of Materials), *cum laude* Institute of Chemistry, University of Tartu
Sept 2004 – June 2007	Bachelor in Science (Material Science) Department of Chemistry, University of Tartu

Professional employment

Jan 2017 – …	Administrative coordinator of the EACH programme/ project manager (1.0), Institute of Chemistry, University of Tartu
Sept 2011 – Dec 2016	Chemist (0.25), Chair of Analytical Chemistry, Institute of Chemistry, University of Tartu
Sept 2008 – March 2017	Senior specialist (0.75), Estonian Health Board Tartu Laboratory

Scientific publications

1. **Teearu, A.**; Vahur, S.; Rodima, T.; Herodes, K.; Bonrath, W.; Netscher, T.; Tshepelevitsh, S.; Trummal, A.; Lõkov, M.; Leito, I. Method development for the analysis of resinous materials with MALDI-FT-ICR-MS: novel internal standards and a new matrix material for negative ion mode. Accepted for publication on 04.05.2017 by *Journal of Mass Spectrometry*, DOI: 10.1002/jms.3943.

2. Vahur, S.; **Teearu, A.**; Peets, P.; Joosu, L.; Leito, I. ATR-FT-IR spectral collection of conservation materials in the extended region of 4000–80 cm^{-1}. *Analytical and Bioanalytical Chemistry*, **2016**, 408 (13), 3373–3379.

3. **Teearu, A.**; Vahur, S.; Haljasorg, U.; Leito, I.; Haljasorg, T.; Toom, L. 2,5-Dihydroxybenzoic acid solution in MALDI-MS: ageing and use for mass calibration. *Journal of Mass Spectrometry*, **2014**, 49 (10), 970–979.

4. Haljasorg, T.; Saame, J.; Kipper, K.; **Teearu, A.**; Herodes, K.; Reinik, M.; Leito, I. Alternative eluent composition for LC–MS analysis of perfluoroalkyl acids in raw fish samples. *Journal of Agricultural and Food Chemistry*, **2014**, 62 (23), 5259–5268.

5. Vahur, S.; **Teearu, A.**; Haljasorg, T.; Burk, P.; Leito, I.; Kaljurand, I. Analysis of dammar resin with MALDI-FT-ICR-MS and APCI-FT-ICR-MS. *Journal of Mass Spectrometry*, **2012**, 47(3), 392–409.

6. Vahur, S.; **Teearu, A.**; Leito, I. ATR-FT-IR spectroscopy in the region of 550–230 cm^{-1} for identification of inorganic pigments. *Spectrochimica Acta Part A-Molecular and Biomolecular Spectroscopy*, **2010**, 75, 1061–1072.

Attended conferences

1. TECHNART 2013 (Analytical Spectroscopy in Art and Archaeology), September 23–26, 2013, Amsterdam, Netherlands.
   Poster presentation: "ATR-FT-IR spectroscopy in the region of 550–225 cm^{-1} for identification of inorganic pigments" (Vahur, S.; Teearu, A.; Leito, I.).

2. 4th scientific conference of of the graduate school of Functional Materials and Technologies, March 7–8, 2013, Tallinn, Estonia.
   Poster presentation: "The application of MALDI-FT-ICR-MS for the analysis of dammar resin" (Teearu, A.; Vahur, S.; Kaljurand, I.; Leito, I.).

3. 3rd scientific conference of of the graduate school of Functional Materials and Technologies, February 29–March 1, 2012, Tartu, Estonia.
   Poster presentation: "Analysis of dammar resin with MALDI- and APCI-FT-ICR-MS" (Teearu, A.; Vahur, S.; Haljasorg, T.; Burk, P.; Kaljurand, I.; Leito, I.).

4. 10th Biennial International Conference of the Infrared and Raman Users Group (IRUG10), March 28–April 1, 2012, Barcelona, Spain.
   Poster presentation: "ATR-FT-IR spectroscopy in the region of 550–230 cm^{-1} for identification of inorganic compounds" (Vahur, S.; Teearu, A.; Leito, I.).

ELULOOKIRJELDUS

Nimi:	Anu Teearu
Sünniaeg:	21.06.1985, Türi
Kodakondsus:	Eesti
Kontaktandmed:	Keemia Instituut, Tartu Ülikool, Ravila 14a, 50411, Tartu, Eesti
Tel:	+372 56 568 216
E-post:	anu.teearu@ut.ee

Hariduskäik

09.2011 – …	Tartu Ülikool, loodus- ja tehnoloogia valdkond, keemia eriala doktorant
09.2007 – 06.2009	tehnikateaduse magistri kraad (keemiline materjalitehnoloogia), *cum laude* Tartu Ülikool, loodus- ja tehnoloogiateaduskond, keemia instituut
09.2004 – 06.2007	tehnikateaduse bakalaureuse kraad (materjaliteadus) Tartu Ülikool, füüsika-keemiateaduskond, keemia-osakond

Teenistuskäik

01.2017 – …	*EACH* programmi administratiivne koordinaator/ projektijuht (1,0) Tartu Ülikool, keemia instituut
09.2011 – 12.2016	Analüütilise keemia õppetool, keemik (0,25)
09.2008 – 03.2017	Terviseameti Tartu labor, vanemspetsialist (0,75)

Publikatsioonide loetelu

1. **Teearu, A.**; Vahur, S.; Rodima, T.; Herodes, K.; Bonrath, W.; Netscher, T.; Tshepelevitsh, S.; Trummal, A.; Lõkov, M.; Leito, I. Method development for the analysis of resinous materials with MALDI-FT-ICR-MS: novel internal standards and a new matrix material for negative ion mode. 04.05.2017 vastu võetud ajakirja *Journal of Mass Spectrometry*, DOI: 10.1002/jms.3943.

2. Vahur, S.; **Teearu, A.**; Peets, P.; Joosu, L.; Leito, I. ATR-FT-IR spectral collection of conservation materials in the extended region of 4000–80 cm^{-1}. *Analytical and Bioanalytical Chemistry*, **2016**, 408 (13), 3373–3379.

3. **Teearu, A.**; Vahur, S.; Haljasorg, U.; Leito, I.; Haljasorg, T.; Toom, L. 2,5-Dihydroxybenzoic acid solution in MALDI-MS: ageing and use for mass calibration. *Journal of Mass Spectrometry*, **2014**, 49 (10), 970–979.

4. Haljasorg, T.; Saame, J.; Kipper, K.; **Teearu, A.**; Herodes, K.; Reinik, M.; Leito, I. Alternative eluent composition for LC-MS analysis of perfluoroalkyl acids in raw fish samples. *Journal of Agricultural and Food Chemistry*, **2014**, 62 (23), 5259–5268.

5. Vahur, S.; **Teearu, A.**; Haljasorg, T.; Burk, P.; Leito, I.; Kaljurand, I. Analysis of dammar resin with MALDI-FT-ICR-MS and APCI-FT-ICR-MS. *Journal of Mass Spectrometry*, **2012**, 47(3), 392–409.

6. Vahur, S.; **Teearu, A.**; Leito, I. ATR-FT-IR spectroscopy in the region of 550–230 cm^{-1} for identification of inorganic pigments. *Spectrochimica Acta Part A-Molecular and Biomolecular Spectroscopy*, **2010**, 75, 1061–1072.

Osalemine konverentsidel

1. TECHNART 2013 (*Analytical Spectroscopy in Art and Archaeology*), 23.09–26.09.2013, Amsterdam, Holland.
   Posterettekanne: "ATR-FT-IR spectroscopy in the region of 550–225 cm^{-1} for identification of inorganic pigments" (Vahur, S.; Teearu, A.; Leito, I.).

2. TÜ ja TTÜ doktorikooli "Funktsionaalsed materjalid ja tehnoloogiad" neljas teaduskonverents, 07.03–08.03. 2013, Tallinn, Eesti.
   Posterettekanne: "The application of MALDI-FT-ICR-MS for the analysis of dammar resin" (Teearu, A.; Vahur, S.; Kaljurand, I.; Leito, I.).

3. TÜ ja TTÜ doktorikooli "Funktsionaalsed materjalid ja tehnoloogiad" kolmas teaduskonverents, 29.02–01.03.2012, Tartu, Eesti.
   Posterettekanne: "Analysis of dammar resin with MALDI- and APCI-FT-ICR-MS" (Teearu, A.; Vahur, S.; Haljasorg, T.; Burk, P.; Kaljurand, I.; Leito, I.).

4. 10^{th} *Biennial International Conference of the Infrared and Raman Users Group* (IRUG10), 28.03–01.04. 2012, Barcelona, Hispaania.
   Posterettekanne: "ATR-FT-IR spectroscopy in the region of 550–230 cm^{-1} for identification of inorganic compounds" (Vahur, S.; Teearu, A.; Leito, I.).

DISSERTATIONES CHIMICAE UNIVERSITATIS TARTUENSIS

1. **Toomas Tamm.** Quantum-chemical simulation of solvent effects. Tartu, 1993, 110 p.
2. **Peeter Burk.** Theoretical study of gas-phase acid-base equilibria. Tartu, 1994, 96 p.
3. **Victor Lobanov.** Quantitative structure-property relationships in large descriptor spaces. Tartu, 1995, 135 p.
4. **Vahur Mäemets.** The ^{17}O and ^{1}H nuclear magnetic resonance study of H_2O in individual solvents and its charged clusters in aqueous solutions of electrolytes. Tartu, 1997, 140 p.
5. **Andrus Metsala.** Microcanonical rate constant in nonequilibrium distribution of vibrational energy and in restricted intramolecular vibrational energy redistribution on the basis of slater's theory of unimolecular reactions. Tartu, 1997, 150 p.
6. **Uko Maran.** Quantum-mechanical study of potential energy surfaces in different environments. Tartu, 1997, 137 p.
7. **Alar Jänes.** Adsorption of organic compounds on antimony, bismuth and cadmium electrodes. Tartu, 1998, 219 p.
8. **Kaido Tammeveski.** Oxygen electroreduction on thin platinum films and the electrochemical detection of superoxide anion. Tartu, 1998, 139 p.
9. **Ivo Leito.** Studies of Brønsted acid-base equilibria in water and non-aqueous media. Tartu, 1998, 101 p.
10. **Jaan Leis.** Conformational dynamics and equilibria in amides. Tartu, 1998, 131 p.
11. **Toonika Rinken.** The modelling of amperometric biosensors based on oxidoreductases. Tartu, 2000, 108 p.
12. **Dmitri Panov.** Partially solvated Grignard reagents. Tartu, 2000, 64 p.
13. **Kaja Orupõld.** Treatment and analysis of phenolic wastewater with microorganisms. Tartu, 2000, 123 p.
14. **Jüri Ivask.** Ion Chromatographic determination of major anions and cations in polar ice core. Tartu, 2000, 85 p.
15. **Lauri Vares.** Stereoselective Synthesis of Tetrahydrofuran and Tetrahydropyran Derivatives by Use of Asymmetric Horner-Wadsworth-Emmons and Ring Closure Reactions. Tartu, 2000, 184 p.
16. **Martin Lepiku.** Kinetic aspects of dopamine D_2 receptor interactions with specific ligands. Tartu, 2000, 81 p.
17. **Katrin Sak.** Some aspects of ligand specificity of P2Y receptors. Tartu, 2000, 106 p.
18. **Vello Pällin.** The role of solvation in the formation of iotsitch complexes. Tartu, 2001, 95 p.
19. **Katrin Kollist.** Interactions between polycyclic aromatic compounds and humic substances. Tartu, 2001, 93 p.

20. **Ivar Koppel.** Quantum chemical study of acidity of strong and superstrong Brønsted acids. Tartu, 2001, 104 p.
21. **Viljar Pihl.** The study of the substituent and solvent effects on the acidity of OH and CH acids. Tartu, 2001, 132 p.
22. **Natalia Palm.** Specification of the minimum, sufficient and significant set of descriptors for general description of solvent effects. Tartu, 2001, 134 p.
23. **Sulev Sild.** QSPR/QSAR approaches for complex molecular systems. Tartu, 2001, 134 p.
24. **Ruslan Petrukhin.** Industrial applications of the quantitative structure-property relationships. Tartu, 2001, 162 p.
25. **Boris V. Rogovoy.** Synthesis of (benzotriazolyl)carboximidamides and their application in relations with *N*- and *S*-nucleophyles. Tartu, 2002, 84 p.
26. **Koit Herodes.** Solvent effects on UV-vis absorption spectra of some solvatochromic substances in binary solvent mixtures: the preferential solvation model. Tartu, 2002, 102 p.
27. **Anti Perkson.** Synthesis and characterisation of nanostructured carbon. Tartu, 2002, 152 p.
28. **Ivari Kaljurand.** Self-consistent acidity scales of neutral and cationic Brønsted acids in acetonitrile and tetrahydrofuran. Tartu, 2003, 108 p.
29. **Karmen Lust.** Adsorption of anions on bismuth single crystal electrodes. Tartu, 2003, 128 p.
30. **Mare Piirsalu.** Substituent, temperature and solvent effects on the alkaline hydrolysis of substituted phenyl and alkyl esters of benzoic acid. Tartu, 2003, 156 p.
31. **Meeri Sassian.** Reactions of partially solvated Grignard reagents. Tartu, 2003, 78 p.
32. **Tarmo Tamm.** Quantum chemical modelling of polypyrrole. Tartu, 2003. 100 p.
33. **Erik Teinemaa.** The environmental fate of the particulate matter and organic pollutants from an oil shale power plant. Tartu, 2003. 102 p.
34. **Jaana Tammiku-Taul.** Quantum chemical study of the properties of Grignard reagents. Tartu, 2003. 120 p.
35. **Andre Lomaka.** Biomedical applications of predictive computational chemistry. Tartu, 2003. 132 p.
36. **Kostyantyn Kirichenko.** Benzotriazole – Mediated Carbon–Carbon Bond Formation. Tartu, 2003. 132 p.
37. **Gunnar Nurk.** Adsorption kinetics of some organic compounds on bismuth single crystal electrodes. Tartu, 2003, 170 p.
38. **Mati Arulepp.** Electrochemical characteristics of porous carbon materials and electrical double layer capacitors. Tartu, 2003, 196 p.
39. **Dan Cornel Fara.** QSPR modeling of complexation and distribution of organic compounds. Tartu, 2004, 126 p.
40. **Riina Mahlapuu.** Signalling of galanin and amyloid precursor protein through adenylate cyclase. Tartu, 2004, 124 p.

41. **Mihkel Kerikmäe.** Some luminescent materials for dosimetric applications and physical research. Tartu, 2004, 143 p.
42. **Jaanus Kruusma.** Determination of some important trace metal ions in human blood. Tartu, 2004, 115 p.
43. **Urmas Johanson.** Investigations of the electrochemical properties of polypyrrole modified electrodes. Tartu, 2004, 91 p.
44. **Kaido Sillar.** Computational study of the acid sites in zeolite ZSM-5. Tartu, 2004, 80 p.
45. **Aldo Oras.** Kinetic aspects of dATPαS interaction with $P2Y_1$ receptor. Tartu, 2004, 75 p.
46. **Erik Mölder.** Measurement of the oxygen mass transfer through the air-water interface. Tartu, 2005, 73 p.
47. **Thomas Thomberg.** The kinetics of electroreduction of peroxodisulfate anion on cadmium (0001) single crystal electrode. Tartu, 2005, 95 p.
48. **Olavi Loog.** Aspects of condensations of carbonyl compounds and their imine analogues. Tartu, 2005, 83 p.
49. **Siim Salmar.** Effect of ultrasound on ester hydrolysis in aqueous ethanol. Tartu, 2006, 73 p.
50. **Ain Uustare.** Modulation of signal transduction of heptahelical receptors by other receptors and G proteins. Tartu, 2006, 121 p.
51. **Sergei Yurchenko.** Determination of some carcinogenic contaminants in food. Tartu, 2006, 143 p.
52. **Kaido Tämm.** QSPR modeling of some properties of organic compounds. Tartu, 2006, 67 p.
53. **Olga Tšubrik.** New methods in the synthesis of multisubstituted hydrazines. Tartu. 2006, 183 p.
54. **Lilli Sooväli.** Spectrophotometric measurements and their uncertainty in chemical analysis and dissociation constant measurements. Tartu, 2006, 125 p.
55. **Eve Koort.** Uncertainty estimation of potentiometrically measured ph and pK_a values. Tartu, 2006, 139 p.
56. **Sergei Kopanchuk.** Regulation of ligand binding to melanocortin receptor subtypes. Tartu, 2006, 119 p.
57. **Silvar Kallip.** Surface structure of some bismuth and antimony single crystal electrodes. Tartu, 2006, 107 p.
58. **Kristjan Saal.** Surface silanization and its application in biomolecule coupling. Tartu, 2006, 77 p.
59. **Tanel Tätte.** High viscosity $Sn(OBu)_4$ oligomeric concentrates and their applications in technology. Tartu, 2006, 91 p.
60. **Dimitar Atanasov Dobchev**. Robust QSAR methods for the prediction of properties from molecular structure. Tartu, 2006, 118 p.
61. **Hannes Hagu**. Impact of ultrasound on hydrophobic interactions in solutions. Tartu, 2007, 81 p.

62. **Rutha Jäger.** Electroreduction of peroxodisulfate anion on bismuth electrodes. Tartu, 2007, 142 p.
63. **Kaido Viht.** Immobilizable bisubstrate-analogue inhibitors of basophilic protein kinases: development and application in biosensors. Tartu, 2007, 88 p.
64. **Eva-Ingrid Rõõm.** Acid-base equilibria in nonpolar media. Tartu, 2007, 156 p.
65. **Sven Tamp.** DFT study of the cesium cation containing complexes relevant to the cesium cation binding by the humic acids. Tartu, 2007, 102 p.
66. **Jaak Nerut.** Electroreduction of hexacyanoferrate(III) anion on Cadmium (0001) single crystal electrode. Tartu, 2007, 180 p.
67. **Lauri Jalukse.** Measurement uncertainty estimation in amperometric dissolved oxygen concentration measurement. Tartu, 2007, 112 p.
68. **Aime Lust.** Charge state of dopants and ordered clusters formation in CaF_2:Mn and CaF_2:Eu luminophors. Tartu, 2007, 100 p.
69. **Iiris Kahn**. Quantitative Structure-Activity Relationships of environmentally relevant properties. Tartu, 2007, 98 p.
70. **Mari Reinik.** Nitrates, nitrites, N-nitrosamines and polycyclic aromatic hydrocarbons in food: analytical methods, occurrence and dietary intake. Tartu, 2007, 172 p.
71. **Heili Kasuk.** Thermodynamic parameters and adsorption kinetics of organic compounds forming the compact adsorption layer at Bi single crystal electrodes. Tartu, 2007, 212 p.
72. **Erki Enkvist.** Synthesis of adenosine-peptide conjugates for biological applications. Tartu, 2007, 114 p.
73. **Svetoslav Hristov Slavov**. Biomedical applications of the QSAR approach. Tartu, 2007, 146 p.
74. **Eneli Härk.** Electroreduction of complex cations on electrochemically polished Bi(*hkl*) single crystal electrodes. Tartu, 2008, 158 p.
75. **Priit Möller.** Electrochemical characteristics of some cathodes for medium temperature solid oxide fuel cells, synthesized by solid state reaction technique. Tartu, 2008, 90 p.
76. **Signe Viggor.** Impact of biochemical parameters of genetically different pseudomonads at the degradation of phenolic compounds. Tartu, 2008, 122 p.
77. **Ave Sarapuu.** Electrochemical reduction of oxygen on quinone-modified carbon electrodes and on thin films of platinum and gold. Tartu, 2008, 134 p.
78. **Agnes Kütt.** Studies of acid-base equilibria in non-aqueous media. Tartu, 2008, 198 p.
79. **Rouvim Kadis.** Evaluation of measurement uncertainty in analytical chemistry: related concepts and some points of misinterpretation. Tartu, 2008, 118 p.
80. **Valter Reedo.** Elaboration of IVB group metal oxide structures and their possible applications. Tartu, 2008, 98 p.

81. **Aleksei Kuznetsov.** Allosteric effects in reactions catalyzed by the cAMP-dependent protein kinase catalytic subunit. Tartu, 2009, 133 p.
82. **Aleksei Bredihhin.** Use of mono- and polyanions in the synthesis of multisubstituted hydrazine derivatives. Tartu, 2009, 105 p.
83. **Anu Ploom.** Quantitative structure-reactivity analysis in organosilicon chemistry. Tartu, 2009, 99 p.
84. **Argo Vonk.** Determination of adenosine A_{2A}- and dopamine D_1 receptor-specific modulation of adenylate cyclase activity in rat striatum. Tartu, 2009, 129 p.
85. **Indrek Kivi.** Synthesis and electrochemical characterization of porous cathode materials for intermediate temperature solid oxide fuel cells. Tartu, 2009, 177 p.
86. **Jaanus Eskusson.** Synthesis and characterisation of diamond-like carbon thin films prepared by pulsed laser deposition method. Tartu, 2009, 117 p.
87. **Marko Lätt.** Carbide derived microporous carbon and electrical double layer capacitors. Tartu, 2009, 107 p.
88. **Vladimir Stepanov.** Slow conformational changes in dopamine transporter interaction with its ligands. Tartu, 2009, 103 p.
89. **Aleksander Trummal.** Computational Study of Structural and Solvent Effects on Acidities of Some Brønsted Acids. Tartu, 2009, 103 p.
90. **Eerold Vellemäe.** Applications of mischmetal in organic synthesis. Tartu, 2009, 93 p.
91. **Sven Parkel.** Ligand binding to 5-HT_{1A} receptors and its regulation by Mg^{2+} and Mn^{2+}. Tartu, 2010, 99 p.
92. **Signe Vahur.** Expanding the possibilities of ATR-FT-IR spectroscopy in determination of inorganic pigments. Tartu, 2010, 184 p.
93. **Tavo Romann**. Preparation and surface modification of bismuth thin film, porous, and microelectrodes. Tartu, 2010, 155 p.
94. **Nadežda Aleksejeva.** Electrocatalytic reduction of oxygen on carbon nanotube-based nanocomposite materials. Tartu, 2010, 147 p.
95. **Marko Kullapere.** Electrochemical properties of glassy carbon, nickel and gold electrodes modified with aryl groups. Tartu, 2010, 233 p.
96. **Liis Siinor.** Adsorption kinetics of ions at Bi single crystal planes from aqueous electrolyte solutions and room-temperature ionic liquids. Tartu, 2010, 101 p.
97. **Angela Vaasa.** Development of fluorescence-based kinetic and binding assays for characterization of protein kinases and their inhibitors. Tartu 2010, 101 p.
98. **Indrek Tulp.** Multivariate analysis of chemical and biological properties. Tartu 2010, 105 p.
99. **Aare Selberg.** Evaluation of environmental quality in Northern Estonia by the analysis of leachate. Tartu 2010, 117 p.
100. **Darja Lavõgina.** Development of protein kinase inhibitors based on adenosine analogue-oligoarginine conjugates. Tartu 2010, 248 p.

101. **Laura Herm.** Biochemistry of dopamine D_2 receptors and its association with motivated behaviour. Tartu 2010, 156 p.
102. **Terje Raudsepp.** Influence of dopant anions on the electrochemical properties of polypyrrole films. Tartu 2010, 112 p.
103. **Margus Marandi.** Electroformation of Polypyrrole Films: *In-situ* AFM and STM Study. Tartu 2011, 116 p.
104. **Kairi Kivirand.** Diamine oxidase-based biosensors: construction and working principles. Tartu, 2011, 140 p.
105. **Anneli Kruve.** Matrix effects in liquid-chromatography electrospray mass-spectrometry. Tartu, 2011, 156 p.
106. **Gary Urb.** Assessment of environmental impact of oil shale fly ash from PF and CFB combustion. Tartu, 2011, 108 p.
107. **Nikita Oskolkov.** A novel strategy for peptide-mediated cellular delivery and induction of endosomal escape. Tartu, 2011, 106 p.
108. **Dana Martin.** The QSPR/QSAR approach for the prediction of properties of fullerene derivatives. Tartu, 2011, 98 p.
109. **Säde Viirlaid.** Novel glutathione analogues and their antioxidant activity. Tartu, 2011, 106 p.
110. **Ülis Sõukand.** Simultaneous adsorption of Cd^{2+}, Ni^{2+}, and Pb^{2+} on peat. Tartu, 2011, 124 p.
111. **Lauri Lipping.** The acidity of strong and superstrong Brønsted acids, an outreach for the "limits of growth": a quantum chemical study. Tartu, 2011, 124 p.
112. **Heisi Kurig.** Electrical double-layer capacitors based on ionic liquids as electrolytes. Tartu, 2011, 146 p.
113. **Marje Kasari.** Bisubstrate luminescent probes, optical sensors and affinity adsorbents for measurement of active protein kinases in biological samples. Tartu, 2012, 126 p.
114. **Kalev Takkis.** Virtual screening of chemical databases for bioactive molecules. Tartu, 2012, 122 p.
115. **Ksenija Kisseljova**. Synthesis of aza-β^3-amino acid containing peptides and kinetic study of their phosphorylation by protein kinase A. Tartu, 2012, 104 p.
116. **Riin Rebane.** Advanced method development strategy for derivatization LC/ESI/MS. Tartu, 2012, 184 p.
117. **Vladislav Ivaništšev.** Double layer structure and adsorption kinetics of ions at metal electrodes in room temperature ionic liquids. Tartu, 2012, 128 p.
118. **Irja Helm.** High accuracy gravimetric Winkler method for determination of dissolved oxygen. Tartu, 2012, 139 p.
119. **Karin Kipper.** Fluoroalcohols as Components of LC-ESI-MS Eluents: Usage and Applications. Tartu, 2012, 164 p.
120. **Arno Ratas.** Energy storage and transfer in dosimetric luminescent materials. Tartu, 2012, 163 p.

121. **Reet Reinart-Okugbeni**. Assay systems for characterisation of subtype-selective binding and functional activity of ligands on dopamine receptors. Tartu, 2012, 159 p.
122. **Lauri Sikk.** Computational study of the Sonogashira cross-coupling reaction. Tartu, 2012, 81 p.
123. **Karita Raudkivi.** Neurochemical studies on inter-individual differences in affect-related behaviour of the laboratory rat. Tartu, 2012, 161 p.
124. **Indrek Saar.** Design of GalR2 subtype specific ligands: their role in depression-like behavior and feeding regulation. Tartu, 2013, 126 p.
125. **Ann Laheäär.** Electrochemical characterization of alkali metal salt based non-aqueous electrolytes for supercapacitors. Tartu, 2013, 127 p.
126. **Kerli Tõnurist.** Influence of electrospun separator materials properties on electrochemical performance of electrical double-layer capacitors. Tartu, 2013, 147 p.
127. **Kaija Põhako-Esko.** Novel organic and inorganic ionogels: preparation and characterization. Tartu, 2013, 124 p.
128. **Ivar Kruusenberg.** Electroreduction of oxygen on carbon nanomaterial-based catalysts. Tartu, 2013, 191 p.
129. **Sander Piiskop.** Kinetic effects of ultrasound in aqueous acetonitrile solutions. Tartu, 2013, 95 p.
130. **Ilona Faustova**. Regulatory role of L-type pyruvate kinase N-terminal domain. Tartu, 2013, 109 p.
131. **Kadi Tamm.** Synthesis and characterization of the micro-mesoporous anode materials and testing of the medium temperature solid oxide fuel cell single cells. Tartu, 2013, 138 p.
132. **Iva Bozhidarova Stoyanova-Slavova.** Validation of QSAR/QSPR for regulatory purposes. Tartu, 2013, 109 p.
133. **Vitali Grozovski**. Adsorption of organic molecules at single crystal electrodes studied by *in situ* STM method. Tartu, 2014, 146 p.
134. **Santa Veikšina**. Development of assay systems for characterisation of ligand binding properties to melanocortin 4 receptors. Tartu, 2014, 151 p.
135. **Jüri Liiv.** PVDF (polyvinylidene difluoride) as material for active element of twisting-ball displays. Tartu, 2014, 111 p.
136. **Kersti Vaarmets.** Electrochemical and physical characterization of pristine and activated molybdenum carbide-derived carbon electrodes for the oxygen electroreduction reaction. Tartu, 2014, 131 p.
137. **Lauri Tõntson**. Regulation of G-protein subtypes by receptors, guanine nucleotides and Mn^{2+}. Tartu, 2014, 105 p.
138. **Aiko Adamson.** Properties of amine-boranes and phosphorus analogues in the gas phase. Tartu, 2014, 78 p.
139. **Elo Kibena**. Electrochemical grafting of glassy carbon, gold, highly oriented pyrolytic graphite and chemical vapour deposition-grown graphene electrodes by diazonium reduction method. Tartu, 2014, 184 p.

140. **Teemu Näykki.** Novel Tools for Water Quality Monitoring – From Field to Laboratory. Tartu, 2014, 202 p.
141. **Karl Kaupmees.** Acidity and basicity in non-aqueous media: importance of solvent properties and purity. Tartu, 2014, 128 p.
142. **Oleg Lebedev**. Hydrazine polyanions: different strategies in the synthesis of heterocycles. Tartu, 2015, 118 p.
143. **Geven Piir.** Environmental risk assessment of chemicals using QSAR methods. Tartu, 2015, 123 p.
144. **Olga Mazina.** Development and application of the biosensor assay for measurements of cyclic adenosine monophosphate in studies of G protein-coupled receptor signalinga. Tartu, 2015, 116 p.
145. **Sandip Ashokrao Kadam.** Anion receptors: synthesis and accurate binding measurements. Tartu, 2015, 116 p.
146. **Indrek Tallo.** Synthesis and characterization of new micro-mesoporous carbide derived carbon materials for high energy and power density electrical double layer capacitors. Tartu, 2015, 148 p.
147. **Heiki Erikson.** Electrochemical reduction of oxygen on nanostructured palladium and gold catalysts. Tartu, 2015, 204 p.
148. **Erik Anderson.** *In situ* Scanning Tunnelling Microscopy studies of the interfacial structure between Bi(111) electrode and a room temperature ionic liquid. Tartu, 2015, 118 p.
149. **Girinath G. Pillai.** Computational Modelling of Diverse Chemical, Bio-chemical and Biomedical Properties. Tartu, 2015, 140 p.
150. **Piret Pikma.** Interfacial structure and adsorption of organic compounds at Cd(0001) and Sb(111) electrodes from ionic liquid and aqueous electrolytes: an *in situ* STM study. Tartu, 2015, 126 p.
151. **Ganesh babu Manoharan.** Combining chemical and genetic approaches for photoluminescence assays of protein kinases. Tartu, 2016, 126 p.
152. **Carolin Siimenson**. Electrochemical characterization of halide ion adsorption from liquid mixtures at Bi(111) and pyrolytic graphite electrode surface. Tartu, 2016, 110 p.
153. **Asko Laaniste.** Comparison and optimisation of novel mass spectrometry ionisation sources. Tartu, 2016, 156 p.
154. **Hanno Evard.** Estimating limit of detection for mass spectrometric analysis methods. Tartu, 2016, 224 p.
155. **Kadri Ligi.** Characterization and application of protein kinase-responsive organic probes with triplet-singlet energy transfer. Tartu, 2016, 122 p.
156. **Margarita Kagan.** Biosensing penicillins' residues in milk flows. Tartu, 2016, 130 p.
157. **Marie Kriisa.** Development of protein kinase-responsive photo-luminescent probes and cellular regulators of protein phosphorylation. Tartu, 2016, 106 p.
158. **Mihkel Vestli.** Ultrasonic spray pyrolysis deposited electrolyte layers for intermediate temperature solid oxide fuel cells. Tartu, 2016, 156 p.

159. **Silver Sepp**. Influence of porosity of the carbide-derived carbon on the properties of the composite electrocatalysts and characteristics of polymer electrolyte fuel cells. Tartu, 2016, 137p.
160. **Kristjan Haav**. Quantitative relative equilibrium constant measurements in supramolecular chemistry. Tartu, 2017, 158 p.